

UNCLASSIFIED

AD NUMBER

ADB053309

LIMITATION CHANGES

TO:

Approved for public release; distribution is unlimited.

FROM:

Distribution authorized to U.S. Gov't. agencies only; Test and Evaluation; JUL 1980. Other requests shall be referred to Ballistic Research Laboratory, Aberdeen Proving Ground, MD, 21005-5066.

AUTHORITY

ALC ltr dtd 22 Nov 1988

THIS PAGE IS UNCLASSIFIED

AD A053309L

## CONTRACT REPORT ARBRL-CR-00432

## A MODEL OF THE TRAVELING CHARGE

Prepared by

Paul Gough Associates, Inc.  
Portsmouth, NH 03801

July 1980



**US ARMY ARMAMENT RESEARCH AND DEVELOPMENT COMMAND**  
**BALLISTIC RESEARCH LABORATORY**  
**ABERDEEN PROVING GROUND, MARYLAND**

Distribution limited to US Government agencies only; Test and Evaluation; Jul 80. Other requests for this document must be referred to Director, USA Ballistic Research Laboratory, ATTN: DRDAR-TSB, Aberdeen Proving Ground, Maryland 21005.

AD

1981-0316

81-0316

CONTRACT REPORT ARBRL-CR-00432

A MODEL OF THE TRAVELING CHARGE

Prepared by

Paul Gough Associates, Inc.  
Portsmouth, NH 03801

July 1980



US ARMY ARMAMENT RESEARCH AND DEVELOPMENT COMMAND  
BALLISTIC RESEARCH LABORATORY  
ABERDEEN PROVING GROUND, MARYLAND

AD B053 309

~~Distribution limited to US Government agencies only; Test and  
Evaluation; Jul 80. Other requests for this document must be  
referred to Director, USA Ballistic Research Laboratory,  
ATTN: DDBRL-158, Aberdeen Proving Ground, Maryland 21005.~~

Distribution Statement A:  
Approved for public release;  
distribution is unlimited.

Destroy this report when it is no longer needed.  
Do not return it to the originator.

Secondary distribution of this report by originating  
or sponsoring activity is prohibited.

Additional copies of this report may be obtained  
from the Defense Technical Information Center, Cameron  
Station, Alexandria, Virginia 22314.

The findings in this report are not to be construed as  
an official Department of the Army position, unless  
so designated by other authorized documents.

*The use of trade names or manufacturers' names in this report  
does not constitute endorsement of any commercial product.*

UNCLASSIFIED

SECURITY CLASSIFICATION OF THIS PAGE (When Data Entered)

REPORT DOCUMENTATION PAGE		READ INSTRUCTIONS BEFORE COMPLETING FORM
1. REPORT NUMBER CONTRACT REPORT ARBRL-CR-00432	2. GOVT ACCESSION NO.	3. RECIPIENT'S CATALOG NUMBER
4. TITLE (and Subtitle) A Model of the Traveling Charge		5. TYPE OF REPORT & PERIOD COVERED Contractor
		6. PERFORMING ORG. REPORT NUMBER
7. AUTHOR(s) P. S. Gough		8. CONTRACT OR GRANT NUMBER(s) DAAK11-79-C-0071
9. PERFORMING ORGANIZATION NAME AND ADDRESS Paul Gough Associates, Inc. Portsmouth, NH 03801		10. PROGRAM ELEMENT, PROJECT, TASK AREA & WORK UNIT NUMBERS
11. CONTROLLING OFFICE NAME AND ADDRESS US Army Armament Research & Development Command US Army Ballistic Research Laboratory (ATTN: DRDAR-BL) Aberdeen Proving Ground, MD 21005		12. REPORT DATE July 1980
		13. NUMBER OF PAGES 150
14. MONITORING AGENCY NAME & ADDRESS (if different from Controlling Office)		15. SECURITY CLASS. (of this report) Unclassified
		15a. DECLASSIFICATION/DOWNGRADING SCHEDULE
16. DISTRIBUTION STATEMENT (of this Report) Distribution limited to US Government agencies only; Test and Evaluation; Jul 80. Other requests for this document must be referred to Director, USA Ballistic Research Laboratory, ATTN: DRDAR-TSB, Aberdeen Proving Ground, MD 21005.		
17. DISTRIBUTION STATEMENT (of the abstract entered in Block 20, if different from Report)		
18. SUPPLEMENTARY NOTES		
19. KEY WORDS (Continue on reverse side if necessary and identify by block number) Traveling Charge Gun 1-D Gas Dynamic Models Ultra-High Burning Rate Propellant High Velocity Guns		
20. ABSTRACT (Continue on reverse side if necessary and identify by block number)  A model is described to permit the theoretical evaluation of the ballistic performance of an end-burning traveling charge. The column of gas between the breech and the regressing propellant surface is analyzed as a one-dimensional, unsteady, inviscid flow with heat loss to the wall. The solid propellant may be represented either as rigid or as an unsteady, one-dimensional, viscoplastic continuum which interacts with the tube wall through the action of friction.		

UNCLASSIFIED

SECURITY CLASSIFICATION OF THIS PAGE(When Data Entered)

To enable the assessment of potential or ideal performance, as well as that currently available from measured rates of burning, the combustion of the propellant may be prescribed according to any of several ideal criteria. The reactants may be required to come to rest, to attain a predetermined Mach number or to induce a predetermined pressure on the unreacted side of the interface or a predetermined acceleration of the projectile. While there are strong arguments to rule out the possibility of a steady combustion wave with supersonic reactants, as viewed from the regressing surface, ideal models of such strong deflagration waves are provided so as to enable the assessment of the performance loss associated with a limitation to weak or subsonic deflagrations.

The breech may be taken to be gas-permeable and the solution can be continued past muzzle exit in order to study blowdown of the tube. The solution is obtained by means of an explicit two-level finite difference scheme and uses the method of characteristics at the external boundaries and at the interface between the gas and the solid propellant.

Sample calculations are provided in order to demonstrate the stability of the method of solution and to benchmark its accuracy. Comparison with a case which admits an exact solution is provided and studies are made of mesh indifference and of the global conservation of mass and energy.

UNCLASSIFIED

SECURITY CLASSIFICATION OF THIS PAGE(When Data Entered)

### Foreword

Technical cognizance for the subject contract  
has been provided by Mr. P. G. Baer  
U.S. Army Ballistic Research Laboratory DRDAR-BLP





## Table of Contents

	<u>Page</u>
Foreword	3
Table of Contents	5
List of Illustrations	7
1.0 INTRODUCTION	9
1.1 Background	9
1.2 Objectives and Scope of Present Study	14
1.3 Summary of Approach	14
2.0 GOVERNING EQUATIONS FOR MODEL	17
2.1 Balance Equations for Gas	17
2.2 Balance Equations for Solid Propellant	19
2.3 Motion of the Projectile	20
2.4 Constitutive Laws	21
2.4.1 Equation of State of Gas	21
2.4.2 Equation of State of Solid Propellant	21
2.4.3 Heat Loss to the Tube	22
2.4.4 Friction Between Propellant and Tube	23
2.4.5 Resistance to Projectile Motion	24
2.4.6 Propellant Burn Rate (Measured)	25
2.5 Boundary Conditions	25
2.5.1 Breech (Closed or Open)	26
2.5.2 Projectile Base and Muzzle Following Projectile Exit	27
2.5.3 Gas/Propellant Interface	28
2.6 Initial Conditions	32
3.0 METHOD OF SOLUTION	35
3.1 Mesh Allocation	35
3.2 Transformed Equations	37
3.3 Integration at Interior Mesh Points	38
3.4 Integration at Boundary Mesh Points	39
3.4.1 Breech (Closed or Open)	41
3.4.2 Projectile Base and Muzzle Following Projectile Exit	41
3.4.3 Gas/Propellant Interface	41
3.4.3.1 Propellant Unreacting	42
3.4.3.2 Measured Burn Rate (With Subsonic Reactants)	42
3.4.3.3 Ideal Burning of Langweiler (Subsonic or Supersonic Reactants)	43
3.4.3.4 Prespecified Value of Pressure on Unreacted Side or of Acceleration of Projectile (With Subsonic Reactants)	44
3.4.3.5 Predetermined Mach Number of Reactants (Subsonic)	44
3.4.3.6 Prespecified Value of Pressure on Unreacted Side or of Acceleration of Projectile (With Supersonic Reactants)	45

3.5	Additional Considerations	45
3.5.1	Choice of Time Step	45
3.5.2	Treatment at Burnout	45
3.5.3	Change of Representation of Solid Propellant	47
3.5.4	Treatment of Friction Between Propellant and Tube Wall	48
3.5.5	Branching of Conditions at the Gas/ Propellant Interface	48
4.0	SOME NUMERICAL RESULTS	50
4.1	Comparison with an Exact Solution	50
4.2	A Nominal Traveling Charge Configuration	51
4.3	Influence of Losses	59
5.0	CONCLUSIONS	61
	REFERENCES	63
	Nomenclature	65
	Appendix A: On the Deflagration Wave with Supersonic Reactants	69
	Appendix B: Code Description and Fortran Listing	79
	DISTRIBUTION LIST	149

## List of Illustrations

<u>Figure</u>	<u>Title</u>	<u>Page</u>
1.1	Schematic illustration of flows associated with conventional granular and end-burning traveling charges	10
4.1	Distributions of pressure and velocity in nominal traveling charge problem at time 0.0 msec	55
4.2	Distributions of pressure and velocity in nominal traveling charge problem at time 0.2 msec	55
4.3	Distributions of pressure and velocity in nominal traveling charge problem at time 0.4 msec	56
4.4	Distributions of pressure and velocity in nominal traveling charge problem at time 0.6 msec	56
4.5	Distributions of pressure and velocity in nominal traveling charge problem at time 1.0 msec	57
4.6	Distributions of pressure and velocity in nominal traveling charge problem at time 1.6 msec	57
4.7	Distributions of pressure and velocity in nominal traveling charge problem at time 2.0 msec	58
4.8	Distributions of pressure and velocity in nominal traveling charge problem at time 2.4 msec	58
A.1	Hugoniot curve for reacted gas	70
A.2	Schematic demonstration of the implausibility of attaining a strong deflagration	73
A.3	Control volume for analysis of a steady heterogeneous reacting flow	75



## 1.0 INTRODUCTION

This report is concerned with the interior ballistic performance of a particular type of gun propelling charge which is attached to the base of the projectile and which burns in successive planar layers, combustion beginning at the rear face of the charge and progressing towards the projectile base. A propelling charge of this type is referred to as an end-burning traveling charge and is of current interest as a potential solution in applications requiring very high muzzle velocities--of the order of 3 km/sec.

In order to permit a theoretical evaluation of the performance to be expected of such a charge, we have developed a model of the one-dimensional continuum dynamics of the solid propellant and its products of combustion, the reaction zone being assumed sufficiently thin that it may be represented as an internal boundary condition. The purpose of the present report is to provide documentation of the model, including the mathematical formulation of the equations, the method of solution, and the structure and use of the computer program into which the model has been encoded.

Subsequent subsections of this introduction enlarge on the concept of the traveling charge, define the scope of the present effort, and summarize the modeling approach.

### 1.1 Background

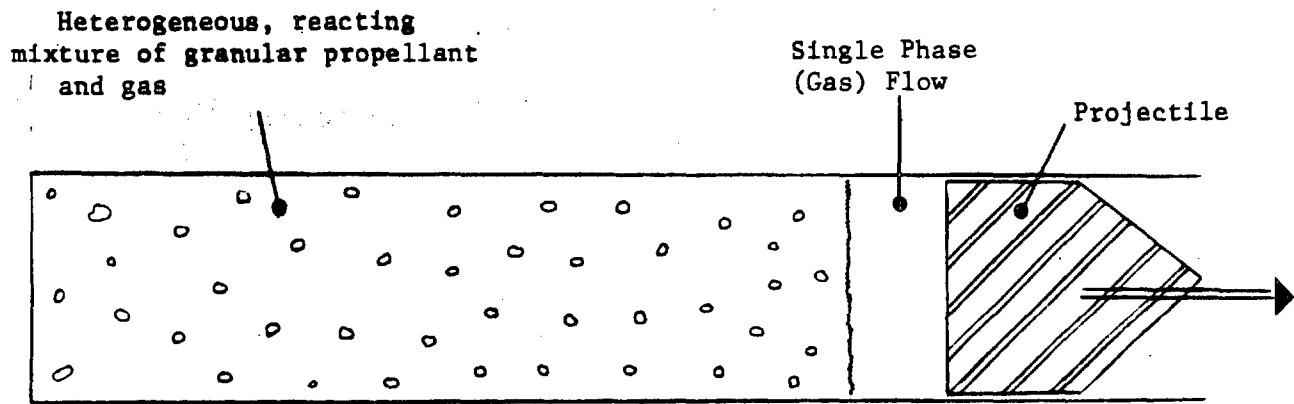
Increasing the muzzle velocity offers two advantages: the time of flight of the projectile is reduced, increasing the likelihood of defeating a highly mobile target; and the terminal velocity is increased, at moderate range, increasing the likelihood of penetration of heavy armor. Present conventional weapons yield muzzle velocities of the order of 1.0-1.5 km/sec. Significant increases in effectiveness against the most mobile or most heavily armored targets would accrue if muzzle velocities as high as 3.0 km/sec could be obtained.

The relevance of the traveling charge concept to the design of weapons yielding such high velocities has been discussed in some detail in a recent review by May et al<sup>1</sup>. In the present report we confine our discussion to certain conceptual aspects of propelling charge performance in order to identify the theoretical factors which have motivated past and present interest in the traveling charge and to note certain questions which may be asked about the traveling charge concept; these questions motivate the present work.

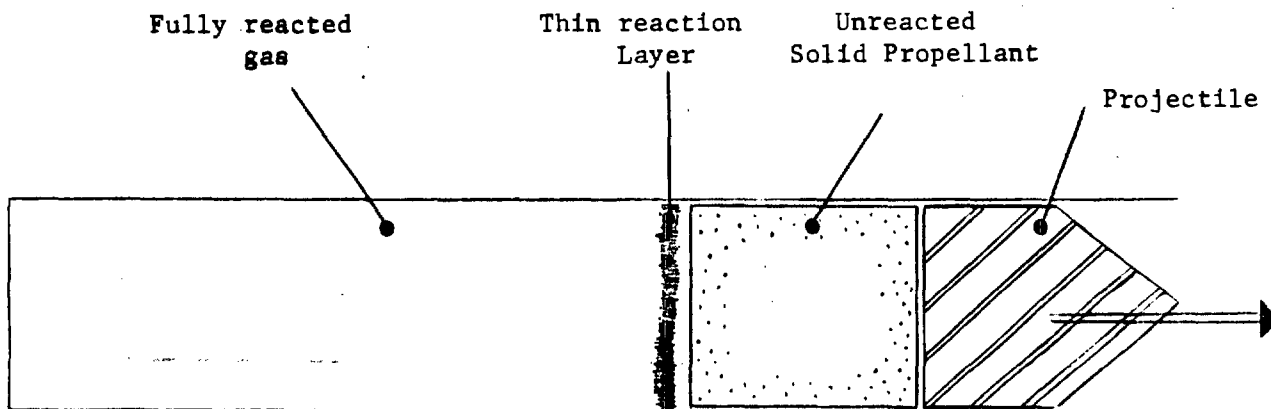
Figure 1.1 illustrates, in a schematic form, the nature of the flows associated with a conventional granular propelling charge and an

---

<sup>1</sup>May, I. W., Baran, A. F., Baer, P. G. and Gough, P. S.  
"The Traveling Charge Effect"  
*Proceedings of the 15th JANNAF Combustion Meeting*



(a) Conventional granular propelling charge



(b) End-burning traveling charge

**Figure 1.1** Schematic illustration of flows associated with conventional granular and end-burning traveling charges

end-burning traveling charge. In neither case do we discuss the details of the ignition process; details pertaining to the conventional charge may be found in the recent AIAA Progress Series volume edited by Krier and Summerfield<sup>2</sup>.

Except for a relatively small region of single phase flow adjacent to the base of the projectile, the granular propellant tends to be found throughout the tube at all times prior to burnout. Therefore the flow is that of a heterogeneous reacting mixture in which the spacewise release of chemical energy is more or less uniform. The tendency of the mixture to become well stirred is due to the action of interphase drag. Conversely the presence of a region of single phase flow adjacent to the projectile base is due to the vanishing of the slip velocity at the base. The departure of the mixture from true well-stirredness can be pronounced in some cases, especially during ignition, and the ballistic consequences may be important<sup>2</sup>. However, by comparison with the end-burning traveling charge, in which the propellant and its products of combustion are separated by a thin layer in which the heat release occurs, the granular propelling charge looks very well-stirred indeed.

Taking the two-phase mixture to be well-stirred and having more or less uniform density leads to the classical one-dimensional solution of Lagrange<sup>3</sup> in which the velocity profile is linear and the pressure profile is parabolic. In particular, one may deduce that at any instant of time the base pressure  $p_{base}$  and the breech pressure  $p_{breech}$  are related according to the formula  $p_{base} = p_{breech} / (1 + W/2)$  where  $W$  is the charge-to-projectile mass ratio. Also, one may show that the ratio of the kinetic energy of the propellant mixture to that of the projectile is  $(W/3) : 1$ .

These elementary classical results define the perspective from which the concept of the traveling charge appears to offer certain ballistic benefits as the charge-to-projectile mass ratio is increased. The relationship between  $p_{breech}$  and  $p_{base}$  describes the degree to which the pressure at the projectile base is reduced by the requirement that a gradient exist to accelerate the mixture. In conventional ammunition, with muzzle velocities of the order of 1 km/sec,  $W$  is approximately 0.50 so that  $p_{base} \sim 0.80 p_{breech}$ . Now the propulsive capacity is clearly due to  $p_{base}$  while either the weapon weight is related to  $p_{breech}$  or, conversely,  $p_{breech}$  is limited by the tube strength. The discrepancy of 20% between propulsive pressure and the structural pressure represents a loss of efficiency in some sense. If we now consider the charge-to-projectile mass ratio necessary to achieve a muzzle velocity of the order of 3 km/sec with a conventional granular charge we find that  $W$  is of the order of 8 so that  $p_{base} \sim 0.2 p_{breech}$ . Evidently we have reached the regime of diminishing returns; much of the propulsive potential of the propellant is lost to self-work. A similar conclusion follows from an examination of the ratio of kinetic energy of the charge to that of the projectile, which takes the values 0.167 and 2.67 for the two cases we have considered.

---

<sup>2</sup>Krier, H. and Summerfield, M., "Interior Ballistics of Guns" *Progress in Astronautics and Aeronautics*, Vol. 66.

American Institute of Aeronautics and Astronautics 1979

<sup>3</sup>Corner, J. "Theory of the Interior Ballistics of Guns"

Wiley, New York, 1950

Now let us consider the end-burning traveling charge configuration also illustrated in figure 1.1. The concept formulated by Langweiler<sup>4</sup> has the following novel aspect. The rate of burning of the propellant is to be controlled in such a fashion that the reacted gas comes to rest with respect to the frame of reference of the gun. Evidently, the burn rate is required initially to be zero and to increase as the projectile accelerates. At any instant, however, the kinetic energy of the gas is zero and, in particular, as burnout is approached, all the propellant is at rest, the kinetic energy being contained only in the projectile. Alternatively, as the gas column is always at rest, suffering neither translation nor dilation, its pressure remains constant at the initial value and is, moreover, uniform with respect to its length. The possibility that these observations can be translated into improved ballistic efficiency has motivated both past and present interest in the traveling charge.

Certain questions come to mind as regards this possibility. We first note those of previous investigators and then add some observations of our own.

The first question is whether the burn rates required by the Langweiler concept can actually be realized. It was observed by Vinti<sup>5</sup> that the regression rate would be required to be of the same order of magnitude as the projectile velocity, namely one or more km/sec. This requirement may be contrasted with the observed rates of burning of conventional propellants which are typically measured in cm/sec at the largest pressures experienced in a gun. The same observation was made by Lee and Laidler<sup>6</sup> who also commented on the extraordinary mechanical properties that would be required to transmit the propellant thrust to the base of the projectile. Apart from the technological difficulties of high strength and high burning rate, Lee and Laidler did not discern any fundamental obstacles to the implementation of the traveling charge concept.

Vinti noted that the pressure on the unreacted side of the gas/propellant interface would exceed that of the reactants and that the excess would be proportional, in some fashion, to the regression rate. The excess is, of course, the contribution of momentum flux to the total propulsive thrust. Accordingly, the Langweiler concept does not

---

<sup>4</sup>Langweiler, H. "A Proposal for Increasing the Performance of Weapons by the Correct Burning of Propellant"  
British Intelligence Objective Sub-Committee, Group 2,  
Ft. Halstead Exploiting Center, Report 1247 undated

<sup>5</sup>Vinti, J. P. "Theory of the Rapid Burning of Propellants"  
Ballistic Research Laboratories Report No. 841 1952

<sup>6</sup>Lee, L. and Laidler, K. J. "The Interior Ballistics of the Impulse Propulsion Gun" Nord 10260 Contract Report CU/F/57.2, August 1951



operate on a constant pressure cycle. The pressure at the base of the propellant increases with travel and it is this pressure, moreover, which the tube must support. In Vinti's opinion, the resulting combination of maximum pressure and muzzle velocity would not differ appreciably from that obtained using a conventional charge.

A more serious objection to the traveling charge concept of Langweiler was also expressed by Vinti. He observed that as the projectile velocity increased to a value exceeding the speed of sound in the reactants, the law of burning would be required to yield supersonic reactants, as perceived by an observer moving with the regressing surface. From the theory of the steady deflagration of a gas it has been shown, for all models of flame structure which have been investigated<sup>7,8,9,10</sup>, that such a process cannot occur. It was concluded by Vinti, therefore, that the Langweiler concept would be inherently incapable of realization once the velocity of the projectile exceeded approximately 1.0-1.5 km/sec, which is the velocity of sound in present day propellant formulations.

We now add to these earlier caveats some considerations of our own. First we observe that the traveling charge is represented as self-supporting. It is not difficult to show that alternative designs in which the propellant is supported by some structural member lead to rather unattractive payload capacities, most of the projectile weight being concentrated in the propellant support system. If the propellant is unsupported, and required to transmit compressive stresses of the order of 500 MPa, we may expect its mechanical response to enter the hydrodynamic regime. That is to say, the components of the stress deviator are not expected to exceed the yield strength--typically of the order of 5-10 MPa in current compositions--so that the stress tensor can be regarded as isotropic, to a good degree of approximation. This implies that the radial stress exerted on the gun tube by the propellant will be approximately equal to the axial stress--as already assumed by Vinti. Therefore the problem of mechanical resistance due to wall friction must surely be considered.

Consider next the conditions as the projectile approaches the muzzle of the gun. Suppose that the ideal combustion model of Langweiler has indeed been realized. The pressure of the gas is therefore some large value. Yet the design constraints associated with muzzle blast require that the pressure be suitably limited. Therefore, either the initial gas pressure must be confined to that limit or burnout must occur prior to muzzle exit.

---

<sup>7</sup> Friedrichs, K. O. "On the Mathematical Theory of Deflagrations and Detonations" NAVORD Report 79-46 1946

<sup>8</sup> Courant, R. and Friedrichs, K. O. "Supersonic Flow and Shock Waves" Interscience, New York 1948

<sup>9</sup> Williams, F. A. "Combustion Theory" Addison-Wesley 1965

<sup>10</sup> Landau, L. D. and Lifschitz, E. M. "Fluid Mechanics" Pergamon Press 1959

If burnout occurs, there will be imposed on the gas column a rarefaction wave which will accelerate it towards the muzzle. If enough projectile travel occurs between burnout and muzzle exit, the velocity profile will resume the distribution characteristic of the conventional charge. From the point of view of a global energy balance, therefore, the potential ballistic benefit of the traveling charge is apparently diminished following burnout of the propellant.

As a final observation we note that when burnout occurs, the velocity of the gas is required instantaneously to adjust to that of the projectile. Since the jump in velocity may be of the order of the speed of sound, the concomitant drop in pressure may be very large. Two consequences follow from this observation. First, the propulsive capacity of the gas after burnout will be diminished due to the sharp drop in base pressure. Second, a strong tensile wave will be transmitted through the projectile and mechanical failure might be a concern if sensitive fuzing or guidance components are present.

The loss of propulsive capacity following burnout suggests that the optimum use of a traveling charge will involve a design in which burnout occurs close to the muzzle. If the pressure drop associated with burnout is sufficiently great, it may be possible to satisfy the constraint associated with blast while operating from a high initial pressure.

From the foregoing discussion it is apparent that the evaluation of the potential merits of the traveling charge concept must be performed in the context of a model capable of recognizing the hydrodynamic implications of certain hypothetical or ideal combustion laws. Specifically, we seek herein to provide a model which is capable of answering questions of the following type. What are the implications, in regard to performance, of limiting the Langweiler combustion model to subsonic or sonic conditions? As the Langweiler combustion model does not in fact yield a constant base pressure on the projectile, would a more favorable ideal combustion model be one in which the stress in the unreacted propellant, or the acceleration of the projectile, were held constant? Would such an ideal law require supersonic combustion? If so, what would be the losses associated with a limitation to subsonic or sonic states in such cases?

## 1.2 Objectives and Scope of Present Study

The objectives of the present study are to formulate, encode and demonstrate a model of an end-burning traveling charge. The model is required to be of sufficient scope as to permit an assessment of the hydrodynamic and ideal combustion limits on performance. However, parametric studies to evaluate the theoretical performance of an end-burning traveling charge and the formation of comparisons with conventional charge performance are not within the scope of the present effort.

## 1.3 Summary of Approach

We first summarize the physical aspects of the model. Subsequently, we will comment on the method of solution. The model is predicated on the nature of the flow illustrated schematically in figure 1.1. The flow is assumed to be one-dimensional without change of area. The gas is assumed to obey a co-volume equation of state and is modeled as a one-dimensional, inviscid, unsteady flow with an allowance for heat loss to the tube. The propellant may be represented either as rigid or as a viscoplastic continuum in which an allowance is made for the friction exerted on the tube.

The breech boundary condition may be represented either as closed or as permeable to the gas. The latter case enables the application of the model to vented chambers and to recoilless rifles. The code also permits a simulation of the blowdown of the tube following the expulsion of the projectile and any unburned propellant.

The interface between the gas and the solid propellant is treated as a discontinuity. A variety of models are provided to describe the rate of burning. We have already noted that there are strong arguments to deny the possibility of a steady deflagration wave with supersonic reactants. These arguments are reviewed in Appendix A. We nevertheless provide models of both subsonic and supersonic deflagrations. Our purpose in providing the latter is principally to permit an assessment of the extent to which the theoretical performance of an end-burning traveling charge is limited by the restriction of burning to the subsonic or sonic conditions.

Considering first the subsonic cases it follows that only one condition may be imposed on the burning process. We admit any one of the following. The burn rate may be described as a function of pressure according to measurements. The burn rate may be required to yield the ideal combustion of Langweiler. The burn rate may be required to yield a predetermined value of pressure on the unreacted side of the gas/propellant interface or to yield a predetermined value of the acceleration of the projectile. Finally, the burn rate may be required to yield a predetermined Mach number of the reactants, provided, of course, that this value is less than one. In all these cases, the subsonic nature of the flow demands that the reactants satisfy a condition of mechanical compatibility with the column of gas.

If the reactants become supersonic, they are no longer required to be mechanically compatible with the gas. The deflagration influences but is not influenced by the motion of the gas unless a shock of sufficient strength is formed to overtake the supersonic boundary. We admit two possible models of a supersonic deflagration. The first is the Langweiler model. In the case of supersonic burning, two conditions may be imposed on the process. The Langweiler process may be interpreted as specifying both the velocity and pressure of the reactants. A second model is defined by specifying the Mach number of the reactants --greater than or equal to unity--and either the pressure on the unreacted side of the gas/propellant interface or the acceleration of the projectile.

Full details of the physical model and the relevant governing equations are given in chapter 2.0. In chapter 3.0 we describe the method of solution which may be summarized as follows. A time dependent mesh is allocated subject to constraints on minimum mesh size and total number of points. A two level explicit marching scheme is used to update the state of interior mesh points and the method of characteristics is used at the boundaries. Chapter 3.0 describes in detail the implementation of the various models of burning and also discusses the rules according to which branching may occur among them during a given interior ballistic cycle.

The method of solution is illustrated in chapter 4.0. A comparison is given with an exact solution for a simple case to provide an absolute benchmark of accuracy. A nominal traveling charge configuration is

discussed to exhibit the degree of mesh indifference of the code and the extent to which mass and energy are conserved on a global basis. We also comment briefly on the ballistic consequences of friction between the propellant and the tube.

The code itself is described in Appendix B which contains tables of the various routines and their linkages, a glossary of variable names, and the format of the data used to run the code. A Fortran IV listing is also attached.

## 2.0 GOVERNING EQUATIONS FOR MODEL

The governing equations for the model consist of one-dimensional time-dependent statements of the balances of mass, momentum and energy supported by constitutive laws and subjected to boundary and initial conditions. The gas is always treated as a continuum as described in section 2.1. The unreacted propellant may be represented either as a continuum or as a rigid body, according to the interests of the user of the model. The equations in the continuum case are described in section 2.2 while the case of rigid body motion is included with the discussion of the motion of the projectile in section 2.3. The constitutive laws are described in section 2.4. The discussion of section 2.4 includes the equations of state for the gas and the solid propellant, heat loss to the tube, friction between the tube wall and the solid propellant, resistance to projectile motion and, finally, the description of non-ideal rates of burning such as those determined experimentally. The analysis of ideal burn rates, in which the reactants are required to come to rest or to attain a prespecified Mach number or to induce a predetermined level of acceleration of the projectile or of stress in the unreacted propellant, are described in section 2.5 which treats the boundary conditions. Finally, section 2.6 of this chapter discusses the initial conditions; when the propellant is burning vigorously at the initial instant, these may be non-trivial. The method of solution of the governing equations is the subject of chapter 3.0.

### 2.1 Balance Equations for Gas

The motion of the gas is assumed to be one-dimensional, unsteady, inviscid and non-heat-conducting. However, the loss of heat to the tube wall is considered in the balance of energy. Using  $t$  to represent time,  $x$  to represent the axial coordinate and  $\rho$ ,  $u$ ,  $p$ ,  $e$  to represent the density, velocity, pressure and internal energy of the gas, the balance equations may be expressed in the usual forms<sup>8</sup>:

#### Balance of Mass

$$\frac{\partial \rho}{\partial t} + \frac{\partial}{\partial x} \rho u = 0 \quad 2.1.1$$

#### Balance of Momentum

$$\frac{\partial \rho u}{\partial t} + \frac{\partial}{\partial x} (\rho u^2 + g_o p) = 0 \quad 2.1.2$$

#### Balance of Energy

$$\frac{\partial}{\partial t} \rho \left( e + \frac{u^2}{2g_o} \right) + \frac{\partial}{\partial x} \rho u \left( e + \frac{p}{\rho} + \frac{u^2}{2g_o} \right) = -q_w \quad 2.1.3$$

Here we have also used  $q_w$  to represent the heat loss per unit volume of gas per unit time and  $g_o$  is a constant used to reconcile units.

It is well known that these equations are of the hyperbolic type<sup>8</sup>. That is to say, there exist real lines on which the equations reduce to ordinary differential forms involving only derivatives along the lines in question. The lines are referred to as characteristics and the differential forms are called conditions of compatibility. The existence of the characteristic lines follows naturally from a consideration of the Cauchy problem for the quasi-linear system<sup>11</sup>

$$A \frac{\partial \psi}{\partial t} + B \frac{\partial \psi}{\partial x} = C \quad 2.1.4$$

where  $\psi$  and  $C$  are  $k$ -dimensional vectors and  $A$  and  $B$  are  $k \times k$  matrices. Consider the transformation  $(x, t) \rightarrow (s, n)$  so that 2.1.4 becomes

$$[A n_t + B n_x] \psi_n = C - [A s_t + B s_x] \psi_s \quad 2.1.5$$

where the subscript denotes a partial derivative. Let the vector  $\psi$  be specified on the initial line  $n = n_0$ . Then the line is called free if 2.1.5 permits the determination of the normal derivatives and characteristic if it does not. The importance of this point is simply that if the normal derivatives can be determined, successive differentiation will permit the determination of derivatives of all orders with respect to  $n$  so that the solution can be obtained in a neighborhood of the initial data by means of Taylor's theorem.

Evidently, the condition that the line  $n = n_0$  be free is that the rank of the matrix

$$\Delta = A n_t + B n_x$$

be  $r(\Delta) = k$  whereupon 2.1.5 has a unique solution for the components of  $\psi_n$ . When  $r(\Delta) < k$  the line  $n = n_0$  is characteristic. However, if the equation 2.1.5 is to hold at each point on such a line, the initial data are not arbitrary, but are constrained by the condition of solvability for the linear system 2.1.5, namely

$$r(\Delta^+) = r(\Delta)$$

where  $\Delta^+ = [\Delta; C - [A s_t + B s_x] \psi_s]$  is the augmented matrix. These conditions of solvability yield the conditions of compatibility for each characteristic line.

A convenient choice for the parameter  $s$  is  $s = t$ . However, it must be borne in mind that  $\psi_s$  is a derivative with  $n$  held constant so that  $\psi_s = \psi_t t_s + \psi_x x_s$ . One may also use the relations  $dx/dt = x_s/t_s = -n_t/n_x$ , where  $dx$  and  $dt$  are understood to be differentials along the line  $n = n_0$ , to recast  $\Delta$  and  $\Delta^+$  as:

$$\Delta = A dx - B dt \quad 2.1.6$$

$$\Delta^+ = [\Delta; C - A \frac{d\psi}{dt}] \quad 2.1.7$$

---

<sup>11</sup> Petrovsky, I. G. "Partial Differential Equations"  
Interscience, New York 1954

By eliminating  $e$  in favor of  $p$  and  $\rho$  in 2.1.3 and introducing the isentropic sound speed  $c$ , it is easy to show that the system 2.1.1, 2.1.2, 2.1.3 yields the following characteristics and conditions of compatibility. On the lines designated by  $\Gamma_g^\pm$  whose slopes satisfy

$$\frac{dx}{dt} = u \pm c \quad 2.1.8$$

we have the conditions of compatibility

$$\frac{dp}{dt} \pm \frac{\rho c}{g_o} \frac{du}{dt} = - \frac{q_w}{\rho \left( \frac{\partial e}{\partial p} \right)_\rho} \quad 2.1.9$$

while on the line  $\Gamma_g^o$  whose slope satisfies

$$\frac{dx}{dt} = u \quad 2.1.10$$

we have the condition of compatibility

$$\frac{dp}{dt} - \frac{c^2}{g_o} \frac{d\rho}{dt} = - \frac{q_w}{\rho \left( \frac{\partial e}{\partial p} \right)_\rho} \quad 2.1.11$$

We will refer to  $\Gamma_g^+$  and  $\Gamma_g^-$  as the acoustic characteristics and  $\Gamma_g^o$  will be referred to as the gas-material characteristic.

## 2.2 Balance Equations for Solid Propellant

When the propellant is represented as a continuum, it is taken to be one-dimensional, unsteady and isothermal. Accordingly, we require only the balances of mass and of momentum. We use  $\rho_p$ ,  $u_p$  and  $\sigma$  to represent the density, velocity and pressure in the propellant. The balance of momentum also incorporates the influence of friction due to the contact of the propellant with the tube wall. We have

### Balance of Mass

$$\frac{\partial \rho_p}{\partial t} + \frac{\partial}{\partial x} \rho_p u_p = 0 \quad 2.2.1$$

### Balance of Momentum

$$\frac{\partial}{\partial t} \rho_p u_p + \frac{\partial}{\partial x} [\rho_p u_p^2 + g_o \sigma] = f_w \quad 2.2.2$$

The pressure is not assumed to be an integrable function of density since the stress response of the propellant is expected to be path dependent in general. We anticipate the discussion of section 2.4.2 by noting that we take the pressure and density to be related by

$$\frac{\partial \sigma}{\partial t} + u_p \frac{\partial \sigma}{\partial x} = \frac{a^2}{g_o} \left[ \frac{\partial \rho_p}{\partial t} + u_p \frac{\partial \rho_p}{\partial x} \right] \quad 2.2.3$$

where  $a$  is the rate of propagation of small disturbances and is, in general, dependent on both density and rate of change of density.

The procedure summarized in the previous section may be applied to equations 2.2.1, 2.2.2 and 2.2.3 to yield the following characteristic lines and conditions of compatibility. On  $\Gamma_p^\pm$  defined by

$$\frac{dx}{dt} = u \pm a \quad 2.2.4$$

we have the conditions

$$\frac{d\sigma}{dt} \pm \rho_p \frac{a}{g_o} \frac{du_p}{dt} = \pm a f_w \quad 2.2.5$$

while on  $\Gamma_p^o$  defined by

$$\frac{dx}{dt} = u_p \quad 2.2.6$$

we have

$$\frac{d\sigma}{dt} = \frac{a^2}{g_o} \frac{d\rho_p}{dt} \quad 2.2.7$$

Equation 2.2.7 is, of course, just a restatement of equation 2.2.3.

### 2.3 Motion of the Projectile

The projectile is treated as a rigid body whose motion is resisted by the pressure of shocked air ahead of it and by friction between its ob-  
turator band and the tube wall. The resistive terms are described in section 2.4.5; here we simply represent the total resistive force by  $F$ . Using  $X_p$  to denote the position of the projectile at any time,  $M_p$  to denote its mass,  $A_b$  to denote the bore area of the tube and  $\sigma(X_p)$  to denote the pressure at the interface between the solid propellant and the projectile base, the equation of motion of the projectile takes the simple form

$$M_p \ddot{X}_p = g_o [A_b \sigma(X_p) - F] \quad 2.3.1$$

where a dot is used to denote a total derivative with respect to time.

In the preceding section we described the analysis of the propellant viewed as a continuum. If its mechanical response is not of interest it may be viewed as a rigid body and its motion incorporated with that of the projectile. Let the position of the regressing propellant surface be denoted by  $x_p$ , relative to the same origin as  $X_p$ ; let the instantaneous mass of the propellant be  $m_p$  and denote by  $r$  the rate of regression relative to the unreacted propellant whose velocity is equal to that of the projectile, namely  $\dot{X}_p$ . Evidently

$$r = \dot{x}_p - \dot{X}_p \quad 2.3.2$$

Moreover, letting  $\rho_{p_o}$  be the constant value of propellant density in the case when it is viewed as a rigid body, we clearly have

$$\dot{m}_p = - A_b \rho_{p_o} r \quad 2.3.3$$



If  $\sigma(x_p)$  is the pressure on the unreacted side of the regressing surface, it follows that the equation of motion of the propellant and the projectile, viewed as a single rigid body, is just

$$(M_p + m_p) \ddot{X}_p = g_o [A_b \sigma(x_p) - F] \quad 2.3.4$$

Equation 2.3.4 can be deduced either from limiting arguments in which  $x_p$  is approached from the unreacted side or by considering a balance of momentum for a control volume which instantaneously envelopes the projectile and unreacted propellant. In the latter case one has

$$\frac{d}{dt} [\dot{X}_p (M_p + m_p)] = g_o [A_b \sigma(x_p) - F] - A_b \rho_p r \dot{X}_p$$

Then the substitution of 2.3.3 into this result yields 2.3.4.

## 2.4 Constitutive Laws

We use the term constitutive law in a broad sense here to denote not only the equations of state for the gas and the solid propellant but also the equations governing heat loss, friction and measured rates of burning.

### 2.4.1 Equation of State of Gas

The gas is assumed to obey a covolume of state. Thus we have

$$e = c_v T = \frac{p(1 - bp)}{(\gamma - 1)\rho} \quad 2.4.1$$

where  $c_v$  is the specific heat at constant volume,  $b$  is the covolume,  $\gamma$  is the ratio of specific heats, and we have used  $T$  to denote the temperature. If  $R$  is the universal gas constant and  $M$  is the molecular weight of the gas we have  $c_v = R/M/(\gamma - 1)$ . Moreover, from 2.4.1, we have the partial derivative

$$\left( \frac{\partial e}{\partial p} \right)_\rho = \frac{1 - bp}{\rho(\gamma - 1)} \quad 2.4.2$$

as required by equations 2.1.9 and 2.1.11. Finally, the isentropic sound speed follows as

$$c^2 = \frac{\gamma g_o p}{\rho(1 - bp)} \quad 2.4.3$$

### 2.4.2 Equation of State of Solid Propellant

From our formulation of the equations of motion of the solid propellant viewed as a continuum, it is evident that we anticipate finite strains. As reflected by equation 2.2.3, we embed the equation of state into the functional dependence of the rate of propagation of small disturbances on density and the rate of change of density. The general constitutive model for the response of the propellant may be thought of as viscoplastic since 2.2.3 expresses a differential relationship between stress and strain. Moreover, the relationship need not be reversible. However, hereditary behavior is not

considered here. Viscoelastic or hereditary behavior requires that derivatives of different orders be applied to stress and strain in the constitutive relationship. For example, strain-rate may be proportional to stress so that elongation continues while the stress is held constant. The use of 2.2.3 implies that density, or strain, will change only under the action of a change in stress. Since propellants do exhibit viscoelastic properties at moderate rates of strain and at ambient temperature, the use of 2.2.3 implies that the characteristic time associated with the application of the load must be short in comparison with the internal relaxation times.

The equation for the rate of propagation of small disturbances has been assumed here to take a particularly simple functional form, namely

$$a = \begin{cases} a_1 \rho_p / \rho_{p_0} & , \text{ loading} \\ a_2 & , \text{ unloading or reloading} \end{cases} \quad 2.4.4$$

Here  $\rho_{p_0}$  is the density at ambient conditions and  $a_1$  is the corresponding rate of propagation of a compressive wave. If  $E$  is the modulus of compression of a laterally confined sample of propellant subjected to small loads, then  $a_1 = \sqrt{g_0 E / \rho_{p_0}}$ . To be physically meaningful, the unloading or reloading wave speed  $a_2$  should exceed the loading wave speed for all values of  $\rho_p$ . In fact 2.4.4 has been encoded so that if  $a_2 = 0$ , a reversible law is used based on the loading branch of 2.4.4.

Unloading, reloading and loading are defined by reference to the rate of compression  $\dot{\rho}_p = \partial \rho_p / \partial t + u_p \partial \rho_p / \partial x$  and the nominal loading curve defined by

$$\sigma_*(\rho_p) = \frac{a_1^2 \rho_{p_0}}{3g_0} \left[ \left( \frac{\rho_p}{\rho_{p_0}} \right)^3 - 1 \right] \quad 2.4.5$$

The propellant is unloading if  $\dot{\rho}_p < 0$ ; loading if  $\dot{\rho}_p > 0$  and  $\sigma = \sigma_*$ ; reloading if  $\dot{\rho}_p > 0$  and  $\sigma < \sigma_*$ .

Expressed in the form 2.4.5, the nominal loading curve is seen to be a special case of that proposed by Murnaghan<sup>12</sup> in connection with the finite deformation of solids; in the general case the value 3 is replaced by  $k$  in both the exponent and the pre-multiplying group of 2.4.5. The functional dependence of  $a$  on  $\rho_p$  and  $\dot{\rho}_p$  has been encoded in a modular fashion so that modifications may be made easily when the availability of data so warrants.

### 2.4.3 Heat Loss to the Tube

We use a very simple model for the heat loss to the tube, it being understood that our interest in heat loss is confined to its ballistic consequences, particularly the degradation of muzzle velocity. The tube wall is treated as though its temperature remained constant at the initial value  $T_w$ . The heat loss is determined by means of an empirical correlation for the film or heat transfer coefficient based on fully

<sup>12</sup> Murnaghan, F. D. "Finite Deformation of an Elastic Solid."  
Dover, New York 1967

developed turbulent flow in a pipe. Both the assumption of constant wall temperature and that relating to the heat transfer coefficient are very crude; however, they involve errors which tend to compensate one another. The wall temperature will, of course, increase substantially during the interior ballistic cycle. A consequence of this increase will be a reduction in heat transfer which is proportional to the difference between gas temperature and wall temperature. On the other hand, the boundary layer is expected to be very much thinner, due to the short time available for its development, than is represented by a correlation based on a fully developed flow, and the film coefficient correspondingly greater. Thus the assumption of constant wall temperature implies an overestimate of heat loss which is compensated by the underestimate based on a film coefficient for fully developed flow.

The film coefficient is represented in the empirical form<sup>13</sup>

$$h = \frac{\kappa}{D} [0.023 \text{Re}_D^{4/5} \text{Pr}^{2/5}] \quad 2.4.6$$

where  $h$  is the film coefficient,  $\kappa$  is the thermal conductivity of the gas,  $D$  is the diameter of the tube,  $\text{Re}_D = \rho |u| D / \mu$  is the Reynolds number based on  $D$ ,  $\text{Pr} = c_p \mu / \kappa$  is the Prandtl number of the gas and  $\mu$  is the viscosity of the gas.

Then the heat loss per unit volume of gas is seen to be related to  $h$  according to

$$q_w = \frac{4}{D} (T - T_w) h \quad 2.4.7$$

Using 2.4.6 and eliminating  $\kappa$  in favor of  $h$  and  $\mu$  we have

$$q_w = Q_w \frac{c_p \mu \text{Pr}^{-3/5}}{D^2} \text{Re}_D^{4/5} (T - T_w) \quad 2.4.8$$

where  $Q_w = 0.092$  according to 2.4.6 and 2.4.7. The precise value of  $Q_w$  is, however, at the discretion of the user, to facilitate ballistic matching.

#### 2.4.4. Friction Between Propellant and Tube

The solid propellant is not expected to be able to sustain the axial stresses induced by the base pressure without the support of radial confinement. Indeed, the strength of current formulations is such that the radial component of stress will be quite close in value to the axial stress at any point. Such hydrodynamic behavior is typical of solids stressed significantly beyond the material yield point. As a consequence, mechanical interaction between the solid propellant and the tube wall is expected to be important and, in particular, the resistance due to friction may be of importance in many cases.

<sup>13</sup> Holman, J. P. "Heat Transfer"

McGraw-Hill, New York 1968

In order to assess the ballistic losses associated with friction between the solid propellant and the tube we provide two simple models. The first model takes the frictional resistance  $f_w$  to be proportional to the local value of the pressure in the form

$$f_w = - \frac{4}{D} \mu_w (u_p) \sigma \operatorname{Sgn}(u_p) \quad 2.4.9$$

where  $\mu_w$  is a velocity dependent coefficient of friction and  $\operatorname{Sgn}$  denotes the sign function.

Alternatively, if a gas film of viscosity  $\mu_f$  and thickness  $\delta_f$  can be interposed between the propellant and the tube wall, the resistance  $f_w$  becomes<sup>10</sup>

$$f_w = - \frac{4}{D} \frac{\mu_f}{\delta_f} u_p \quad 2.4.10$$

and is proportional to velocity rather than pressure.

#### 2.4.5 Resistance to Projectile Motion

The resistance to projectile motion is considered to stem from two sources. We write

$$F = A_b (p_a + p_{band}) \quad 2.4.11$$

where  $p_a$  is the pressure exerted by the air in front of the projectile and  $p_{band}$  reflects the resistance due to the obturator or rotating band and is also expressed as a pressure. The resistance due to the air in front of the projectile is determined from the pressure behind a shock whose strength is such that the compressed gas has a velocity equal to that of the projectile at any instant. Then if the unshocked air is taken to be at rest with pressure  $p_o$  and speed of sound  $c_o$ , it follows that  $p_a$  is given by

$$p_a = p_o \left\{ (1 + \mu^2) \left[ \frac{\dot{x}_p^2 + [\dot{x}_p^2 + 4(1 - \mu^2)^2 c_o^2]^{1/2}}{2(1 - \mu^2) c_o} \right]^2 - \mu^2 \right\} \quad 2.4.12$$

where  $\mu^2 = (\gamma_a - 1)/(\gamma_a + 1)$  and  $\gamma_a$  is the ratio of specific heats of air.

The resistance due to the obturator may be given in one of two forms. Either it is prespecified as a tabular function of projectile travel or it follows from an estimate of the normal force between the obturator and the tube wall as follows.

Let  $\sigma_z$  and  $\sigma_r$  represent the axial and radial components of stress in the projectile and, following the usual convention, let them be positive in tension. Let the length of the obturator,  $l_b$  be sufficiently small that we can typify adequately the state of stress by the values at its midpoint. Let  $M_b$  be the projectile mass which is supported by a section through the

midpoint of the obturator and let  $\mu_{wb}$  be the coefficient of friction between the tube and the obturator. A balance of axial forces yields

$$\frac{\pi D^2}{4} \sigma_z - \frac{\pi D \ell_b}{2} \mu_{wb} \sigma_r + \frac{M_b}{g_o} \ddot{X}_p = 0 \quad 2.4.13$$

On the other hand, taking the tube to be sufficiently stiff that radial strains do not occur, and supposing the behavior of the projectile to be elastic, the axial and radial strains are related according to<sup>14</sup>

$$\sigma_r = \frac{\nu}{1 - \nu} \sigma_z \quad 2.4.14$$

where  $\nu$  is Poisson's ratio. Substitution of 2.4.14 into 2.4.13 yields the value of  $\sigma_r$  whereupon the resistive pressure due to the obturator takes the form

$$p_{band} = \frac{4\mu_{wb} \ell_b}{g_o \pi D} \frac{M_b \ddot{X}_p}{\frac{1 - \nu}{\nu} \frac{D^2}{4} - \frac{\mu \ell_b D}{2}} \quad 2.4.15$$

Equation 2.4.15 is appropriate to the case when there is no initial interference between the band and the tube. If such an interference does exist, we assume it to be characterized by an initial shot start pressure  $p_s$ . Then the value of  $p_{band}$  given by 2.4.15 is augmented by the quantity  $\mu_{wb}(\dot{X}_p)p_s/\mu_{wb}(0)$  in which the coefficient of friction is assumed to depend on velocity.

#### 2.4.6 Propellant Burn Rate (Measured)

It is assumed that if data are available to describe the burn rate of the propellant, the functional relationship has the usual form

$$r = B_1 + B_2 p^n \quad 2.4.16$$

in which  $B_1$ ,  $B_2$  and  $n$  are parameters which may take different values for successive segments of the propellant. The value of  $p$  is assumed here to pertain to the reacted material. Burn rates of the form given by equation 2.4.16 are only well posed physically when the reactants have a subsonic velocity relative to the regressing surface. Further discussion of this point is contained in Appendix A.

#### 2.5 Boundary Conditions

The boundary conditions are of several types and are discussed in several subsections. Conditions at the breech, which may be either closed or open, are discussed in section 2.5.1. In section 2.5.2 we consider first the conditions at the base of the projectile when the propellant has not burned out. Subsequently we consider the change in conditions

---

<sup>14</sup>Fung, Y. C. "Foundations of Solid Mechanics" Prentice-Hall, 1965

at burnout. Finally, we note the conditions which apply following the exit of the projectile, if blowdown of the tube is of interest. The boundary conditions then apply to the open muzzle and the discussion is similar to that of section 2.5.1. The conditions at the regressing interface between the reacted and unreacted propellant are discussed in section 2.5.3. This section also addresses the analysis of the ideal rates of burning.

### 2.5.1 Breech (Closed or Open)

The boundary conditions at the breech are taken to apply only to the gas as the solid propellant is assumed never to approach the breech. When the breech is closed there is but one condition to consider, namely the vanishing of the velocity of the gas. If we take the breech as the origin of the axial coordinate  $x$  we therefore require

$$u(0,t) = 0, \text{ all } t \quad 2.5.1$$

When the breech is open it is assumed to be connected to the exterior via a nozzle whose throat area is  $A_*$  and whose discharge coefficient is  $C_{DB}$ . We assume  $C_{DB}A_* \leq A_b$ . The external pressure is assumed to be negligible by comparison with the stagnation pressure at the boundary. Therefore, we do not consider the possibility of a totally subsonic efflux and the external venting area is of no concern.

The critical mass flow rate corresponding to sonic conditions at the throat may be approximated with sufficient accuracy by the equation<sup>3</sup>

$$\dot{m}_* = C_{DB}A_*p_{STAG} \sqrt{\frac{\gamma g_o^M}{RT_{STAG}} \left(\frac{2}{\gamma+1}\right)^{\frac{\gamma+1}{\gamma-1}}} \{1 - 0.224\gamma + 0.104\gamma^2\} \quad 2.5.2$$

where  $\gamma = (bp_{STAG}^M)/(RT_{STAG})$ . This result is strictly true only for the case  $\gamma = 1.25$ , but we regard the evaluation of the covolume correction for other values of  $\gamma$  to be unnecessary in view of the smallness of the correction. The stagnation temperature and pressure are related to the boundary values according to

$$p_{STAG} = p \left(\frac{T_{STAG}}{T}\right)^{\frac{\gamma}{\gamma-1}} \quad 2.5.3$$

and

$$T_{STAG} = T + \frac{u^2/2g_o + b(p - p_{STAG})}{c_p} \quad 2.5.4$$

where the unsubscripted quantities represent the boundary values.

Because the flow is unsteady, it is not necessarily the case that the Mach number  $M = |u|/c$  is limited to values less than or equal to unity. However, we suppose that quasi-steady arguments do apply to the gas between the boundary and the exterior. Then the rules governing the discharge may be stated as either  $M > 1$  and  $\dot{m} = \rho A_b |u| < \dot{m}_*$  or else  $\dot{m} = \dot{m}_*$ . As noted above, the case  $M < 1$  and  $\dot{m} < \dot{m}_*$  is not of interest since the external pressure is assumed too low to allow a totally subsonic discharge. Since discharge is expected to commence with a Mach number less than or equal to unity, a transition to supersonic venting requires that a sufficiently strong compression wave impinge upon the boundary, the strength increasing with the excess of  $A_b$  over  $C_{DB} A_*$ . In principle, if  $A_b > C_{DB} A_*$ , a shock is required.

A different situation arises in the case of venting through the muzzle after the projectile has exited. Then the flow may initially be supersonic as we comment further in the next section.

### 2.5.2 Projectile Base and Muzzle Following Projectile Exit

Considering the conditions which apply at the base of the projectile it is clear that prior to burnout, when the propellant is represented as a continuum, we have

$$u_p(X_p, t) = \dot{X}_p \quad 2.5.5$$

and, following burnout of the propellant, we have the corresponding condition on the gas, namely

$$u(X_p, t) = \dot{X}_p \quad 2.5.6$$

The transition from 2.5.5 to 2.5.6 occurs at the instant of burnout. Because the sudden application of 2.5.6 to the gas may represent an instantaneous increase in velocity comparable in magnitude to the speed of sound, it is accompanied by a rather large drop in pressure. This point is discussed further in chapter 3.0 when we consider the numerical determination of the boundary values.

In some instances it will be of interest to continue the solution following the exit of the projectile from the muzzle. The histories of muzzle pressure and temperature are of interest since they are connected with problems of blast and flash. In almost all cases of interest the flow will be supersonic at exit, provided that burnout has occurred. The discharge at the muzzle is presumed to be characterized by a discharge coefficient  $C_{DMUZ}$ . Critical flow is determined by equation 2.5.2 with  $C_{DMUZ}$  in place of  $C_{DB}$  and  $A_b$  in place of  $A_*$ . If  $C_{DMUZ} = 1$ , and the discharge is initially supersonic, it will remain so until the Mach number reaches the value unity whereupon 2.5.2 will govern the discharge and the Mach number will remain equal to one. As with the treatment of the breech, subsonic venting is not considered. If the discharge is initially supersonic but  $C_{DMUZ} < 1$ , an abrupt transition will occur when the Mach number

decreases to a point at which the flow cannot be passed through the effective throat area  $A_b C_{DMUZ}$ . Physically, the occurrence of choking will result in the rearward propagation of a shock or strong compression wave to decelerate the supersonic flow. The magnitude of the jump will be proportional to the degree of departure of  $C_{DMUZ}$  from unity.

On the other hand, if the discharge is initially subsonic, choking will occur at the instant of expulsion of the projectile and a rarefaction will be propagated rearward to accelerate the flow.

### 2.5.3 Gas/Propellant Interface

The layer in which the unreacted propellant is thermally stimulated, decomposes, and releases its energy of chemical bonding, is assumed to be sufficiently thin that it may be represented as a surface of discontinuity. Further discussion of this assumption is given in Appendix A. Using the previously established nomenclature, we may express the principles of conservation of mass, momentum and energy for the propellant transported across the surface of discontinuity in the following forms.<sup>8</sup>

$$\rho(u - \dot{x}_p) = -\rho_p r \quad 2.5.7$$

$$p + \frac{\rho}{g_o} (u - \dot{x}_p)^2 = \sigma + \frac{\rho_p}{g_o} r^2 \quad 2.5.8$$

$$e + \frac{p}{\rho} + \frac{1}{2g_o} (u - \dot{x}_p)^2 = e_p + \frac{\sigma}{\rho_p} + \frac{r^2}{2g_o} \quad 2.5.9$$

Here  $e_p$  may be understood to mean the chemical energy released following decomposition of the propellant. We also note

$$\dot{x}_p = u_p + r \quad 2.5.10$$

which is identical with 2.3.2 when the propellant is taken to be rigid. Of course, if the propellant is not burning as may be required in certain ideal cases, 2.5.7, 2.5.8 and 2.5.9 are replaced by the conditions of continuity of pressure and velocity.

Because the regressing surface is presumed to be a deflagration wave, its velocity of advance relative to the unreacted propellant must always be subsonic<sup>8</sup>. Accordingly, when the propellant is treated as a continuum, it follows that the characteristic lines  $\Gamma_p^o$  and  $\Gamma_p^-$  both intercept the regressing surface and impose conditions of compatibility between the boundary values on the unreacted side and values in the interior of the propellant. Further discussion of the application of this observation is given in chapter 3.0. Because of the two conditions of compatibility, the three quantities  $\sigma$ ,  $u_p$  and  $\rho_p$  are not all independent of the state of the interior. We may regard  $\sigma$  as the independent member which, when specified, yields unique values of  $u_p$  and  $\rho_p$  which are compatible with the interior state of the propellant. On the other hand, if the propellant is treated as rigid we have  $\rho_p = \rho_{p0}$ , a constant, and  $u_p = \dot{x}_p$  which is, in turn, a function of  $\sigma$ . Accordingly, we may consider  $\sigma$  as the only unknown quantity pertaining to the state of the unreacted



propellant and that  $u_p$  and  $\rho_p$  are either given or follow from the conditions of compatibility. From this perspective therefore, we have five independent quantities to be determined at the interface, namely  $p$ ,  $\rho$ ,  $u$ ,  $\sigma$  and  $r$ . The internal energy  $e$  is, of course, given as a function of  $p$  and  $\rho$  and  $\dot{x}_p$  is related to  $u_p$  and  $r$  via equation 2.5.10. Thus we have three conditions, equations 2.5.7, 2.5.8 and 2.5.9 to determine five quantities. Clearly, we need two additional independent relations.

When the reactants are subsonic, as viewed from the regressing surface, it follows that characteristics of the  $\Gamma_g^+$  family intercept the boundary and impose a condition of compatibility with the state of the interior of the gas. Thus, whenever the reactants are subsonic there remains just one additional condition which may be applied to the boundary values independently of the principles of conservation of mass, momentum and energy and of the requirement that the state of each side of the interface be compatible with the contiguous substance.

In the event that the reactants are subsonic we consider that the remaining boundary condition may be any one of the following.

(a) Measured Burn Rate (With Subsonic Reactants)

When measurements of the burn rate as a function of the pressure of the fully reacted gas are available, the burning rate law, in the form 2.4.16 completes the determination of the boundary values.

(b) Ideal Burning of Langweiler (With Subsonic Reactants)

According to the ideal traveling charge model of Langweiler<sup>4</sup> the reactants are to be brought to rest once reaction is complete. The condition  $u = 0$  serves to complete the determination of the boundary values.

(c) Prespecified Value of Pressure on Unreacted Side or of Acceleration of Projectile (With Subsonic Reactants)

It is easy to see that if the ideal combustion of Langweiler commences from some initially quiescent state then the pressure of the reactants remains constant in time and uniform over the length of the gas column. However, the pressure on the unreacted side of the interface exceeds that in the gas by an amount which increases with the velocity of the projectile, the excess being due to the momentum jump at the interface and representing the contribution of momentum flux to the total thrust. From this point of view, therefore, the Langweiler concept departs from the traditional concept of an ideal interior ballistic cycle. The continual increase in the pressure of the unreacted propellant implies that the tube must be able to support a value which is higher than the average value used to propel the projectile. In addition, while the pressure is increasing, the total mass of the propelled

body, namely the projectile plus the unreacted propellant, is diminishing due to consumption of the propellant. Thus the acceleration of the projectile increases even faster than the pressure. In some cases the maximum allowable acceleration of the projectile may be constrained by structural considerations.

A direct statement of the traditional concept of a constant base pressure gun may be expressed by requiring that the pressure on the unreacted side of the interface be equal to some predetermined value. Such a condition then allows the determination of all the boundary values. If, alternatively, the structural limitations of the projectile are of concern, it may be desired to hold the acceleration equal to some limiting value. When the propellant is treated as a rigid body, equation 2.3.1 enables the direct translation of the condition on acceleration into a condition on the instantaneous value of the pressure on the unreacted side of the interface whereupon all the boundary values may be determined.

When the propellant is treated as a continuum it does not necessarily follow that the maximum pressure will occur at the interface since transient phenomena govern the distribution throughout the unreacted propellant. The pressure on the unreacted side may nevertheless be prespecified and, once given, will allow the determination of all the boundary values.

Similarly, the use of 2.3.1, in the case when the propellant is treated as a continuum, enables an instantaneous value of the pressure on the unreacted side to be determined. However, it no longer follows that the acceleration of the projectile will be equal to the desired value.

Therefore, while we have encoded the possibility of an ideal combustion which yields either a predetermined value of pressure on the unreacted side or an equivalent value based on equation 2.3.1 and a prespecified value of acceleration, it should be understood that only when the propellant is treated as rigid will the desired ballistic consequence--control of maximum pressure or of projectile acceleration--be attained precisely. Transient phenomena, which will be determined by a continuum representation, may defeat the intended objective of the ideal law.

(d) Predetermined Mach Number of Reactants (Subsonic)

A final condition which we have considered is that the Mach number of the reactants be equal to some predetermined value. Given such a value, less than unity, all the boundary values may be found.

The preceding discussion has addressed several different conditions which may be applied, singly, to complete the specification of the boundary values when the reactants are subsonic. It may be of interest, as already mentioned in chapter 1.0, to consider an interior ballistic cycle in which the combustion is limited by more than one of the foregoing, the most limiting being considered at each stage of the cycle, with branching from one to another as the cycle unfolds. Further discussion of the manner in which the branching is conducted is given in chapter 3.0.

To conclude the present discussion we comment on the conditions to be considered when the reactants are supersonic as viewed from the regressing interface. As discussed in Appendix A, there are strong arguments to suggest that a steady combustion process with supersonic reactants cannot occur or, if it does occur, is completely unstable. Possibly, if the flame is sufficiently thick and sufficiently unsteady, supersonic reactants could result. In any case, it may be of interest to ascertain whether there is indeed any ballistic benefit to be gained from a combustion process with supersonic reactants. For this purpose we have encoded conditions which do admit the possibility of a so-called strong deflagration wave.

When the reactants are supersonic it is no longer the case that they have to be compatible with the flow in the interior of the gas. They influence, but are not influenced by the contiguous fluid as signals do not propagate from the interior to the boundary once the flow at the boundary becomes supersonic. In contrast to the preceding discussion of the subsonic case, therefore, we require two independent conditions to determine all the boundary values. We consider the two following combinations.

(a) Ideal Burning of Langweiler (With Supersonic Reactants)

When the reactants are subsonic and the initial state is quiescent and uniform, the ideal combustion of Langweiler involves the single requirement  $u = 0$  whereupon the condition of compatibility on  $\Gamma_g^+$  yields  $p = p_{ST}$  where  $p_{ST}$  is the initial pressure of the quiescent gas column. When the reactants are supersonic, members of  $\Gamma_g^+$  no longer intercept the regressing surface and the condition  $u = 0$  does not imply  $p = p_{ST}$  necessarily. However we may require  $p = p_{ST}$  as an independent condition on the supersonic reactants. Thus in the supersonic case, the ideal burning of Langweiler is described by two conditions  $u = 0$  and  $p = p_{ST}$  whereupon all the boundary values may be determined and, moreover, the gas column remains quiescent.

(b) Prespecified Value of Pressure on Unreacted Side or of Acceleration of Projectile (With Supersonic Reactants)

The previous discussion of this case subject to subsonic reactants remains unchanged insofar as the

relationship between the pressure and the acceleration limitations is concerned. Therefore we predicate our subsequent discussion on the assumption that the pressure on the unreacted side is predetermined. To complete the determination of the boundary values we require an additional relationship which replaces the condition of compatibility on  $\Gamma_g^+$ . We assume that this condition is furnished as a predetermined value of the Mach number  $M \geq 1$ . It should be noted therefore that this case does not require the regularity of the gas phase properties which results from the continuation of the Langweiler combustion into the supersonic regime.

## 2.6 Initial Conditions

The initial values for these quantities governed by ordinary differential equations are the intuitively natural set. The projectile is initially at rest, its position is known, and the propellant has some predetermined initial mass. In cases when parametric studies are to be performed, it may be desirable to compute these initial values so as to satisfy certain system constraints. In many cases of interest it is desirable to assume that the ignition charge is of sufficient energy as to elevate the chamber pressure to several hundred MPa, the initial pressure being equal to the maximum pressure. In such cases, the contribution of the igniter to the total mass and energy of the propelling charge may be significant and must be accounted for in a parametric study based, say, on a constant ratio of charge mass to projectile mass. We therefore note some relationships among the charge parameters which are useful in describing the initial conditions according to various alternative schemes. The schemes admitted by the code are described in Appendix B.

Let the initial volume of the gas be  $V = A_b x_{b0}$  where  $x_{b0}$  is the length of the column at the initial instant. Let  $p_{ST}$  be the initial pressure. Let  $m_{g0}$  and  $m_{p0}$  be the initial masses of the gas and the solid propellant and let  $W$  be the charge to projectile mass ratio. If we assume that the ignition gas is of the same composition as the propellant and that it has been fully decomposed without the performance of external work or heat loss, its internal energy will be the energy of bonding  $e_p$ . Thus we have

$$m_{g0} = V\rho = \frac{V}{(\gamma - 1)\frac{e_p}{p_{ST}} + b} \quad 2.6.1$$

Therefore the following relationship holds between the mass of the projectile and the total mass of the propelling charge

$$WM_p = m_{p0} + \frac{V}{(\gamma - 1)\frac{e_p}{p_{ST}} + b} \quad 2.6.2$$

When an ideal burn rate is used such that the regression rate is zero at the initial instant, the initial acceleration  $a$  is given by

$$a = \frac{A_b g_o p_{ST}}{M_p + m_{p_o}} \quad 2.6.3$$

provided that the propellant is viewed as rigid. Substitution of 2.6.3 into 2.6.2 yields a formula which relates the initial pressure to given values of  $a$  and  $W$ , namely

$$p_{ST} = -\frac{1}{2b} \left[ K_1 - \sqrt{K_1^2 + K_2} \right] \quad 2.6.4$$

where

$$K_1 = \frac{Va}{A_b g_o} + (\gamma - 1)e_p - \frac{ab}{A_b g_o} (1 + W)M_p$$

$$K_2 = 4 \frac{(\gamma - 1)ab}{A_b g_o} e_p M(1 + W)$$

It should be kept in mind that 2.6.1 and 2.6.4 which depend on the assumption that the initial energy of the gas is equal to  $e_p$  are only strictly true when the regression rate is initially zero, as will be clear from the subsequent discussion of the continuum variables.

In principle, the initial conditions for the continuum variables should express the state of the combustion chamber and the solid propellant directly after loading into the gun. That is to say, the gas should be air at ambient temperature and pressure, the propellant should be at ambient pressure, and both should be at rest. The model should then reflect the influence of the igniter products which simultaneously pressurize the chamber and provide a thermal stimulus to the propellant. However, the present model does not reflect explicitly the influence of the igniter. The characteristics of the igniter are taken to be embedded directly into the initial conditions.

In those cases in which the propellant is taken to have a non-zero burning rate at the initial instant, either due to a prespecified pressure dependent burning rate or as a consequence of satisfying the predetermined condition on the pressure on the unreacted side of the interface, the initial velocity distribution in the gas is taken to vary linearly from the value zero in the breech to the value determined on the fully reacted side of the interface. This provision eliminates the necessity for dealing with a non-analytic initial condition. The pressure and density are, however, uniform and are taken to be equal to the boundary values on the reacted side of the interface.

The solid propellant is always taken to be at rest. However, when wall friction is considered we assume that the initial distribution of pressure is such as to satisfy the condition of mechanical equilibrium.

Then if  $\sigma$  is the value at the unreacted side of the interface, the pressure within the propellant is given by the distribution

$$\sigma(x) = \sigma \exp \left\{ -\frac{4\mu}{D}(x - x_p) \right\} \quad 2.6.5$$

where  $\mu$  is the coefficient of friction corresponding to  $u_p = 0$ . This initial distribution reflects the possibility of lockup of the charge when its aspect ratio is sufficiently large.

The initial length of the solid propellant depends on the distribution of pressure. Evidently we have the relation

$$m_{p_0} = A_b \int_{x_p}^{X_p} \rho_p(x) dx \quad 2.6.6$$

where  $\rho_p$  is assumed to be related to  $\sigma$  according to the nominal loading curve 2.4.5. The length is determined iteratively using a midpoint search so that more complicated constitutive data can be accommodated without changing the method.

### 3.0 METHOD OF SOLUTION

Having summarized the governing equations for the model, we turn now to the method of solution. The method of solution may be summarized as follows. The physical domain occupied instantaneously by the gas is mapped onto a unit line to yield a stationary equally spaced mesh for the purpose of obtaining a finite difference solution of the balance equations. The same is true of the domain occupied by the solid propellant when it is represented as a continuum. In each case the solution is advanced in time by means of a two level predictor/corrector algorithm which uses the physical balance equations at the interior mesh points and the characteristic forms at the boundaries.

The mesh allocation algorithm is described in section 3.1 and the computational form of the equations is described in 3.2. The procedures for interior and boundary mesh points are described in sections 3.3 and 3.4 respectively. The chapter concludes with a discussion of special considerations, such as the treatment at burnout, in section 3.5.

#### 3.1 Mesh Allocation

The mesh is allocated dynamically, the number of mesh points varying from time to time in accordance with the following algorithm. The user specifies two parameters which we refer to by their Fortran names, see Appendix B, namely DXMIN, the minimum allowable mesh spacing in the physical plane, and MAXDIM, the maximum allowable total number of mesh points to be used in the calculation. Then a total of NDIM mesh points is allocated to the representation of the gas and a total of NDIM2 - NDIM mesh points is allocated for the representation of the propellant, if it is treated as a continuum. The allocation is subject to the following constraints.

$$\frac{x_p}{NDIM - 1} \geq DXMIN \quad 3.1.1$$

$$\frac{x_p - x_p}{NDIM2 - NDIM1} \geq DXMIN \quad 3.1.2$$

where NDIM1 = NDIM + 1, and the total number NDIM2 is required to satisfy

$$NDIM2 \leq MAXDIM \quad 3.1.3$$

If the propellant is not treated as a continuum, 3.1.2 is not used and 3.1.3 is replaced by NDIM ≤ MAXDIM. In addition, it is required that each continuum region be sufficiently large that 3.1.1 and 3.1.2 will admit at least three mesh points.

When the propellant becomes so short, as a consequence of burning, that 3.1.2 will no longer admit three or more mesh points for its representation, the code automatically resets an internal switch and the calculation is concluded with the propellant treated according to a lumped parameter formulation. Further discussion of this point is given in section 3.5.

The constraints 3.1.1 and 3.1.2 are used first to establish a total number of mesh points to yield a resolution DXMIN. If 3.1.3 is satisfied, the values NDIM, NDIM2 given by 3.1.1 and 3.1.2 are used to represent the solution. If 3.1.3 is violated, the total number MAXDIM is allocated on a pro rata basis in accordance with the numbers proposed by 3.1.1 and 3.1.2.

The mesh allocation algorithm is exercised at the beginning of each integration step. From time to time the total number of mesh points allocated to a region may vary. It then becomes necessary to interpolate the existing arrays in order to create the new representation of the solution.

We use the cubic spline interpolation scheme of Walsh et al<sup>15</sup>, simplified to take advantage of the fact that the data are equally spaced. Let  $\phi(x)$  be the interpolating function for data  $y_j = y(x_j)$ ,  $j = 1, \dots, n$  and  $x_{j+1} - x_j = d$  where  $d$  is a constant. Let  $\mu_j = \phi''(x_j)$ , then we have the interpolation formula

$$\begin{aligned} \phi(x) = & \{(x - x_j)y_{j+1} + (x_{j+1} - x)y_j\}/d \\ & - (x - x_j)(x_{j+1} - x)\{(d + x_{j+1} - x)\mu_j + (d + x - x_j)\mu_{j+1}\}/6d \end{aligned} \quad 3.1.4$$

One may show that if we take  $S_1 = 1$  and put

$$S_j = 1 - 1/(16S_{j-1}) \quad 3.1.5$$

$$Z_j = \frac{3}{2d^2} (y_{j+1} + y_{j-1} - 2y_j) \quad 3.1.6$$

then, defining  $Z_2' = Z_2$  and putting

$$Z_j' = Z_j - \frac{Z_{j-1}'}{4S_{j-2}}, \quad j > 2 \quad 3.1.7$$

the values of  $\mu_j$  follow as  $\mu_1 = \mu_n = 0$  and

$$\mu_{n-1} = Z_{n-1}'/S_{n-2} \quad 3.1.8$$

.

$$\mu_j = (Z_j' - \frac{1}{4} \mu_{j+1})S_{j-1} \quad 3.1.9$$

---

<sup>15</sup>Walsh, J. L., Ahlberg, J. H. and Nilson, E. N., "Best Approximation Properties of the Spline Fit"

*J. Math. Mech.* 11, 225-234 1962



### 3.2 Transformed Equations

Taking the origin to be at the breech it follows that the gas may be mapped onto a unit line by the transformation

$$\zeta = x/x_p \quad 3.2.1$$

It follows that the balance equations must be transformed according to the rules

$$\frac{\partial}{\partial x} \rightarrow \frac{1}{x_p} \frac{\partial}{\partial \zeta} \quad 3.2.2$$

$$\frac{\partial}{\partial t} \rightarrow \frac{\partial}{\partial t} - \frac{\dot{\zeta} x_p}{x_p} \frac{\partial}{\partial \zeta} \quad 3.2.3$$

We also note that for arbitrary  $\psi$

$$\frac{1}{x_p} \frac{\partial}{\partial \zeta} [\psi(u - \eta)] = \frac{1}{x_p} \frac{\partial}{\partial \zeta} \psi u - \frac{\eta}{x_p} \frac{\partial \psi}{\partial \zeta} - \psi \frac{\dot{x}_p}{x_p} \quad 3.2.4$$

and where we have introduced  $\eta = \zeta \dot{x}_p$ .

We now introduce the dependent variables

$$G_1 = \rho x_p \quad 3.2.5$$

$$G_2 = G_1 u = \rho u x_p \quad 3.2.6$$

$$G_3 = G_1 (e + u^2/2g_0) = \rho x_p (e + u^2/2g_0) \quad 3.2.7$$

The transformed, or computational, form of the balance equations 2.1.1, 2.1.2 and 2.1.3 is then seen to be as follows.

$$\frac{\partial G_1}{\partial t} + \frac{\partial}{\partial \zeta} \left[ \frac{G_1}{x_p} (u - \eta) \right] = 0 \quad 3.2.8$$

$$\frac{\partial G_2}{\partial t} + \frac{\partial}{\partial \zeta} \left[ \frac{G_2}{x_p} (u - \eta) + g_0 p \right] = 0 \quad 3.2.9$$

$$\frac{\partial G_3}{\partial t} + \frac{\partial}{\partial \zeta} \left[ \frac{G_3}{x_p} (u - \eta) + p u \right] = -q_w x_p \quad 3.2.10$$

The balance equations for the solid propellant can be put into a form analogous to 3.2.8 and 3.2.9. However, because of the differential constitutive law 2.2.3, it is convenient to keep the total time derivative of  $\rho_p$  isolated. The computational form of the equations 2.2.1, 2.2.2 and 2.2.3 is as follows.

$$\frac{\partial \rho_p}{\partial t} + \frac{u_p - \eta_p}{X_p - x_p} \frac{\partial \rho_p}{\partial \zeta} + \frac{\rho_p}{X_p - x_p} \frac{\partial u_p}{\partial \zeta} = 0 \quad 3.2.11$$

$$\frac{\partial u_p}{\partial t} + \frac{u_p - \eta_p}{X_p - x_p} \frac{\partial u_p}{\partial \zeta} + \frac{g_o}{\rho_p (X_p - x_p)} \frac{\partial \sigma}{\partial \zeta} = \frac{f_w}{\rho_p} \quad 3.2.12$$

$$\frac{\partial \sigma}{\partial t} + \frac{u_p - \eta_p}{X_p - x_p} \frac{\partial \sigma}{\partial \zeta} = \frac{a^2}{g_o} \left\{ \frac{\partial \rho_p}{\partial t} + \frac{u_p - \eta_p}{X_p - x_p} \frac{\partial \rho_p}{\partial \zeta} \right\} \quad 3.2.13$$

where, by analogy with 3.2.1, we have  $\zeta = (x - x_p)/(X_p - x_p)$  and  $\eta_p = \dot{x}_p + \zeta(\dot{X}_p - \dot{x}_p)$ .

### 3.3 Integration at Interior Mesh Points

The balance equations for the gas phase are integrated at interior mesh points using the two-level predictor/corrector scheme of MacCormack<sup>16</sup>. Let  $\psi_j^n$  be understood to mean the value of  $\psi$  at the  $j$ -th mesh point and the  $n$ -th step of the integration. Then 3.2.8, 3.2.9, 3.2.10 are put into a finite difference form according to the following rules of discretization.

$$\frac{\partial \psi}{\partial t} \rightarrow \begin{cases} (\tilde{\psi}_j - \psi_j^n)/\Delta t & , \text{ predictor} \\ (\psi_j^{n+1} - 1/2(\tilde{\psi}_j + \psi_j^n))/(\Delta t/2) & , \text{ corrector} \end{cases} \quad 3.3.1$$

and

$$\frac{\partial \psi}{\partial \zeta} \rightarrow \begin{cases} (\psi_{j+1}^n - \psi_j^n)/\Delta \zeta & , \text{ predictor} \\ (\tilde{\psi}_j - \tilde{\psi}_{j-1})/\Delta \zeta & , \text{ corrector} \end{cases} \quad 3.3.2$$

where  $\Delta \zeta$  is the nondimensional mesh spacing in the computational plane and  $\Delta t$  is the time step through which the solution is being advanced. The substitution of 3.3.1 and 3.3.2 into 3.2.8, 3.2.9, 3.2.10 at the predictor level yields a system of linear algebraic equations for the predictor quantities  $\tilde{\psi}_j$ . Then the corrector level of the scheme is performed to yield the values  $\psi_j^{n+1}$ .

Somewhat different rules are used to perform the discretization of 3.2.11, 3.2.12 and 3.2.13. The rules for the time derivatives are as expressed by 3.3.1. However, first order upstream differencing is always used for the convective terms and the remaining spacewise derivatives are treated by centered differencing. That is

---

<sup>16</sup> MacCormack, R. W. "The Effect of Viscosity in Hypervelocity Impact Cratering" AIAA Paper 69-354 1969

$$(u_p - \eta_p) \frac{\partial \psi}{\partial \zeta} = \begin{cases} (\psi_{j+1} - \psi_j) / \Delta \zeta & \text{if } u_p - \eta_p < 0 \\ (\psi_j - \psi_{j-1}) / \Delta \zeta & \text{if } u_p - \eta_p \geq 0 \end{cases} \quad 3.3.3$$

at both predictor and corrector levels. But

$$\frac{\partial \psi}{\partial \zeta} = \frac{\psi_{j+1} - \psi_{j-1}}{2\Delta \zeta} \quad 3.3.4$$

applies to  $\partial u_p / \partial \zeta$  in 3.2.11 and to  $\partial \sigma / \partial \zeta$  in 3.2.12 at both predictor and corrector levels.

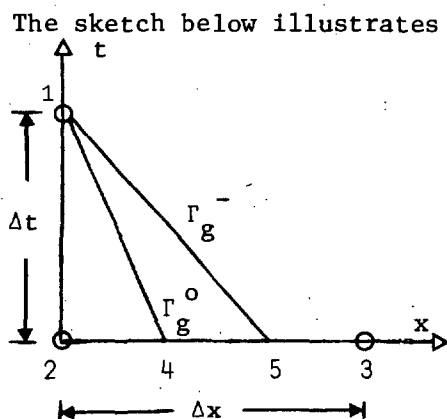
We also note that the rule expressed by 3.3.1 serves to define an algorithm for the integration of the ordinary differential equations such as 2.3.1, for example.

In order to assure stability of the method it is necessary that the time step be constrained. This point is discussed in section 3.5.

### 3.4 Integration at Boundary Mesh Points

The algorithms for the boundary points may be summarized in the following general form. The conditions of compatibility on those characteristic lines which intersect both the boundary and the line bearing the data at the present step are used to determine linear relationships between the boundary values of velocity and pressure and between the boundary values of density and pressure. These linear relationships are combined with the physical boundary conditions and the combination is then solved as a possibly nonlinear algebraic system, the method of solution varying in complexity in accordance with the nature of the boundary conditions.

We first indicate the manner in which the characteristic forms of the equations are used to establish linear relationships among certain of the boundary values, taking the gas-permeable breech as an example. The procedure at other boundaries is completely analogous. Subsequently, we will consider the impact of the physical boundary conditions, proceeding case by case through a number of subsections.



efflux of gas through the breech and is expressed in terms of the physical coordinate  $x$ . The point 1 is understood to correspond to the state of the boundary at the next step of the integration. The points 2 and 3 correspond to the boundary and the adjacent mesh point at the present step. The point 5 corresponds to the intersection with the line of present data of the characteristic  $\Gamma_g^-$  which also intercepts the point 1. Similarly,

$\Gamma_g^0$ , the material characteristic intercepts the boundary at 1 and the line of present data at 4. If the boundary were impermeable the point 4 would coincide with 2. If, on the other hand, the efflux were sufficiently intense as to become supersonic, there would also be a member of the family  $\Gamma_g^+$  which would have an intersection with 1 and the segment 2-3.

Knowing  $\Delta x$  and  $\Delta t$ , the points of intersection 4 and 5 are deduced using 2.1.10 and 2.1.8 respectively, with the values of  $u$  and  $c$  determined at 2 on the predictor level and at 1 on the corrector level, the values in the latter case following from the predictor level solution. The conditions of compatibility 2.1.9 and 2.1.11 are interpreted as finite difference formulae with the state variables evaluated at 1 and 5 or at 1 and 4 as the case may be. The values of  $p$ ,  $\rho$ ,  $u$  at 4 and 5 are deduced from the values at 2 and 3 by linear interpolation. The coefficients of the differential terms in 2.1.9 are evaluated as averages of the values at 2 and 5 on the predictor step and 1 and 5 on the corrector step. A similar procedure is followed in the case of equation 2.1.11. No iteration is involved.

From this analysis it is easy to see that 2.1.9 will yield a linear relationship of the form

$$p = \alpha u + \beta \quad 3.4.1$$

Similarly, 2.1.11 will yield a relationship of the form

$$\rho = \theta p + \phi \quad 3.4.2$$

where  $p$ ,  $u$ ,  $\rho$  are all understood to be values at 1. Equation 3.4.2 remains valid if the boundary becomes impermeable but may not be used if the flow corresponds to influx. Similarly, 3.4.1 may be supplemented by a second such relationship if the efflux becomes supersonic and two acoustic characteristics intercept the boundary from the interior. We note that in such a case, therefore,  $p$  and  $u$  are completely determined as the solution of the two linear equations. On the other hand, if the state corresponds to a supersonic influx, then 3.4.1 may not be used at all; acoustic waves no longer reach the boundary from the interior of the flow. All these possibilities will be exercised in the subsequent discussion of the physical boundary conditions.

Our comments thus far have pertained specifically to the gas. Perfectly analogous considerations apply to the solid propellant. For future reference we state the characteristic forms as

$$\sigma = \alpha_p u_p + \beta_p \quad 3.4.3$$

corresponding to a member of  $\Gamma_p^+$  or  $\Gamma_p^-$  and

$$\rho_p = \theta_p \sigma + \phi_p \quad 3.4.4$$

which corresponds to a member of  $\Gamma_p^0$ . In the present study we shall be concerned only with boundary conditions which express either impermeability to the solid propellant or subsonic efflux.

### 3.4.1 Breech (Closed or Open)

When the breech is closed, the physical boundary condition 2.5.1 yields  $u = 0$  directly. Then the pressure follows directly from a condition of compatibility in the form 3.4.1 and the density from 3.4.2. The solution is therefore complete.

If the breech is open and the efflux is supersonic, then as noted above,  $p$  and  $u$  follow from the two relations of the form 3.4.1 corresponding to the two acoustic characteristic intersections. The density follows from 3.4.2. Before the solution can be accepted it is necessary to test that the mass flux does not exceed  $\dot{m}_*$  given by equation 2.5.2. If the value  $\dot{m}_*$  is exceeded, or if the flow is subsonic, the efflux is required to be as given by 2.5.2 and the condition of compatibility on the characteristic  $\Gamma_g^+$  is not applicable. The boundary values are found iteratively, using a midpoint search.

### 3.4.2 Projectile Base and Muzzle Following Projectile Exit

At the projectile base, whether we are concerned with the continuum response of the solid propellant or with the behavior of the gas following burnout, the condition 2.5.5 or 2.5.6 yields the velocity. Then the pressure follows from 3.4.1 or 3.4.3, as the case may be, and the density from 3.4.2 or 3.4.4. The projectile velocity  $\dot{X}$  is always updated prior to the determination of the boundary values.<sup>P</sup>

The analysis of the boundary values at the muzzle following expulsion of the projectile is completely analogous to that pertaining to the open breech.

### 3.4.3 Gas/Propellant Interface

We consider several possible cases in accordance with the manner of specification of the burn rate. The discussion given for each case is predicated on the assumption that the solid propellant is treated as rigid so that its density is known as a constant value and its velocity, equal to that of the projectile, is given according to an update of the equation of motion 2.3.4. Therefore, we preface the analysis of each case by commenting on the consequences of a continuum representation of the solid propellant. In the event that the propellant is to be treated as a continuum we are required to satisfy two conditions of compatibility of the form 3.4.3 and 3.4.4. This is accomplished iteratively as follows.

A trial value for  $u_p$  is proposed, based on current storage for the boundary values on the unreacted side of the interface. Compatible values  $\sigma$  and  $\rho_p$  are deduced from 3.4.3 and 3.4.4. The values of  $u_p$  and  $\rho_p$  are used together with the remaining boundary conditions to determine consistent values for the state of the gas and also the pressure  $\sigma'$ . The latter value will not, in general be equal to  $\sigma$ . Accordingly, the proposed value of  $u_p$  is modified by an amount  $\Delta u_p = (\sigma' - \sigma)/a_p$ ,  $\sigma$  is

replaced by the now compatible value  $\sigma'$  and  $\rho_p$  is similarly adjusted. This procedure is continued until the pressure  $\sigma$  changes by an amount less than 6.9 Pa.

Branching from one condition to another is discussed in section 3.5.

#### 3.4.3.1 Propellant Unreacting

This case may arise if, for example, an ideal burn rate is specified to yield a value of pressure on the unreacted side which is less than the current pressure on the reacted side. The ideal rate would therefore be negative and is replaced by the condition that the propellant is not burning. Given  $u_p$ , the value  $u$  is known at once as  $u = u_p$  and the analysis is identical with that following burnout.

#### 3.4.3.2 Measured Burn Rate (With Subsonic Reactants)

Substitution of 2.5.7 into 2.5.8 yields

$$\frac{\sigma}{\rho_p} = \frac{p}{\rho_p} + \frac{r^2}{g_o} \left[ \frac{\rho_p}{\rho} - 1 \right] \quad 3.4.5$$

Similarly, substitution of 2.5.7 into 2.5.9 yields

$$\frac{\sigma}{\rho_p} = e + \frac{p}{\rho} - e_p + \frac{r^2}{2g_o} \left[ \left( \frac{\rho_p}{\rho} \right)^2 - 1 \right] \quad 3.4.6$$

Then, combining 3.4.5 and 3.4.6 to eliminate  $\sigma$  and making use of the equation of state 2.4.1 to eliminate  $e$  we have

$$\frac{p}{\rho_p} \left[ \frac{\gamma}{\gamma - 1} \frac{\rho_p}{\rho} - 1 - \frac{b\rho_p}{\gamma - 1} \right] = e_p - \frac{r^2}{2g_o} \left[ \frac{\rho_p}{\rho} - 1 \right]^2 \quad 3.4.7$$

Furthermore, as the reactants are presumed subsonic, we may combine 2.5.7 with the condition of compatibility 3.4.1 to obtain

$$\frac{\rho_p}{\rho} = \frac{u_p + r - (p - \beta)/\alpha}{r} = \psi(p) \quad 3.4.8$$

Then 3.4.8 may be used to permit the interpretation of 3.4.7 as a function of  $p$  alone, namely

$$\Phi(p) = \frac{p}{\rho_p} \left[ \frac{\gamma}{\gamma - 1} \psi(p) - 1 - \frac{b\rho_p}{\gamma - 1} \right] - e_p + \frac{r^2}{2g_o} \left[ \psi(p) - 1 \right]^2 = 0 \quad 3.4.9$$

Equation 3.4.9 may be solved iteratively using Newton's method according to which the trial value  $p$  is replaced by the better approximation  $p - \Phi(p)/\Phi'(p)$ . We note the following derivatives which are required in the iterative process.

$$\begin{aligned} \phi'(p) = & \frac{1}{\rho_p} \left[ \frac{\gamma}{\gamma - 1} \psi(p) - 1 - \frac{b p}{\gamma - 1} \right] - \frac{p}{\rho_p} \frac{\gamma}{\gamma - 1} \psi'(p) \\ & + \frac{r(p)r'(p)}{g_o} [\psi(p) - 1]^2 + \frac{r^2(p)}{g_o} [\psi(p) - 1] \psi'(p) \end{aligned} \quad 3.4.10$$

$$\psi'(p) = r^{-2}(p) \{ r(p) [r'(p) - 1/\alpha] - [u_p + r(p) - (p - \beta)/\alpha] r'(p) \} \quad 3.4.11$$

Once  $p$  is determined the remaining boundary values follow from the chain of calculations:

$$u = (p - \beta)/\alpha \quad 3.4.12$$

$$r = r(p) \quad 3.4.13$$

$$\rho = \frac{r \rho_p}{u_p + r - u} \quad 3.4.14$$

$$\sigma = p + \frac{\rho_p r^2}{g_o} \left( \frac{\rho_p}{\rho} - 1 \right) \quad 3.4.15$$

$$e = \frac{p(1 - b\rho)}{(\gamma - 1)\rho} \quad 3.4.16$$

As noted in the preamble to this section, if  $u_p$  was a trial value, the quantity  $\sigma$  given by 3.4.15 must be compared with the value which is compatible with  $u_p$  according to 3.4.3. If they differ,  $u_p$  must be adjusted appropriately and the boundary values redetermined.

### 3.4.3.3 Ideal Burning of Langweiler (Subsonic or Supersonic Reactants)

In this case the determination of the boundary values for the gas is almost trivial since  $u = 0$  and the pressure  $p$  is equal to the constant initial value. Only the density at the boundary, and hence the internal energy, vary with time. When  $u = 0$ , 2.5.7 yields

$$\frac{\rho_p}{\rho} = \frac{u_p}{r} + 1 \quad 3.4.17$$

Substituting this result into 3.4.7 and rearranging yields the ideal rate of burning as a function of the instantaneous velocity of the propellant.

$$r = \left\{ \frac{\frac{\gamma}{\gamma - 1} \frac{p}{\rho_p}}{e_p + \frac{b p}{\gamma - 1} - \frac{p}{(\gamma - 1)\rho_p} - \frac{u_p^2}{2g_o}} \right\}^{u_p} \quad 3.4.18$$

Given  $r$ ,  $\rho$  follows from 3.4.17 whereupon  $\sigma$  and  $e$  are determined by 3.4.15 and 3.4.16 respectively.

#### 3.4.3.4 Prespecified Value of Pressure on Unreacted Side or of Acceleration of Projectile (With Subsonic Reactants)

As discussed in section 2.5.3 we assume that both of these conditions amount to the same thing, namely the specification of  $\sigma$ . Substitution of 3.4.5 into 3.4.6 to eliminate  $r$  yields, after rearrangement

$$\frac{\rho}{\rho_p} = \frac{\frac{p}{\rho_p} \frac{\gamma}{\gamma - 1} - \frac{p - \sigma}{2\rho_p}}{e_p - \frac{p - \sigma}{2\rho_p} + \frac{p}{\rho_p} \left(1 + \frac{b\rho_p}{\gamma - 1}\right)} \quad 3.4.19$$

By combining 3.4.19 with 3.4.8 we may deduce

$$r = \frac{\left[u_p - \frac{p - \beta}{\alpha}\right] \left[\sigma + \frac{\gamma + 1}{\gamma - 1} p\right]}{2\rho_p \left[e_p + \frac{b\rho_p}{\gamma - 1} - \frac{p}{\rho_p (\gamma - 1)}\right]} \quad 3.4.20$$

This may be viewed as an effective or ideal burn rate equation yielding  $r = r(p)$ . Then the method of section 3.4.3.2 may be followed with 3.4.20 in place of the measured burn rate law.

#### 3.4.3.5 Predetermined Mach Number of Reactants (Subsonic)

We may state the condition in the form

$$M = \frac{\dot{x}_p - u}{\sqrt{\frac{\gamma g_o p}{\rho(1 - b\rho)}}} \quad 3.4.21$$

where  $M < 1$  is the predetermined value of the Mach number. In view of 2.5.7 this may be solved to yield

$$\frac{\rho}{\rho_p} = \rho_p \left[ b + \frac{\gamma g_o p M^2}{\rho_p^2 r^2} \right] \quad 3.4.22$$

Moreover, combining 3.4.22 with 3.4.8 we may deduce an effective burn rate law,  $r = r(p)$

$$r = \frac{\frac{p - \beta}{\alpha} - u_p + \left\{ \left( \frac{p - \beta}{\alpha} - u_p \right)^2 + \frac{4(1 - b\rho_p)}{\rho_p} \gamma g_o p M^2 \right\}^{1/2}}{2(1 - b\rho_p)} \quad 3.4.23$$

Then the analysis of 3.4.3.2 applies with  $r$  defined by 3.4.23.



### 3.4.3.6 Prespecified Value of Pressure on Unreacted Side or of Acceleration of Projectile (With Supersonic Reactants)

In this case 3.4.22, which expresses the additional requirement that the Mach number  $M > 1$  of the reactants be given, may be combined with 3.4.5 to yield

$$r(p) = \left[ \frac{g_o}{\rho_p} \frac{\sigma - (1 + \gamma M^2)p}{b p - 1} \right]^{1/2} \quad 3.4.24$$

as an effective burn rate law. However, in making use of the analysis of section 3.4.3.2 it is necessary to use not only 3.4.24 to define  $r(p)$  but also 3.4.22 to define  $\Psi(p)$ . The expression 3.4.8 incorporates the assumption that  $u$  and  $p$  are compatible with the interior flow of the gas which is no longer true in this case. Moreover, following the determination of  $p$ , it is necessary to deduce  $\rho$  from 3.4.22 whereupon  $u$  follows from 3.4.14.

### 3.5 Additional Considerations

We conclude this chapter by noting some additional considerations relating to the method of solution.

#### 3.5.1 Choice of Time Step

As is well known<sup>17</sup>, explicit finite difference schemes demand, for their numerical stability, that the time step be suitably constrained. We constrain  $\Delta t$  according to the Courant-Friedrichs-Lewy (C-F-L) condition

$$\Delta t \leq \frac{x_p \Delta \zeta}{\max[|u - \eta| + c]} \quad 3.5.1$$

where  $\Delta \zeta$  is the nondimensional mesh spacing in the gas, and by a similar relation expressed in terms of the properties of the propellant when it, too, is treated as a continuum.

The maximum allowable value of  $\Delta t$  thus defined is further divided by a user-supplied safety factor, SAFE, which must be equal to at least one.

#### 3.5.2 Treatment at Burnout

If the combustion zone is represented as a discontinuity of infinitesimal thickness, it follows that the boundary value of the velocity of the gas will undergo a sudden jump as burnout occurs. The flow which will have been represented as blowing away from the base of the projectile will now be required to follow it. If the Mach number of the

---

<sup>17</sup> Richtmyer, R. D. and Morton, K. W. "Difference Methods for Initial Value Problems" 2nd Ed. John Wiley, New York 1967

reactants, just prior to the instant of burnout, was comparable to unity, the sudden change in velocity will be accompanied by a sharp drop in pressure. A strong rarefaction will be formed to communicate the change in the boundary condition to the column of gas. Indeed, the sudden drop in pressure may be sufficiently large as to strain the numerical method of solution. Therefore, we employ an analytical solution to describe the boundary values for a short period after burnout. The analysis also provides a simple exact solution which may be used to benchmark the accuracy of the program, as we discuss in chapter 4.0. We therefore deduce the solution in some detail before commenting on its application to the determination of the boundary values in the computer program.

Consider the motion of a piston propelled by a semi-infinite column of gas which is initially at rest and has uniform properties. At any subsequent time, the gas may be divided into two regions, one still quiescent and uniform, and the other undergoing expansion to follow the projectile. A flow of this type is called a simple wave<sup>8</sup>. If we assume the piston to be moving to the right, it follows that all characteristics of the family  $\Gamma_g^+$  emanate from the uniform region so that their corresponding condition of compatibility is impressed uniformly on the flow. We therefore have, throughout the expansion region

$$u + \int \frac{dp}{c \rho} = \text{constant} \quad 3.5.2$$

Using the covolume equation of state to perform the thermodynamic integral and denoting the properties of the quiescent region by a subscript 1 we have

$$u + \frac{2}{\gamma - 1} (1 - b\rho)c = \frac{2}{\gamma - 1} (1 - b\rho_1)c_1 \quad 3.5.3$$

This relation applies, in particular, at the base of the piston where  $u = \dot{X}_p$ . Moreover, the isentropic nature of the flow implies

$$\frac{p}{p_1} = \left[ \frac{(1 - b\rho)c}{(1 - b\rho_1)c_1} \right]^{\frac{2\gamma}{\gamma - 1}} \quad 3.5.4$$

Combining 3.5.3 and 3.5.4 yields the base pressure as a function of the velocity of the piston

$$p = p_1 \left[ 1 - \frac{\gamma - 1}{2} \frac{\dot{X}_p}{(1 - b\rho_1)c_1} \right]^{\frac{2\gamma}{\gamma - 1}} \quad 3.5.5$$

From the equation of motion of the projectile it is a simple matter to deduce the following.

$$\dot{X}_p = \frac{2c_1'}{\gamma - 1} \left\{ 1 - \left[ \left( 1 - \frac{\gamma - 1}{2} \frac{\dot{X}_p}{c_1'} \right)^{-\frac{\gamma + 1}{\gamma - 1}} + \frac{\gamma + 1}{2c_1'} \frac{A_b g_o p_1}{M_p} (t - t_o) \right]^{-\frac{\gamma - 1}{\gamma + 1}} \right\} \quad 3.5.6$$

$$X_p = X_{p_0} + \frac{2c_1'}{\gamma - 1} \left\{ (t - t_0) + \frac{M_p c_1'}{A_b g_0 p_1} \left[ \left(1 - \frac{\gamma - 1}{2} \frac{\dot{X}_{p_0}}{c_1'}\right)^{-\frac{2}{\gamma - 1}} - \left(1 - \frac{\gamma - 1}{2} \frac{\dot{X}_{p_0}}{c_1'}\right)^{-\frac{\gamma + 1}{\gamma - 1}} + \frac{\gamma + 1}{2c_1'} \frac{A_b g_0 p_1}{M_p} (t - t_0) \right]^{\frac{2}{\gamma + 1}} \right\} \quad 3.5.7$$

It should be noted that we have taken the initial instant to be  $t_0$  and we have denoted the initial position and velocity of the piston by  $X_{p_0}$  and  $\dot{X}_{p_0}$  respectively. Also, we have used

$$c_1' = (1 - b p_1) c_1 \quad 3.5.8$$

The relations 3.5.6 and 3.5.7 with  $\dot{X}_{p_0} = 0$  provide an exact solution which may be used to benchmark the accuracy of the computer program. Since the code must be exercised with a finite column of gas, the comparison will only be valid until such a time as the reflection of the expansion front from the breech overtakes the piston or projectile.

When the ideal combustion of Langweiler has been in effect up to the instant of burnout, the gas is quiescent as assumed above. Then 3.5.5 may be used to determine the boundary value of pressure. We note that if, at the instant of burnout we have a near sonic condition  $\dot{X}_p = c_1'$  and  $\gamma = 1.2$ , then  $p/p_1 = 0.282$  so that the pressure drops instantaneously to 28% of its value prior to burnout. This implies a sharp drop in the propulsive capacity of the gas which is exacerbated by the fact that prior to burnout, propulsion was due not just to  $p_1$  but also to the contribution of thrust.

When the combustion is due to other than the ideal model of Langweiler, the state of the gas adjacent to the projectile at burnout is, in general, neither uniform nor quiescent. We nevertheless use 3.5.5, where  $p_1$  and  $c_1$  are predicated on the conditions at the boundary just prior to burnout, and we replace  $\dot{X}_p$  by  $\dot{X}_p - u_1$  where  $u_1$  is the velocity of the gas just prior to burnout.

In all cases, equation 3.5.5 is used to determine the boundary value of pressure for five integration steps following burnout. Thereafter, the previously described numerical algorithm is used.

### 3.5.3 Change of Representation of Solid Propellant

As the solid propellant is consumed, it will reach a point at which it is too short to be treated as a continuum in accordance with the constraint  $(X_p - x_p)\Delta\zeta \geq DX_{MIN}$  on the mesh spacing  $\Delta\zeta$ . At this point, if a continuum representation had been elected, an internal switch is reset and the calculation concludes with the propellant treated as rigid. A value of the density is computed from a knowledge of the remaining mass of propellant and its length. Friction between the propellant and the wall is not treated in cases in which the propellant is initially taken

to be rigid. When a transformation from a continuum to a rigid representation is made, near burnout, the resistance per unit bearing area due to friction is frozen at the value it had at the time of transition.

#### 3.5.4 Treatment of Friction Between Propellant and Tube Wall

The friction term, when taken to be proportional to pressure in accordance with equation 2.4.9, with values of  $\mu_w \gtrsim 0.1$ , becomes very large and tends to create numerical wiggles in the solution. A number of different schemes were attempted in order to resolve this problem. Indeed, the use of centered differencing rather than the alternating scheme of MacCormack, in the integration of the momentum equation of the propellant, was predicated on the desire to express as accurately as possible the competition between  $\partial\sigma/\partial x$  and  $f_w$  at both predictor and corrector levels. Possibly, calculations with values of  $\mu_w$  as large as 0.1 will not be of interest since the ballistic loss will be seen to be significant, at least in the sample cases described in chapter 4.0.

Nevertheless, to stabilize properly such solutions we have smoothed the term  $f_w$ . In the numerical evaluation of equation 2.4.9 the pressure is expressed as  $(p_{j-1} + p_{j+2} + 2p_j)/4$  at internal mesh points and as an average of the boundary value with its neighbor at boundary points. Also, the expression for  $f_w$  is made implicit in the pressure at the boundaries when using the characteristic forms. That is to say the term  $f_w$  is multiplied by  $p_1/p_2$  in the nomenclature of section 3.4 prior to making use of the characteristic form 3.4.3.

#### 3.5.5 Branching of Conditions at the Gas/Propellant Interface

As we have noted previously, the program is structured so as to allow the combustion model to vary in nature as the ballistic cycle unfolds. Our purpose in this concluding section is to state the rules according to which the internal branching has been structured. The following are the combinations of constraints which may be involved during a given cycle.

##### (a) Measured Burn Rate/Mach Number Limit

If measured burn data are supplied, a search is made for boundary values based on these data. The values so found are then tested to ensure that the Mach number of the reactants does not exceed the limit  $M$ , provided  $M > 0$ . If  $M$  is exceeded or, if the search for boundary values based on the measured burn rate was unsuccessful, branching occurs to determine values which yield the specified value of  $M$ .

This combination is limited to subsonic combustion, that is,  $M < 1$ . If the measured data yield a Mach number greater than unity and the user has specified  $M = 0$  or  $M \geq 1$ , the calculation terminates with an error message and the program proceeds to the next case.

##### (b) Langweiler Combustion/Mach Number Limit

The Langweiler ideal combustion model will yield boundary values

which are only limited thermodynamically by the covolume limit  $p = 1/b$  at which point the reactants are at zero temperature. If a value  $0 < M < 1$  has been furnished by the user, the boundary values according to the Langweiler model are tested to ensure that the Mach number of the reactants does not exceed  $M$ . If it does, branching will occur to yield the indicated Mach number. It should be noted that while the Langweiler model will admit supersonic combustion, the branch to the Mach number limit will be admitted only if  $M < 1$ .

(c) Prespecified Propellant Pressure or Acceleration/Mach Number Limit

It is simple to branch between a constraint on the pressure on the unreacted side of the interface and a constraint on the acceleration, as both of these constraints can be expressed in terms of the pressure on the unreacted side of the interface. A search for suitable boundary values is undertaken. When they are found, the Mach number is compared with the input limit  $M$ , provided  $M > 0$ . If  $M < 1$  and the limit has been exceeded, branching to the Mach number limitation will occur. If the computed Mach number and the input limit  $M$  are both greater than or equal to one, branching occurs to the supersonic combustion process to satisfy both  $M$  and the required value of pressure simultaneously. The flow is no longer required to be compatible with the state of the gas.

If the original search for subsonic boundary values to yield the designated pressure on the unreacted side was unsuccessful, and  $M > 0$ , branching will occur to the Mach number limited processes, using  $M$  alone if  $M < 1$  and using both the designated pressure and  $M$  if  $M \geq 1$ .

There is one further branch to be considered in this case. If the value of the indicated pressure on the unreacted side is less than or equal to the current pressure of the gas, the reaction is assumed to terminate since the regression rate would otherwise be required to be negative.

## 4.0 SOME NUMERICAL RESULTS

The model which we have described in chapter 2.0 admits a large variety of possible cases. A systematic exploitation of the model capacity is beyond the scope of the present study. The solutions which we discuss in the present chapter are intended principally to demonstrate the operability of the computer program and to provide an assessment of the magnitude of the errors associated with the method of solution. However, we also comment briefly on the potential magnitude of some of the losses associated with the end-burning traveling charge. First, in section 4.1, we consider a case for which an exact solution is available in order to provide an absolute benchmark of accuracy. Second, in section 4.2, we discuss a nominal traveling charge configuration, paying attention to properties of mesh indifference and global conservation of mass and energy. Finally, in section 4.3, we comment on the losses due to friction, heat transfer to the tube, and the pressure of shocked air in front of the projectile.

### 4.1 Comparison with an Exact Solution

In section 3.5 we presented an exact solution for the motion of a piston propelled by a semi-infinite column of initially quiescent, uniform gas. While the present model can only be used in the context of a finite tube, its predictions may be compared with the exact solution for that period of time prior to the interaction of the expansion wave with the finite boundary. Such a comparison is made in Table 4.1. The solutions were based on values  $D = 4.0$  cm,  $\gamma = 1.239$ ,  $M = 25.0$  gm-mol/gm,  $b = 1.06$  cm<sup>3</sup>/gm,  $M_p = 160$  gm, an initial pressure of 551.6 MPa and an initial temperature of 3271°K. The numerical solutions were deduced for a tube of length 254 cms. Inasmuch as the speed of sound in the quiescent gas is 1.78 km/sec, it follows that equations 3.5.5 and 3.5.6 may be used to describe the pressure at the base of the piston and the piston velocity for a period of at least 1.4 msec, after which time the wave reflection from the finite boundary begins to invalidate the exact solution.

Table 4.1 Comparison of Numerical Solutions with an Exact Solution

Time (msec)	Base Pressure (MPa)			Piston Velocity (km/sec)		
	Exact	21 pts	100 pts	Exact	21 pts	100 pts
0.2	281.8	284.9	281.9	0.610	0.612	0.610
0.4	186.1	186.0	186.1	0.967	0.970	0.967
0.6	137.7	137.8	137.7	1.217	1.221	1.217
0.8	108.7	108.9	108.7	1.409	1.412	1.409
1.0	89.5	89.5	89.5	1.564	1.567	1.564

The table provides a comparison between the exact solution and numerical solutions generated with 21 and with 100 mesh points. The agreement is seen to be very good. Even with 21 mesh points, the base pressure is predicted to within approximately 1% of the exact value at 0.2 msec and

to within less than 0.1% at later times. With 100 points the error is less than 0.03% at 0.2 msec. As expected, the results pertaining to the piston velocity are similar. The results are indicative not only of good absolute accuracy but also of mesh indifference. It is worth noting that the expansion is really very strong. Evidently, due to the large initial pressure and the relatively low piston mass, the pressure drops to roughly 50% of its initial value by 0.2 msec.

#### 4.2 A Nominal Traveling Charge Configuration

To illustrate further the operability of the computer program we now present a solution for a nominal end-burning traveling charge configuration. The problem of interest corresponds to a 40 mm tube with 100 calibers of projectile travel. An ideal burning law is assumed in which the pressure on the unreacted side of the gas/propellant interface is required to be 700 MPa provided that the Mach number of the reactants does not exceed 0.999. In accordance with the logic for branching which we have discussed in the previous chapter, a solution yielding the requisite pressure will be sought at each stage of the calculation. If the Mach number limitation is exceeded, branching will occur to yield values satisfying the limiting value of the Mach number. As the input value is less than unity, the reactants will be required to satisfy a condition of mechanical compatibility with the column of gas.

We first solve this problem treating the propellant as rigid. Three solutions are generated using a maximum of 21, 41, and 81 mesh points and minimum spacings of 0.508, 0.254 and 0.127 cms respectively. Some aspects of these three solutions are compared in order to permit an assessment of the mesh indifference of the predictions. We also consider the degree to which mass and energy are conserved globally in these three calculations as a further indication of the magnitude of the numerical errors of integration. Subsequently, we present some details of a fourth calculation of the same problem based on a continuum representation of the propellant. In this last case we illustrate the solution by means of plots of the pressure and velocity distributions at various times.

The data base for the nominal problem is contained in Table 4.2. The values for the wave speed in the propellant only pertain, of course, to the case in which continuum behavior is considered.

---

Table 4.2 Data Base for Nominal Traveling Charge Problem

---

Tube Diameter	4.0 cm
Maximum Projectile Travel	4.0 m
Projectile Mass	160 gm
Propellant Chemical Energy	4450 J/gm
Covolume	1.05 cm <sup>3</sup> /gm
Molecular Weight	23.253 gmol/gm
Density	1.66 gm/cc
Ratio of Specific Heats	1.2414 (-)
Compressive Wave Speed	1.07 km/sec

Unloading Wave Speed*	0 m/sec
Initial position of rear propellant face relative to breech	2.54 cm
Initial Pressure	700 MPa
Maximum allowable pressure on unreacted side of gas/propellant interface	700 MPa
Maximum allowable reactant Mach number	0.999
Charge-to-projectile mass ratio	3.54
Loading density	1.2 gm/cc

\* Code action is to treat solid propellant constitutive law as reversible in case of continuum representation.

In Table 4.3 we compare the values of projectile velocity and breech and base pressure in the gas for the three calculations based on a representation of the propellant as rigid. The base pressure corresponds to the state of the reactants at the gas/propellant interface.

Table 4.3 Dependence of Nominal Solution on Mesh

Time (msec)	Projectile Velocity (km/sec)			Breech Pressure (MPa)			Base Pressure		
	21 pts	41 pts	81 pts	21 pts	41 pts	81 pts	21 pts	41 pts	81 pts
0.2	0.249	0.249	0.249	664.4	664.4	664.4	663.5	663.5	663.5
0.4	0.511	0.511	0.511	583.1	583.1	583.1	579.1	579.1	579.1
0.6	0.804	0.804	0.804	492.6	492.6	492.6	481.1	481.2	481.2
0.8	1.144	1.144	1.144	410.0	410.0	410.0	384.9	384.9	385.0
1.0	1.559	1.559	1.559	340.1	340.1	340.1	291.6	291.6	291.6
1.6	2.456	2.458	2.460	199.5	199.8	199.8	84.8	85.1	85.3
2.0	2.821	2.825	2.828	140.7	142.1	142.9	52.4	52.6	52.7
2.34*	3.068	3.073	3.076	103.8	102.9	102.1	38.0	38.1	38.2

\* Muzzle Exit

The quantities of ballistic interest are the maximum pressures and the muzzle velocity. These do not exhibit a mesh dependence beyond 0.2% as we pass from 21 to 41 points or beyond 0.1% as we pass from 41 to 81 points. The greatest numerical error seems to be associated with the breech pressure at muzzle exit which exhibits a mesh dependence of approximately 0.7%. As the value of the breech pressure at muzzle exit is not normally of ballistic interest, it appears from Table 4.3 that 41 mesh points are sufficient in simulations of this type.



Next, in Table 4.4, we present the histories of the defects in total mass and energy at the same set of times, for the three calculations. Since there are no losses in the physical problem, both mass and energy should be conserved on a global basis. As the present numerical scheme does not automatically assure such a global conservation, the mass and energy defects provide an indication of the magnitude of the errors of numerical integration. The total mass is computed using a trapezoidal rule. The result is subtracted from the initial value and the defect is then expressed as a percentage of the original value. The energy defect is computed similarly.

Table 4.4 Global Mass and Energy Defects in Nominal Problem

Time (msec)	Mass Defect (%)			Energy Defect (%)		
	21 pts	41 pts	81 pts	21 pts	41 pts	81 pts
0.2	-0.01	0.00	0.00	0.00	0.00	0.00
0.4	0.00	0.00	0.00	0.00	0.00	0.00
0.6	0.00	0.00	0.00	0.00	0.00	0.00
0.8	0.02	0.00	0.00	0.00	0.00	0.00
1.0	0.07	0.01	0.00	0.00	0.00	0.00
1.6	0.26	0.06	0.01	-0.01	0.00	0.00
2.0 *	0.38	0.10	0.02	0.02	0.01	0.00
2.34 *	0.45	0.11	0.02	0.04	0.02	0.01

\* Muzzle Exit

The results of Table 4.4 essentially confirm those of Table 4.3. If the maximum defect is taken as an indicator of the probable error of any given ballistic prediction, it follows from Table 4.4 that errors of the order of 0.5% are to be expected if one uses a maximum 21 mesh points and of the order of 0.1% if one uses 41 points.

We turn now to a discussion of a solution for the nominal problem based on a continuum representation of the propellant. The solution is illustrated by the distributions of pressure and velocity shown in figures 4.1 through 4.8.

It should be noted that the solid propellant is assumed to have a nonlinear, but reversible, equation of state. A maximum of 31 mesh points is allowed with a minimum spacing of 0.508 cms. The maximum time step as computed from the Courant-Friedrichs-Lewy condition is divided by two so that the maximum Courant number is, by definition, 0.5.

The initial distributions of pressure and velocity are shown in figure 4.1. As the initial pressure is equal to the maximum value required on the unreacted side of the interface, the burn rate is initially zero according to the ideal law. Both the gas and the solid propellant are at rest and pressurized uniformly to the initial value. Friction between the propellant and the tube wall is not considered. We will

comment on the influence of the loss terms in the next section of this chapter.

Because of the high pressure exerted on the projectile base, the projectile begins to accelerate and, analogously with the example of section 4.1, an expansion wave is propagated through the solid propellant. Figure 4.2 shows the conditions at 0.2 msec. The drop in pressure across the propellant is seen to be considerable. At this time, burning of the propellant has begun but is still rather weak since the gas pressure is still high. By 0.4 msec, as shown in figure 4.3, significant displacement of the projectile and traveling charge has occurred and the gas/propellant interface manifests itself quite clearly as a discontinuity in the distributions of both pressure and velocity.

Although the ideal combustion model is not that corresponding to the Langweiler process, it may be seen that the kinetic energy of the gas, as inferred from the velocity distribution, is still quite small at this stage. The same is true at 0.6 msec, figure 4.4, and even at 1.0 msec, figure 4.5, in which the propellant is seen to be approximately 50% burnt. The wave dynamics in the solid propellant should also be noted. In both figures 4.4 and 4.5, the pressure gradient in the solid propellant is seen to have reversed as a consequence of transient phenomena. Of equal interest, although not shown in the figures, is the fact that tensile stresses are predicted to occur at the interface between the propellant and the projectile base. However, undue significance should not be attached to this observation since the wave dynamics are associated to a large degree with the assumed highly pressurized initial condition.

The three concluding figures 4.6, 4.7 and 4.8 show the evolution of the solution until muzzle exit occurs. The propellant does not quite burn out in this example. It should be noted, in these last three figures, that branching to a Mach number limited burning process has occurred. The pressure at the base of the propellant is no longer 700 MPa but is, instead, roughly twice that in the gas. As the burn rate becomes limited by the Mach number constraint, the velocity profile of the gas develops and the gas does begin to store increasing amounts of kinetic energy. Nevertheless, it is easy to see, from figure 4.8, that the kinetic energy of the propellant is approximately 25% of what would be expected in a conventional charge. In the latter, the velocity of the **gas** at the projectile base would be equal to that of the projectile whereas in the present calculation it is seen to be approximately one-half of the projectile velocity.

In the latter figures there are still signs of the transient phenomena we noted previously in connection with the solid propellant. They are manifested here in the pressure distribution of the gas which has no mechanism for damping. Thus the variations in the ideal burn rate due to the interaction of traveling waves in the solid propellant with the gas/propellant interface have been preserved in the pressure field of the gas.

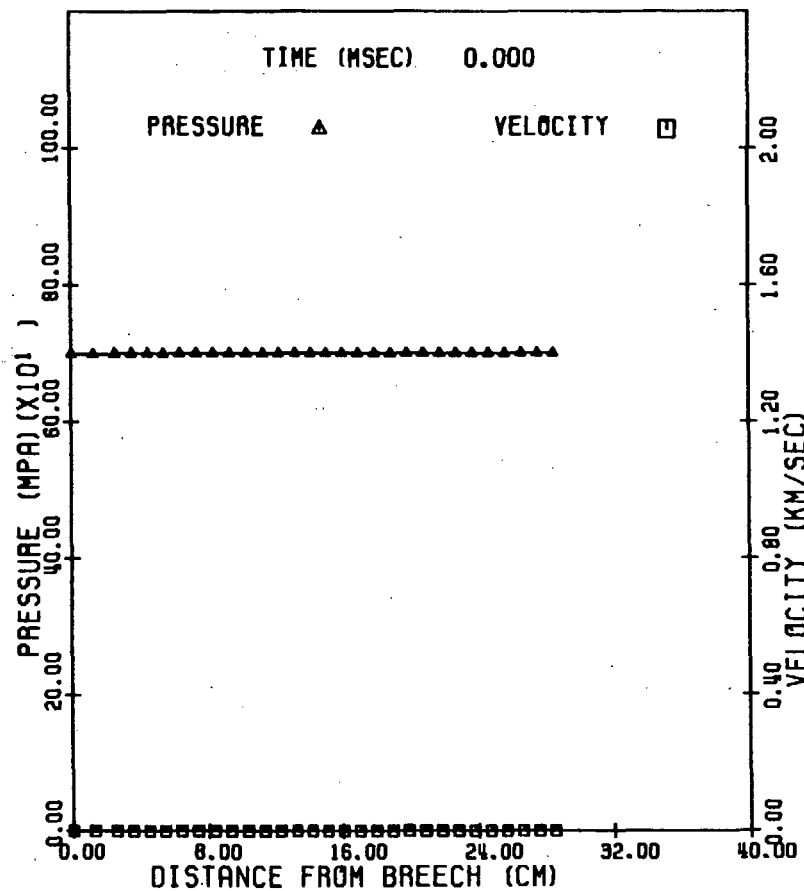


Figure 4.1 Distributions of pressure and velocity in nominal traveling charge problem at time 0.0 msec

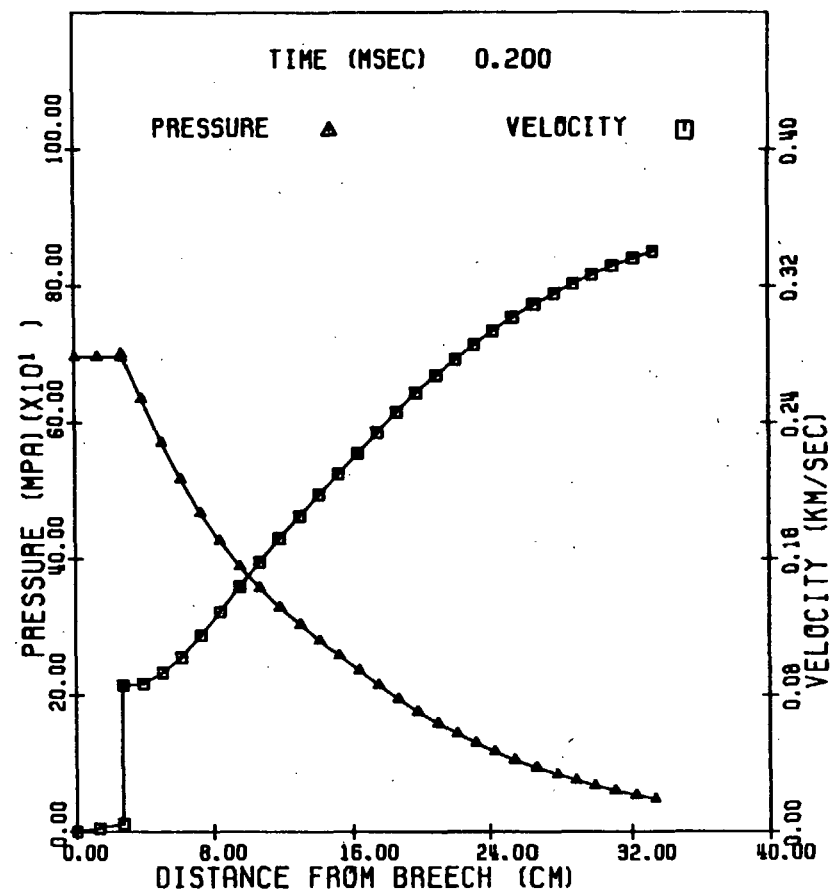


Figure 4.2 Distributions of pressure and velocity in nominal traveling charge problem at time 0.2 msec

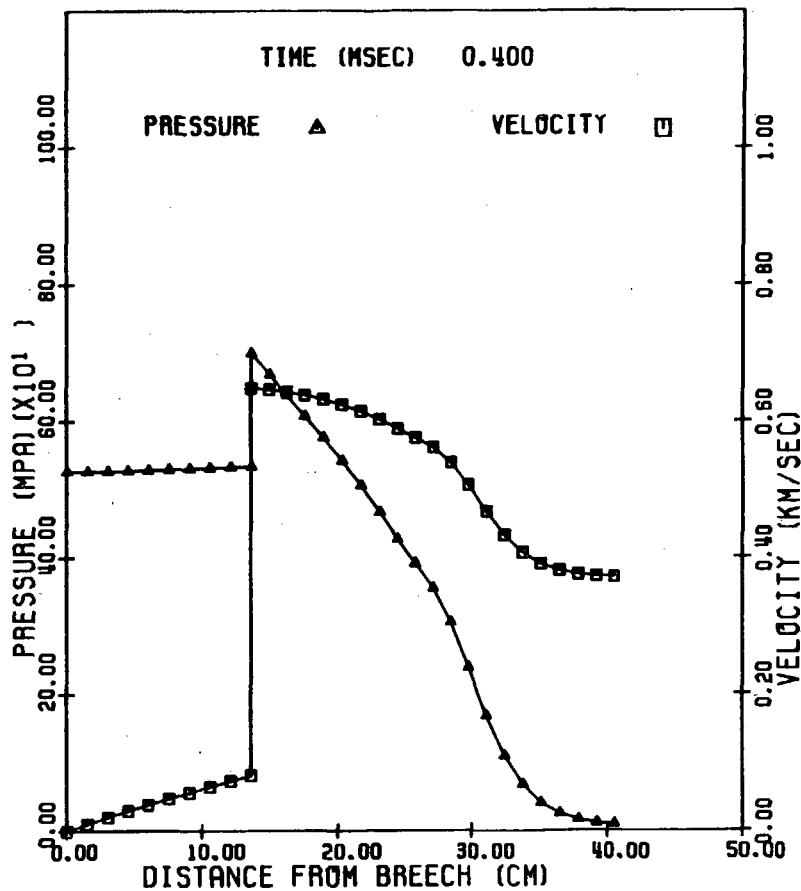


Figure 4.3 Distributions of pressure and velocity in nominal traveling charge problem at time 0.4 msec

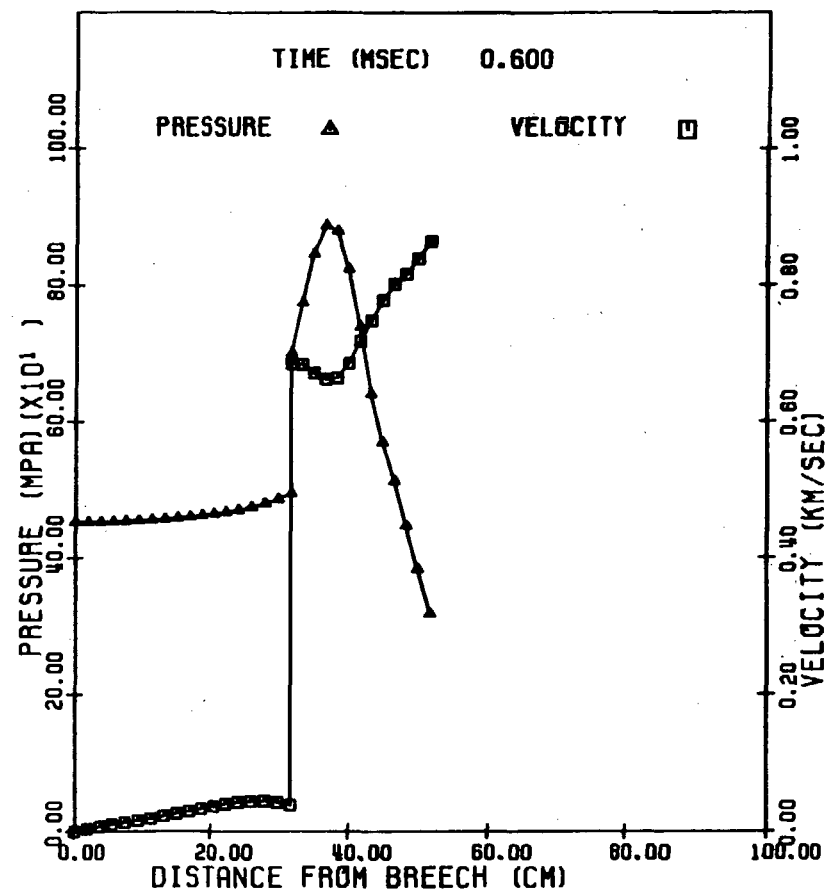


Figure 4.4 Distributions of pressure and velocity in nominal traveling charge problem at time 0.6 msec

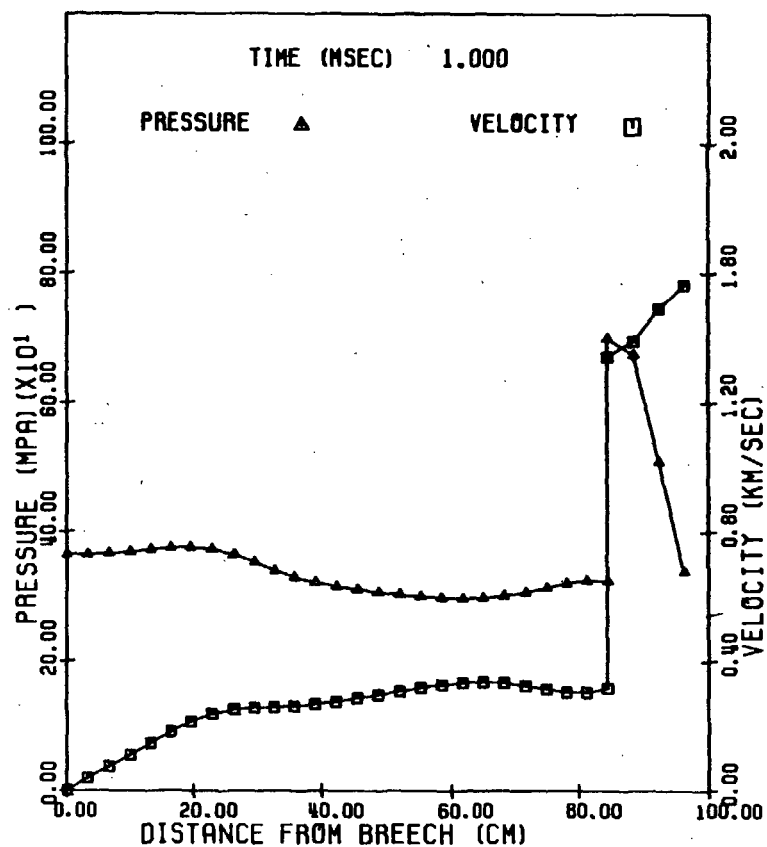


Figure 4.5 Distributions of pressure and velocity in nominal traveling charge problem at time 1.0 msec

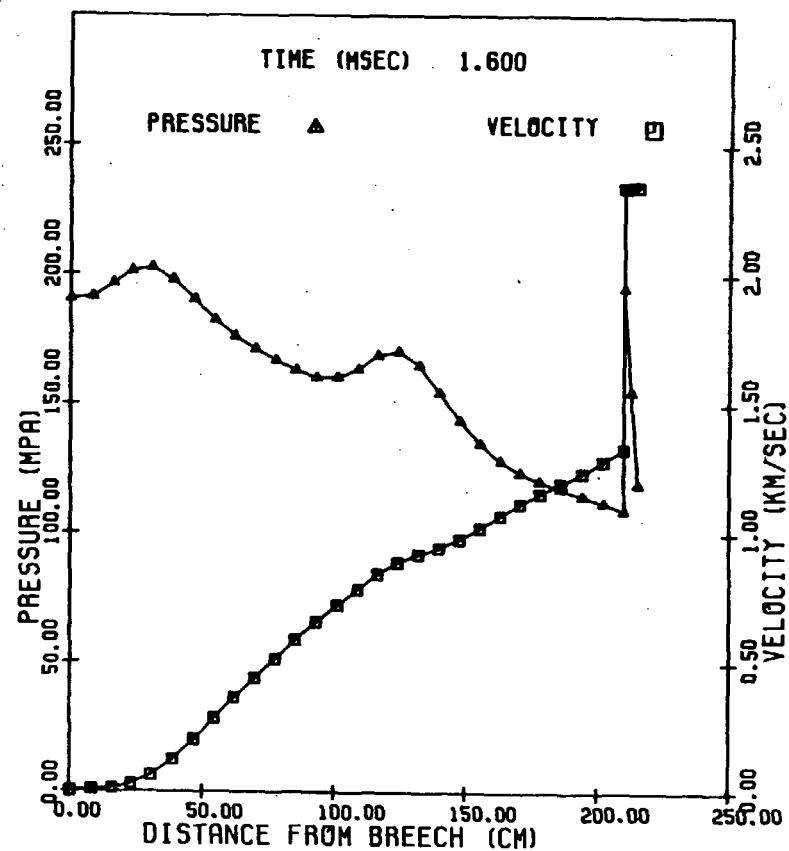


Figure 4.6 Distributions of pressure and velocity in nominal traveling charge problem at time 1.6 msec

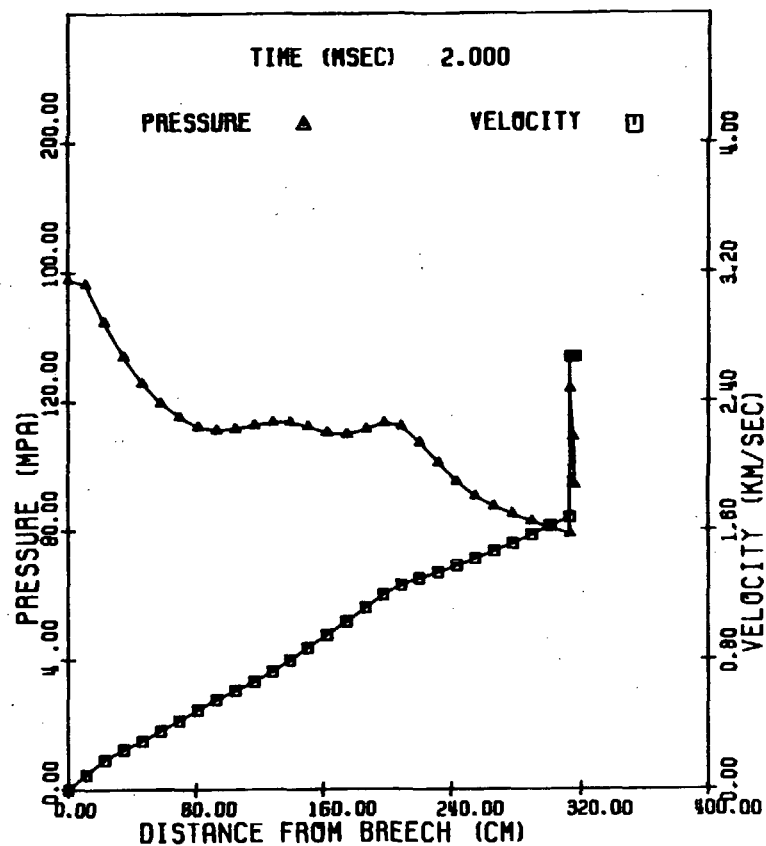


Figure 4.7 Distributions of pressure and velocity in nominal traveling charge problem at time 2.0 msec

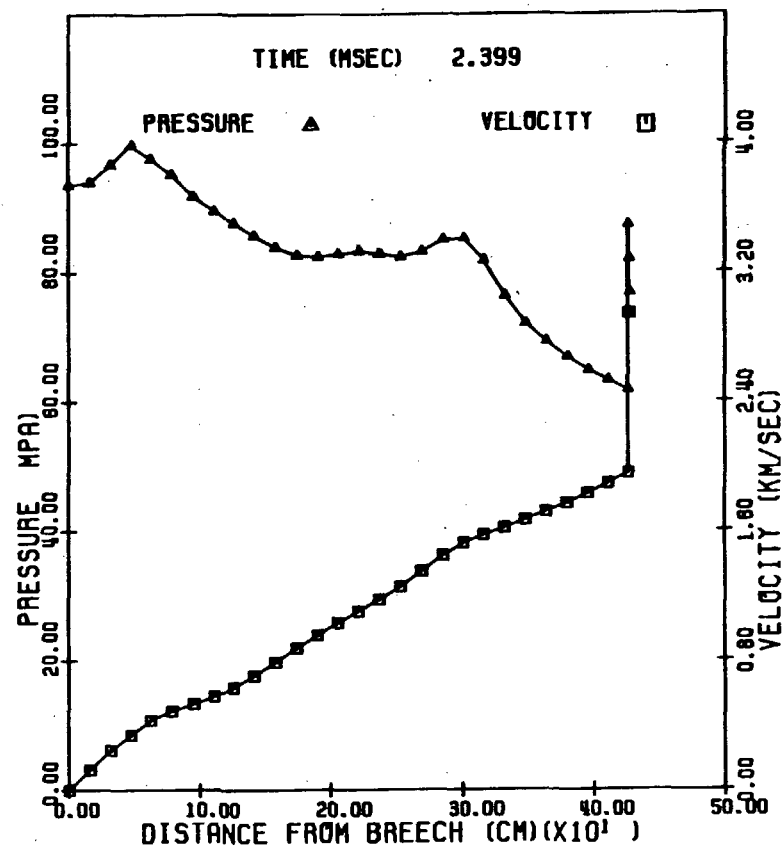


Figure 4.8 Distributions of pressure and velocity in nominal traveling charge problem at time 2.4 msec

### 4.3 Influence of Losses

To conclude, we summarize the results of calculations performed during the testing of the code, with a view to forming an assessment of the magnitudes of the losses to be expected in the traveling charge. These results are summarized in Table 4.5.

Table 4.5 Influence of Losses on Muzzle Velocity

Case	Comments	Muzzle Velocity (km/sec)								
1	Nominal with rigid propellant	3.068								
2	Propellant treated as a continuum	2.941								
3	Propellant treated as a continuum with wall friction due to constant coefficient of friction equal to 0.1	2.194								
4	Propellant treated as a continuum with wall friction coefficient given as following table of values	2.981								
	<table><tr><td>Velocity (km/sec)</td><td><math>\mu</math> (-)</td></tr><tr><td>0.</td><td>0.06</td></tr><tr><td>0.152</td><td>0.02</td></tr><tr><td>0.304</td><td>0.01</td></tr></table>	Velocity (km/sec)	$\mu$ (-)	0.	0.06	0.152	0.02	0.304	0.01	
Velocity (km/sec)	$\mu$ (-)									
0.	0.06									
0.152	0.02									
0.304	0.01									
5	Propellant treated as a continuum with wall friction due to gas film bearing with $\mu_f = 1.79 \times 10^{-3}$ gm/cm-sec and $\delta_f = 0.254$ mm	2.937								
6	Rigid propellant and heat losses	2.997								
7	Rigid propellant and resistance due to shocked air	3.025								
8	Rigid propellant and constant resistance, due to obturator, of 3.45 MPa	3.059								
9	Rigid propellant and resistance due to setback load on obturator of length 2.54 cms with forward mass of projectile equal to 160 gm and coefficient of friction given according to the following table of values	2.986								
	<table><tr><td>Velocity (km/sec)</td><td><math>\mu</math> (-)</td></tr><tr><td>0.</td><td>0.6</td></tr><tr><td>0.152</td><td>0.2</td></tr><tr><td>0.304</td><td>0.1</td></tr></table>	Velocity (km/sec)	$\mu$ (-)	0.	0.6	0.152	0.2	0.304	0.1	
Velocity (km/sec)	$\mu$ (-)									
0.	0.6									
0.152	0.2									
0.304	0.1									

From this table it is evident that the only losses of significance are likely to be associated with friction between the propellant and the tube. A comparison of cases 2 and 3 shows that a friction coefficient of 0.1 simply cannot be tolerated. On the other hand, a mild coefficient of friction, such as that considered in case 4, may actually increase the muzzle velocity. This is a consequence of the failure of case 2 to yield burnout of the propellant whereas the friction in case 4 delays the projectile exit sufficiently for complete burnout to occur. The influence of the resistance in this case is therefore similar to that of a shot start pressure which, as is well known, often acts to increase the muzzle velocity in conventional ammunition.



## 5.0 CONCLUSIONS

The following conclusions are drawn in respect to the present study.

(1) A model of the end-burning traveling charge has been formulated, encoded, and demonstrated. The model is suitable for assessing the hydrodynamic and ideal combustion limits on the ballistic performance of traveling charge guns.

(2) Good agreement has been shown with an exact solution for a simplified case. Studies of mesh indifference and global conservation of mass and energy indicate that the numerical error associated with ballistic predictions of a nominal traveling charge configuration based on 41 mesh points is of the order of 0.1%-1.0%.

(3) A review of the arguments which deny the admissibility of a strong steady deflagration wave has revealed that this combustion limit is a manifestation of the well known steady flow process of choking by heat addition. It does not appear likely that this limit can be circumvented without sacrificing ballistic performance by the incorporation of condensed additives to control the effective flow area of the gas phase within the flame.

(4) Preliminary calculations have shown the importance of proper lubrication of the interface between the traveling charge and the tube. A coefficient of friction equal to 0.1 resulted in a loss of 30% of the muzzle velocity predicted without friction.



## REFERENCES

1. May, I. W.; Baran, A. F.; Baer, P. G. and Gough, P. S.  
 "The Traveling Charge Effect"  
 Proceedings of the 15th JANNAF Combustion Meeting 1978
  
2. Krier, H. and Summerfield, M.  
 "Interior Ballistics of Guns"  
 Progress in Astronautics and Aeronautics, Vol. 66  
 American Institute of Aeronautics and Astronautics 1979
  
3. Corner, J.  
 "Theory of the Interior Ballistics of Guns"  
 Wiley, New York 1950
  
4. Langweiler, H.  
 "A Proposal for Increasing the Performance of Weapons  
 by the Correct Burning of Propellant"  
 British Intelligence Objective Sub-committee, Group 2,  
 Ft. Halstead Exploiting Center, Report 1247 undated
  
5. Vinti, J. P.  
 "Theory of the Rapid Burning of Propellants"  
 Ballistic Research Laboratories Report No. 841 1952
  
6. Lee, L. and Laidler, K. J.  
 "The Interior Ballistics of the Impulse Propulsion Gun"  
 Nord 10260 Contract Report CU/F/51.2 August 1951
  
7. Friedrichs, K. O.  
 "On the Mathematical Theory of Deflagrations and  
 Detonations"  
 NAVORD Report 79-46 1946
  
8. Courant, R. and Friedrichs, K. O.  
 "Supersonic Flow and Shock Waves"  
 Interscience, New York 1948
  
9. Williams, F. A.  
 "Combustion Theory"  
 Addison-Wesley 1965
  
10. Landau, L. D. and Lifschitz, E. M.  
 "Fluid Mechanics"  
 Pergamon Press 1959
  
11. Petrovsky, I. G.  
 "Partial Differential Equations"  
 Interscience, New York 1954
  
12. Murnaghan, F. D.  
 "Finite Deformation of an Elastic Solid"  
 Dover, New York 1967

13. Holman, J. P.  
"Heat Transfer"  
McGraw-Hill, New York 1968
14. Fung, Y. C.  
"Foundations of Solid Mechanics"  
Prentice-Hall 1965
15. Walsh, J. L.; Ahlberg, J. H. and Nilson, E. N.  
"Best Approximation Properties of the Spline Fit"  
J. Math. Mech. 11, 225-234 1962
16. MacCormack, R. W.  
"The Effect of Viscosity in Hypervelocity Impact  
Cratering"  
AIAA Paper 69-354 1969
17. Richtmyer, R. D. and Morton, K. W.  
"Difference Methods for Initial Value Problems"  
2nd Edition John Wiley, New York 1967
18. Shapiro, A.  
"The Dynamics and Thermodynamics of Compressible  
Fluid Flow"  
Ronald Press, New York 1953

## Nomenclature

$A_b$	Cross sectional area of tube
$A_*$	Throat area of gas-permeable breech
$a$	Wave speed in solid propellant
$a_1$	Value of $a$ at zero pressure
$a_2$	Value of $a$ during unloading or reloading
$\alpha$	Acceleration
$B_1$	Additive constant in measured burn rate law
$B_2$	Pre-exponential factor in measured burn rate law
$b$	Covolume of gas
$C_{DB}$	Discharge coefficient of gas-permeable breech
$C_{DMUZ}$	Discharge coefficient of muzzle
$c$	Isentropic sound speed in gas
$c_p$	Specific heat at constant pressure
$c_v$	Specific heat at constant volume
$D$	Diameter of tube
$e$	Internal energy of gas
$e_p$	Chemical energy of propellant
$F$	Resistance to projectile motion
$f_w$	Force of friction exerted on wall by propellant
$g_o$	Constant used to reconcile units of measurement
$h$	Film coefficient
$l_b$	Length of bearing section of obturator
$M_b$	Mass of projectile in front of midpoint of obturator
$M_p$	Mass of projectile
$M$	Molecular weight of gas
$m_p$	Mass of propellant
$n$	Burn rate exponent
$Pr$	Prandtl number
$p$	Pressure in gas
$p_a$	Pressure in shocked air ahead of projectile
$p_{band}$	Resistive pressure due to obturator
$p_s$	Shot start pressure
$p_{ST}$	Initial pressure of gas
$p_o$	Initial pressure of air ahead of projectile

$Q_w$	Coefficient in correlation for heat loss to tube
$q_w$	Heat loss to tube
$Re_D$	Reynolds number based on D
$R$	Gas constant
$r$	Regression rate of propellant
$T$	Gas temperature
$T_w$	Wall temperature
$t$	Time
$u$	Gas velocity
$u_p$	Propellant velocity
$W$	Charge to Projectile Mass Ratio
$x$	Axial coordinate
$x_p$	Position of projectile base relative to breech
$x_p$	Position of gas/propellant interface relative to breech
$\alpha$	Coefficient in acoustic characteristic form for gas
$\alpha_p$	Coefficient in acoustic characteristic form for propellant
$\beta$	Additive term in acoustic characteristic form for gas
$\beta_p$	Additive term in acoustic characteristic form for propellant
$\Gamma_g^o, \Gamma_g^\pm$	Gas-material, gas-acoustic characteristic lines
$\Gamma_p^o, \Gamma_p^\pm$	Propellant-material, propellant-acoustic characteristic lines
$\gamma$	Ratio of specific heats of gas
$\gamma_a$	Ratio of specific heats of air
$\Delta t$	Time step
$\Delta \zeta$	Spacewise mesh increment in computational plane
$\delta_f$	Thickness of gas film used to lubricate propellant
$\zeta$	Nondimensional axial coordinate in computational plane
$\eta$	Velocity of convective mesh
$\theta$	Coefficient in material characteristic form for gas
$\theta_p$	Coefficient in material characteristic form for propellant
$\kappa$	Thermal conductivity of gas
$\mu$	Viscosity of gas

$\mu_f$	Viscosity of lubricating film
$\mu_w$	Coefficient of friction between propellant and tube wall
$\mu_{wb}$	Coefficient of friction between obturator and tube wall
$\nu$	Poisson ratio of projectile
$\rho$	Density of gas
$\rho_p$	Density of propellant
$\rho_{p_0}$	Value of $\rho$ at zero pressure
$\sigma$	Pressure in propellant
$\sigma_*$	Value of $\sigma$ on nominal loading curve

---

A dot over a quantity indicates a total derivative with respect to time.





## Appendix A: On the Deflagration Wave with Supersonic Reactants

The purpose of this appendix is to note briefly the arguments which have been advanced to deny the possibility of a steady deflagration with supersonic reactants as perceived by an observer moving with the flame. These arguments are based on the details of the structure of the flame and have been established in the context of a single phase gas flow. Subsequently, we comment on the implications of a heterogeneous two-phase structure in regard to the possibility of supersonic flow. Finally, we note the implications of our findings as regards the traveling charge.

The theory of detonations and deflagrations, as it affects our present discussion, is treated fully in the monograph of Courant and Friedrichs<sup>8</sup>. From their development we shall abstract only those results which bear directly on the present discussion. In particular, we will note their treatment of the allowable states which may be reached in a steady exothermic flow without the restrictions imposed by considerations of the structure of the reaction zone. This discussion will provide the essential nomenclature and conceptual framework within which the basis for denial of the possibility of a deflagration with supersonic reactants can be understood. Following the presentation of this denial we will note the comments of other authors in relation to the single phase deflagration.

The basic constraints on the allowable steady state processes with properties observed at two stations, which we designate by subscripts 0 and 1 respectively, are the laws of conservation of mass, momentum and energy. We have already noted these in the present report. In order to keep the discussion of this appendix self-contained we restate them here and we introduce somewhat different nomenclature. The symbols used in this appendix will be defined as they are introduced.

Using  $p$  and  $\rho$  to denote pressure and density and letting  $v$  be the gas velocity in a frame of reference moving with the reaction zone we have

$$\rho_0 v_0 = \rho_1 v_1 = m \quad (\text{A.1})$$

$$p_0 + \rho_0 v_0^2 = p_1 + \rho_1 v_1^2 \quad (\text{A.2})$$

$$E^{(0)}(\tau_0, p_0) + p_0 \tau_0 + \frac{1}{2} v_0^2 = E^{(1)}(\tau_1, p_1) + p_1 \tau_1 + \frac{1}{2} v_1^2 \quad (\text{A.3})$$

and where we have also introduced  $\tau = 1/\rho$  and  $E$  is the internal energy, assumed to be given as a function of  $\tau$  and  $p$ . The superscripts on the values of internal energy in (A.3) indicate that due to changes of composition, the functional form may vary from station 0 to station 1. The nomenclature used here is identical with that of Courant and Friedrichs. We will adopt the convention that the gas flows from station 0 to station 1.

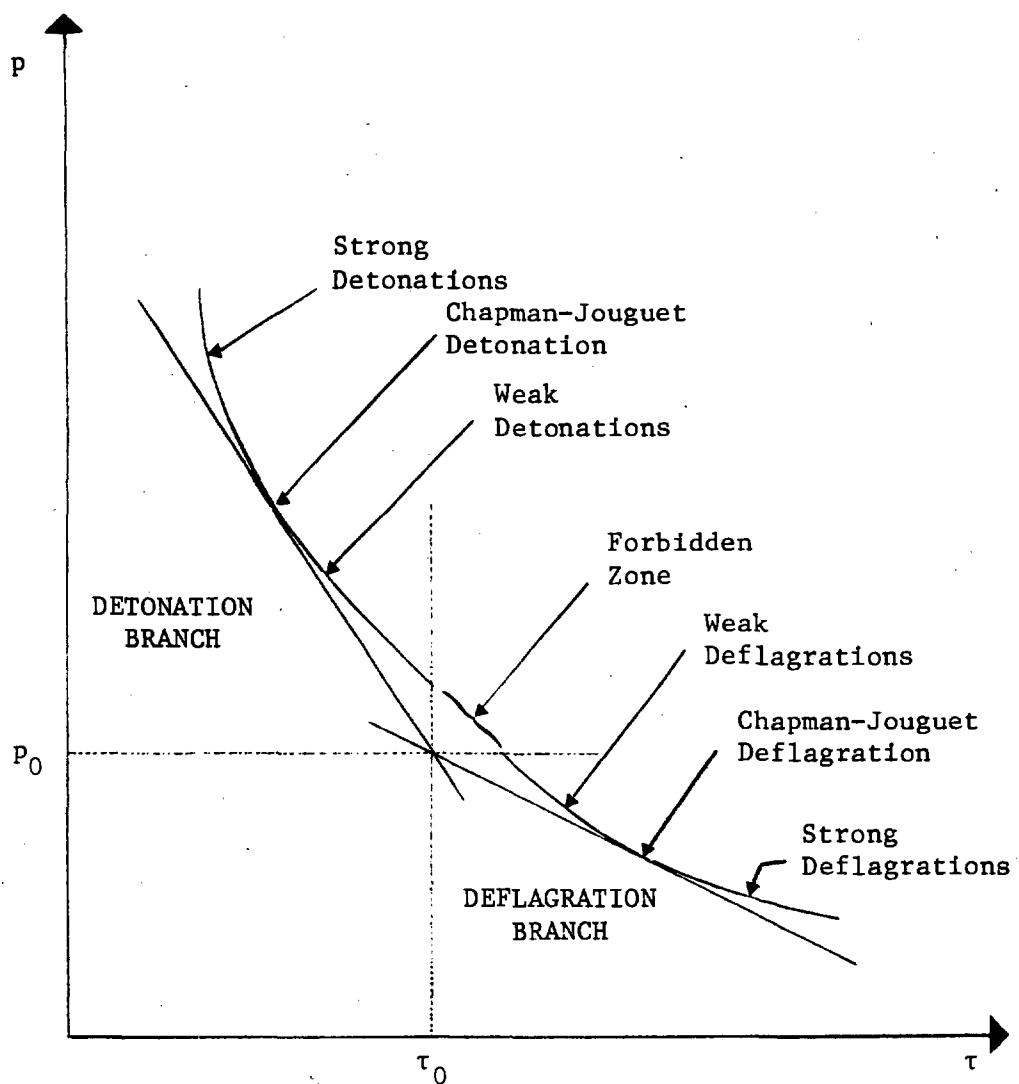


Figure A.1 Hugoniot curve for reacted gas

It should be noted that nothing has been said concerning the proximity of stations 0 and 1 or of the structure of the flow between them. It is assumed only that the flow is steady and that viscous stresses and heat conduction may be neglected at the two stations. In many cases of practical interest the flow may fail to be truly steady. Yet the present results may be regarded as approximately correct provided that the rates of change of mass, momentum and energy in the region bounded by stations 0 and 1 may be neglected by comparison with the fluxes of these quantities. Such conditions will be favored when the reaction zone is thin and the environment changes slowly.

From the conservation laws (A.1), (A.2) and (A.3) we may deduce two important relationships. First, from (A.1) and (A.2) we may deduce that

$$\frac{p_1 - p_0}{\tau_1 - \tau_0} = -m^2 \quad (\text{A.4})$$

Thus it is apparent that only those processes are possible in which the sign of the change in pressure is opposed to that of the specific volume. Observe, moreover, that when the reaction zone has finite thickness, but is steady, and viscous stresses may be neglected, then (A.4) applies throughout the reaction zone and shows that the pressure and specific volume are linearly related throughout the process.

Next, introduce the Hugoniot function for the burnt gas

$$H^{(1)}(\tau, p) = E^{(1)}(\tau, p) - E^{(1)}(\tau_0, p_0) + \frac{1}{2}(\tau - \tau_0)(p + p_0)$$

Then (A.3) may be written as

$$H^{(1)}(\tau, p) = E^{(0)}(\tau_0, p_0) - E^{(1)}(\tau_0, p_0) \quad (\text{A.5})$$

If the reaction is assumed to be exothermic as the gas flows from station 0 to station 1, it follows that the right hand side of (A.5) is positive.

Now suppose that the initial state  $\tau_0, p_0$  is given and regard (A.5) as a locus of possible final states. The graph of (A.5) appears as shown in figure A.1, subject to certain thermodynamic assumptions<sup>8</sup>. Because of (A.4) the accessible portion of (A.5) is confined to two separate branches, the upper corresponding to increases in pressure and the lower corresponding to decreases in pressure. These are referred to as the detonation and deflagration branches respectively. Equation (A.4) provides some immediate insight into an important difference between the two branches. It is apparent that the limiting constant pressure process--a deflagration--travels with an infinitesimal velocity. On the other hand, the limiting constant volume process--a detonation--travels with an infinite velocity. For the present discussion, only the deflagration branch is of interest.

The deflagration branch may itself be divided into two branches, identified in figure A.1 as weak and strong deflagrations, according to the magnitude of the pressure drop, and separated by a point identified as the Chapman-Jouguet deflagration. If one considers an arbitrary straight line emanating from  $(\tau_0, p_0)$  and intersecting with the deflagration branch it follows, subject to certain thermodynamic assumptions<sup>8</sup>, that the line has at most two points of intersection--one on the weak deflagration branch and the other on the strong deflagration branch. At the Chapman-Jouguet point, the straight line is tangent to the deflagration branch.

It may be shown that in the case of a weak deflagration, the reactants are subsonic relative to the reaction front and that in the case of a strong deflagration, they are supersonic. Naturally, the Chapman-Jouguet point is distinguished by the fact that the reactants are sonic with respect to the reaction front. In each case the speed of sound is understood to be that of the reacted gas. It is also shown by Courant and Friedrichs that in the case of an ideal gas, at least, a deflagration wave is always subsonic relative to the unreacted gas.

The foregoing discussion has distinguished between deflagrations with subsonic and supersonic reactants but has not identified any reasons to deny the admissibility of either. Indeed both the weak and strong deflagrations are clearly admitted by the principle of conservation of mass, momentum and energy. In order to show the impossibility of a steady strong deflagration wave it is necessary to consider the finite rate of reaction. Then the following geometrical argument may be employed.

Consider figure A.2. We show, schematically, the Hugoniot for the unreacted gas, the fully reacted gas, and the gas in several stages of partial reaction. That is to say, the preceding analysis is assumed to apply at all stages of the reaction. Now there are just two types of steady process which may occur between 0 and 1. The state may change continuously due to the finite rate of heat release by the reaction in which case we are required to traverse the straight line (A.4). Or, a compressive shock may occur, in which case we may traverse the Hugoniot corresponding to the state of reactedness at which the shock was encountered, the direction of the process being such as to lead to an increase in pressure.

It is evident, from the assumed shape of the Hugoniot curves illustrated in figure A.2, that a continuous process of heat release from 0 to 1 must inevitably intercept the weak deflagration branch when the reaction is complete. Accordingly, a transition to the second intersection point in the strong deflagration branch would require an expansion shock, which is inherently unstable. On the other hand, any admissible shock transition at a state of partial reactedness, can only lead to higher pressure from which only an intersection with the weak deflagration branch is possible, unless a detonation is admitted.

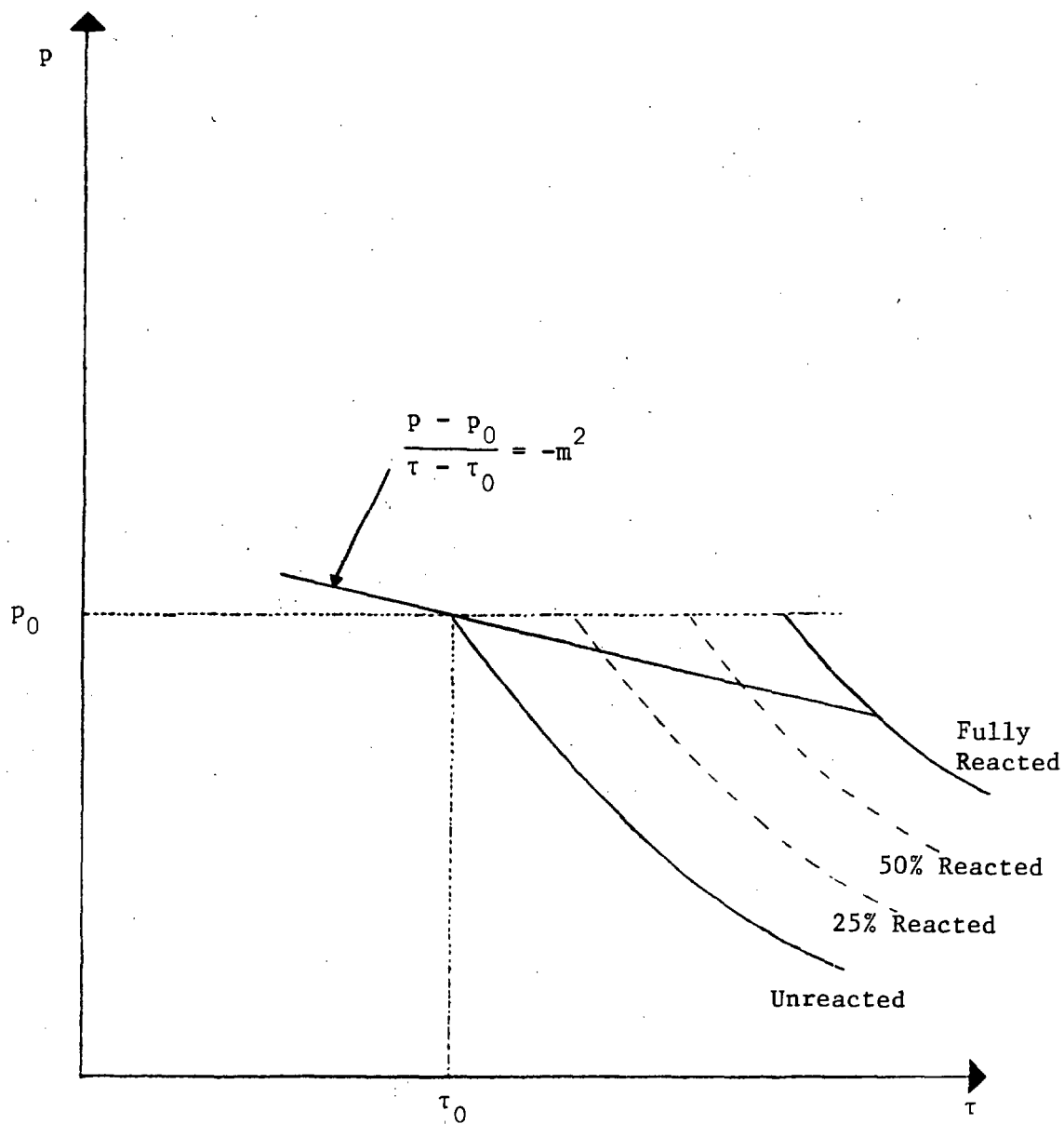


Figure A.2 Schematic demonstration of the implausibility of attaining a strong deflagration

This geometrical argument was also formalized by Courant and Friedrichs to provide an analytical demonstration that a simple flame model would reach a state of complete reactedness on the weak deflagration branch. The earlier work of Friedrichs<sup>7</sup> and the book by Williams<sup>9</sup> may also be consulted for demonstrations based on the structure of the solutions of particular models of the reaction zone. Landau and Lifschitz<sup>10</sup> have considered the problem from the point of view of the stability of the process. Considering the characteristic data on each side and assuming that just one internal condition is specified by the flame structure leads to the conclusion that a perturbation about a strong deflagration is underdetermined. Accordingly, exponentially growing solutions are admitted and the flame is unstable. The discussion of the inadmissibility of the strong deflagration wave given by Vinti<sup>5</sup> is essentially the same as the geometrical argument given here.

An alternative way of understanding the limitation of the reaction process to weak or at most sonic deflagrations follows from a consideration of the laws of choking in quasi-one-dimensional compressible flow. Moreover, this alternative point of view enables one to consider directly the consequences of a multiphase structure of the flame.

Consider a generalized quasi-one-dimensional steady flow in the manner described by Shapiro<sup>18</sup>. From the balance equations for a control volume as shown in figure A.3 one may deduce the following functional dependence of the Mach number  $M$  on the processes associated with the flow, namely cross sectional area, heat and mass addition and drag.

$$\begin{aligned} \frac{dM^2}{M^2} = & - \frac{2[1 + \frac{\gamma-1}{2} M^2]}{1 - M^2} \frac{dA}{A} + \frac{1 + \gamma M^2}{1 - M^2} \frac{dQ - dW_x + dH}{c_p T} \\ & + \frac{\gamma M^2 [1 + \frac{\gamma-1}{2} M^2]}{1 - M^2} \left\{ 4f \frac{dx}{D} + \frac{dX}{\frac{1}{2}\gamma p A M^2} - 2y \frac{d\omega}{\omega} \right\} \\ & + \frac{2(1 + \gamma M^2)(1 + \frac{\gamma-1}{2} M^2)}{1 - M^2} \frac{d\omega}{\omega} - \frac{1 + \gamma M^2}{1 - M^2} \frac{dW}{W} - \frac{d\gamma}{\gamma} \end{aligned} \quad (A.6)$$

The nomenclature of this equation is taken directly from Shapiro and has the following significance.

$M$  is the Mach number based on the ideal gas equation of state for which the speed of sound  $c$  is given by  $c^2 = \gamma RT/W$ .

$A$  is the net flow area for the gas. That is, the area of the duct less the area of the entrained liquid or droplets or particles.

<sup>18</sup> Shapiro, A. "The Dynamics and Thermodynamics of Compressible Fluid Flow" Ronald Press, New York 1953

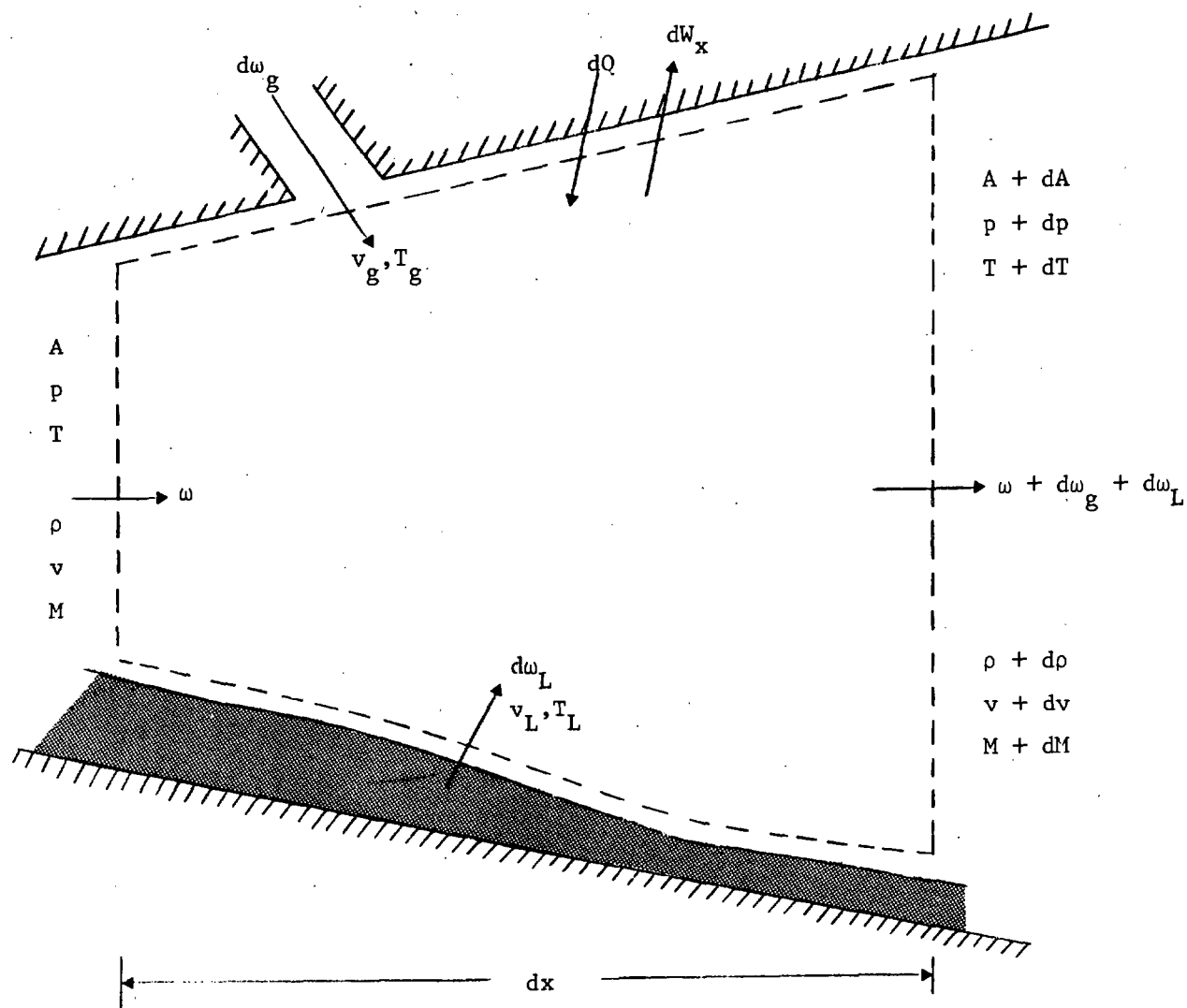


Figure A.3 Control volume for analysis of steady heterogeneous reacting flow (Shapiro, ref. 18)

$\gamma$  is the ratio of specific heats

$dQ$  is the net heat added to the gas stream by conduction or radiation from external sources, per unit mass of gas entering the control surface.

$dW_x$  is the net external work to outside bodies per unit mass entering the control surface.

$$dH = dh_{pr} - [\bar{c}_{pg} (T - T_{og}) + v^2/2] \frac{d\omega_g}{\omega} - [h_L - h_v + \frac{v^2 - v_L^2}{2}] \frac{d\omega_L}{\omega}$$

$dh_{pr}$  is the heat release per unit mass of gas stream due to decomposition, positive for an exothermic reaction.

$f$  is the wall friction factor.

$D$  is the hydraulic radius.

$dX$  is the sum of the drag of stationary bodies, the drag of droplets, particles and filaments traveling more slowly than the gas stream, and the body or gravity forces.

$$y = [y_g \frac{d\omega_g}{\omega} + y_L \frac{d\omega_L}{\omega}] / (\frac{d\omega}{\omega})$$

$$y_g = v'_g/v \quad y_L = v'_L/v$$

$$d\omega = d\omega_L + d\omega_g \quad \text{See Figure A.3}$$

$W$  is the molecular weight.

$R$  is the gas constant.

$h_L$  is the enthalpy of liquid about to evaporate as it enters the control volume.

$h_v$  is the enthalpy of evaporated liquid  $d\omega_L$  at temperature  $T$ .

$T_{og}$  is the stagnation temperature of the injected gas stream.

$\bar{c}_{pg}$  is the average value of  $c_p$  between  $T_{og}$  and  $T$ .

The remaining symbols may be identified from figure A.3 and the convention that  $v'_g$  and  $v'_L$  are the streamwise components of the velocities of the injected gas and liquid.

From a consideration of equation (A.6), which is seen to embed extremely complex behavior, the following conclusions may be drawn<sup>18</sup>.

- (1) An increase in area acts to decrease the value of  $M$  if  $M < 1$  and to increase  $M$  if  $M > 1$ .



- (2) Heat addition or combustion acts to increase  $M$  if  $M < 1$  and to decrease  $M$  if  $M > 1$ .
- (3) The effect of friction, or drag of internal bodies, acts to increase  $M$  if  $M < 1$  and to decrease  $M$  if  $M > 1$ .
- (4) Mass addition with  $y < 1$  acts to increase  $M$  if  $M < 1$  and to decrease  $M$  if  $M > 1$ .
- (5) An increase in  $W$  acts to decrease  $M$  if  $M < 1$  and to increase  $M$  if  $M > 1$ .
- (6) An increase in  $\gamma$  always acts to reduce  $M$ .

These results permit us to understand the denial of the admissibility of the strong deflagration wave from an alternative point of view. The previous discussion, based on the assumed shape of the Hugoniot of the reactants, corresponds to a process in which only heat addition due to combustion was of interest. Evidently, if we consider an arbitrary initial state, presumed subsonic, the Mach number increases steadily as we pass towards the fully reacted state. If, however, the Mach number increases to unity, there is no longer a solution to the steady flow problem unless the initial state may be altered. Thus the inadmissibility of the strong deflagration wave is perceived to be a manifestation of the well-known phenomenon of choking.

In the heterogeneous flame we must also consider mass addition and drag. These, too, always drive the Mach number towards unity just as the heat addition does. Only one possibility appears to exist in the heterogeneous flame whereby the sonic point can be passed in a continuous manner. The cross-sectional area of the flow will increase due to consumption of the dispersed condensed phase and also, possibly, due to separation of the droplets or particles as a consequence of the drag. If, as the sonic point is encountered, the effect of change of area is such as to dominate the opposing effects of heat addition, mass addition and drag, then a continuous transition to supersonic flow would be possible. A trivial example of such a case is, of course, the converging-diverging rocket nozzle in which the cross-sectional area of the duct is used to effect the transition from subsonic to supersonic flow.

The possibility of obtaining such continuous transitions by means of the area change associated with condensed phase fuel consumption and dispersal may be determined only by parametric studies of equation (A.6). Such studies are beyond the scope of the present enquiry. However, we may speculate that the conditions under which the transition could be made would correspond to fuels of rather low ballistic efficiency in which inert components would play the role of a conventional rocket nozzle.

We conclude with some comments on the implications of these results as regards the end-burning traveling charge. First, we concur with Vinti's conclusion that the Langweiler process would be inherently incapable of realization once the projectile velocity exceeded the speed of sound in the reacted gas. Only by making the reaction zone sufficiently thick that unsteady effects become important can we expect to develop supersonic reactants. Of course, as the reaction zone becomes

thicker, we approach the configuration of a conventional propelling charge in which, as discussed in the introduction to this report, the reaction zone effectively fills the tube. However, the rejection of the Langweiler scheme does not necessarily defeat the concept of the traveling charge as a potentially useful ballistic solution. Because the thrust associated with the Langweiler scheme increases continually as the projectile accelerates, the gun is required to operate at a condition which is far removed from the ideal constant pressure cycle. Moreover, the pressure on the unreacted side of the gas/propellant interface is found to rise very sharply as the Mach number increases beyond unity.

Hence, the present findings are more appropriately considered in the context of an ideal constant base pressure scheme for the burning rate. In this context, the denial of the possibility of a strong deflagration wave is not necessarily restrictive. It is merely necessary that the Chapman-Jouguet point be reached so that the combustion zone is just uncoupled from the pressure of the column of reactants. In such a case the propellant will burn under a choked condition. However, it seems probable that the pressure of the unreacted propellant would be influenced not only by the chemical formulation of the propellant but also by its mechanical behavior during the interior ballistic cycle.

## Appendix B: Code Description and Fortran Listing

The model of the end burning traveling charge has been encoded in the FORTRAN IV language for implementation on the CYBER 7600 computer and is documented by the listing which forms the principal part of this appendix. We provide a summary of the routines, their purpose and their linkages to other routines, in Table B.1. In Table B.2 we provide a glossary of those variables which are contained in the common block areas of storage. Local variables are not described. Table B.3 summarizes, in detail, the input files used to run the program.

In addition to the tabular information, we provide the following brief discussion of the code structure, paying particular attention to the manner in which the physical problem is represented. We also comment on the code output.

The program consists of a main routine, TCMAN, which is supported by a total of twenty subfunctions and subprograms. For ease of maintenance, particularly in connection with the constitutive laws, a largely modular approach has been followed in writing the code. Only the co-volume equation of state of the gas is intrinsically bound into the code; the remaining constitutive laws are expressed by individual subroutines. With the exception of subroutine BASE, which embeds the rather complicated logic associated with the various combustion models and the branching among them, the programming is extremely straightforward.

The principal computational arrays are GS1(100,3), GS2(100,3) and GS3(100,3) as described in Table B.2. The first index of these arrays points to a mesh location, a maximum of 100 points being admitted by the present dimension statements. The second index points to a storage level and is assigned the values 1,2,3 on a rotating basis. At any level, the index NI points to current storage; that is to say, NI points to the present data at the outset of a predictor step and is advanced to point to the predicted future data on the corrector step. The index NF points to the storage level which contains the future data. Finally, the index NP is used, on the corrector step, to point to the present data. The principal integration step counter is NDT, which is incremented by one on each predictor and each corrector level.

At any time, the gas column is represented by NDIM mesh points whose data occupy the first NDIM locations of GS1, GS2 and GS3. If the propellant is treated as a continuum, its data occupy the storage locations NDIM1 to NDIM2 of GS1, GS2 and GS3, where  $NDIM1 = NDIM + 1$ .

The execution of the program is controlled by the data described in Table B.3. Multiple runs may be performed as follows. For a given problem, a parametric series may be run using an array of values of the ratio of charge-to-projectile mass. At the conclusion of this series, the program returns to its starting point and looks for another complete set of data. If none is furnished, exit occurs. When a parametric series is to be conducted, the input datum IDEALI, which defines the

combustion model, is also consulted. The basic values of IDEALI are zero, if measured burn rate data are used; one, if Langweiler burning is used; and two, if the pressure on the unreacted side of the gas/propellant interface, or the projectile acceleration is specified. By setting IDEALI equal to three or four, initial conditions are deduced, using the relations described in section 2.6, to yield the appropriate value of pressure or acceleration in combination with the designated charge-to-projectile mass ratio. Following the evaluation of the initial data in such cases, IDEALI defaults internally to the value two. It should also be noted that when the initial properties are deduced from the charge-to-projectile mass ratio, the propellant density is determined from a user-supplied value of the loading density and may differ from the value typical of the homogeneous substance.

We also note, in regard to those data which are defined in a tabular fashion, that, except for the measured burn rate data, the following interpretation is made in a consistent manner. Values of the dependent variable are deduced for an argument lying within the table range of the independent variable by means of linear interpolation. When an argument is furnished which lies below or above the table range, the dependent variable is assigned the first or the last entry, accordingly. The measured burn rate coefficients are assumed to be constant until the mass fraction consumed at any time exceeds the corresponding value ZR assigned to the coefficients. Interpolation does not occur.

We conclude by commenting on the output of the code. The principal logical index in this regard is the input quantity NPRO. If it is zero, the continuum state variables are printed at times which are integer multiples of the input quantity TINOM. By setting NPRO equal to one, two or three, various bodies of compressed output can be obtained in place of the full tables of continuum data. If NPRO is four, no intermediate results are printed. In all cases, the calculation concludes with a table of summary data of ballistic interest. The code also tracks the total mass and energy of the system at any time. At the conclusion of the run the maximum and final percentage defects of these quantities, from the initial values, are printed. These may be used to assess the approximate magnitude of the errors of numerical integration in cases where physical losses do not occur due to dissipation or outflow.

Table B.1 Summary of Routines - Purpose and Linkages

**TCMAIN**                    Called by: NONE  
                          Calls:     BAR1, BAR2, BAR3, BAR4, BASE  
  BASEPR, BREECH, GETK, OUTFLO,  
  REFIT, SIGCHK, VELCHK  
                          Purpose:     Main program and principal executive  
routine. TCMAIN reads and prints problem data, initializes constants,  
and then either calls BAR1 to initialize the state variables or reads  
data from unit 8 if problem is restarted. TCMAIN organizes the two-  
level integration scheme and is supported by specialized subroutines  
which handle interior mesh points (BAR3) and the various boundary  
conditions (BASE, BASEPR, BREECH, OUTFLO). TCMAIN provides printed  
output and disc storage of solution in accordance with user-supplied  
data. Summary data are accumulated and are printed at the termination  
of each case.

**BAR1**                    Called by: TCMAIN  
                          Calls:     BURN, RNOM, REFIT, RESP  
                          Purpose:     BAR1 initializes continuum arrays and,  
through the call to REFIT, establishes the initial mesh.

**BAR2**                    Called by: TCMAIN, BAR3, CARAC  
                          Calls:     None  
                          Purpose:     Utility routine, BAR2 transforms  
computational variables into ordinary state variables.

**BAR3**                    Called by: TCMAIN  
                          Calls:     BAR2, HTW, WFR  
                          Purpose:     Integration of all continuum equations  
at all interior mesh points. Called twice per integration step, once  
for each level.

**BAR4**                    Called by: TCMAIN  
                          Calls:     DSDR  
                          Purpose:     Computes maximum time step allowable  
according to Courant-Friedrichs-Lewy stability condition and safety  
factor SAFE.

**BASE**                    Called by: TCMAIN  
                          Calls:     BURN, CARAC, DSDR, RESP, RNOM  
                          Purpose:     Subroutine BASE is responsible for the  
determination of the boundary values at the base of the projectile, fol-  
lowing burnout, and at the gas/propellant interface for all the com-  
bustion models. If the propellant is treated as a continuum, its boun-  
dary values at the interface are also deduced by BASE. The routine is  
called twice per update step, once at each level.

**BASEPR**                  Called by: TCMAIN  
                          Calls:     CARAC, DSDR, RNOM  
                          Purpose:     Updates boundary values at base of  
projectile when the propellant is treated as a continuum. Called twice  
per integration step.

BREECH                    Called by:    TCMAIN  
                           Calls:        CARAC  
                           Purpose:      Updates boundary values at breech of  
 tube when breech is closed or impermeable to gas.

BURN                     Called by:    BAR1, BASE  
                           Calls:        None  
                           Purpose:      Computes measured burn rate as a function  
 of pressure of reactants.

CARAC                   Called by:    BASE, BASEPR, BREECH, OUTFLO  
                           Calls:        BAR2, DSDR  
                           Purpose:      Given a value of the velocity at a  
 boundary mesh point, CARAC deduces a value of pressure which is compatible  
 with the given value and also with the flow in the interior.

DSDR                    Called by:    BAR4, BASE, BASEPR, CARAC  
                           Calls:        SNOM  
                           Purpose:      Computes wave speed in propellant as  
 a function of density and rate-of-change of density.

GETK                    Called by:    TCMAIN  
                           Calls:        RESP  
                           Purpose:      Computes time derivatives of state  
 variables governed by ordinary differential equations. Called twice  
 per integration step, once at each level.

HTW                     Called by:    BAR3  
                           Calls:        None  
                           Purpose:      Computes heat loss per unit volume  
 due to heat transfer from gas to tube wall.

OUTFLO                  Called by:    TCMAIN  
                           Calls:        CARAC  
                           Purpose:      Computes boundary values at gas permeable  
 breech and also at muzzle following expulsion of the projectile. Called  
 twice per integration step.

REFIT                   Called by:    TCMAIN, BAR1  
                           Calls:        None  
                           Purpose:      Allocates mesh and performs spline  
 interpolation of data when mesh changes.

RESP                    Called by:    BAR1, BASE, GETK  
                           Calls:        None  
                           Purpose:      Computes resistance to projectile motion  
 due to friction on obturator and pressure of shocked air in barrel.

RNOM                    Called by:    BAR1, BASE, BASEPR  
                           Calls:        None  
                           Purpose:      Computes propellant density as a  
 function of pressure on nominal loading curve.

SIGCHK                    Called by:    TCMAIN  
                          Calls:        SNOM  
                          Purpose:        Checks that state of continuum propellant does not lie above nominal loading curve.

SNOM                     Called by:    DSDR, SIGCHK  
                          Calls:        None  
                          Purpose:        Computes propellant pressure as a function of density on nominal loading curve.

VELCHK                   Called by:    TCMAIN  
                          Calls:        None  
                          Purpose:        Checks that continuum propellant velocity has not reversed sign as a consequence of friction.

WFR                      Called by:    BAR3  
                          Calls:        None  
                          Purpose:        Computes friction between continuum propellant and tube wall.

Table B.2

## Glossary of Principal Fortran Variables

---

AB	Bore Area
ADWN	Unload/Reload wave speed in propellant
AIRGAM	Ratio of specific heats of air in barrel in front of projectile
AIRMW	Molecular weight of air in barrel
AIRPO	Pressure of unshocked air in barrel
AIRTO	Temperature of unshocked air in barrel
AMU(10)	Array of coefficients of friction between propellant and tube
AMUV(10)	Array of velocities corresponding to AMU
ANU	Poisson ratio of projectile
APMAX	Maximum allowable acceleration of projectile
ASBR	Throat area of gas-permeable breech
AUP	Loading wave speed in propellant
BMU(10)	Array of coefficients of friction between obturator and tube wall
BMUV(10)	Array of velocities corresponding to BMU
BR(10)	Array of resistive pressures due to obturator
BRX(10)	Array of projectile displacements corresponding to BR
BN(20)	Array of burn rate exponents
BV	Covolume of gas
B1(20)	Array of burn rate additive constants
B2(20)	Array of burn rate pre-exponential factors
CDBR	Discharge coefficient of gas-permeable breech
CDMUZ	Discharge coefficient of muzzle



CHTW	Coefficient of wall heat transfer correlation
CM	Unreacted propellant mass
CV	Specific heat of gas at constant volume
DB	Diameter of barrel
DELTAX	Non-dimensional mesh spacing in gas column
DELTBX	Non-dimensional mesh spacing in propellant
DELYR	Thickness of gas film used to lubricate propellant
DRHO(2)	Total time derivative of density of propellant at boundaries
DXMIN	Minimum allowable mesh spacing in physical plane
E(100)	Array of values of internal energy
ECHEM	Chemical energy of propellant
ELB	Length of bearing section of obturator
ETA(100)	Array of values of velocity of mesh
GAM	Ratio of specific heats of gas
GS1(100,3)	Computational array. If I corresponds to the gas GS1(I,J) contains the quantity $\rho x_p$ at the I-th mesh point at the J-th level of integration. Otherwise GS1(I,J) contains the value of $\rho_p$
GS2(100,3)	Computational array. If I corresponds to the gas, GS2(I,J) contains the quantity $\rho u x_p$ at the I-th mesh point and the J-th integration level. Otherwise GS2(I,J) contains $u_p$ .
GS3(100,3)	Computational array. If I corresponds to the gas, GS3(I,J) contains the quantity $\rho x_p (e + u^2/2g_0)$ at the I-th mesh point and the J-th level of integration. Otherwise, GS3(I,J) contains $\sigma$ .
IDEAL	Burn rate indicator. See File 2 discussion of IDEALI.
INT	Set equal to 1 on predictor level and 0 on corrector level of integration step

K(4,2)	Array of derivatives of $X_p$ , $\dot{X}_p$ , $M_p$ and $x_p$ at predictor and corrector levels.
MACH	Maximum allowable Mach number of reactants relative to regressing interface
MAXDIM	Maximum allowable number of mesh points
MOL	Molecular weight of gas
NBR	Number of increments of propellant for tabular description of burn rate coefficients
NBRES1	Number of entries in tabular description of resistance due to obturator
NBRES2	Indicator for calculation of resistance due to shocked air in front of projectile
NBRES3	Number of entries in tabular description of coefficient of friction of obturator as a function of projectile velocity
NBRV	Indicator that breech is gas-permeable or otherwise
NCJ	Error indicator
NDIM	Number of mesh points allocated to gas
NDIM1	NDIM + 1
NDIM2	Total number of mesh points allocated when propellant is treated as a continuum
NDT	Integration counter. Incremented on both predictor and corrector levels
NF	Pointer to next integration level of storage
NHTW	Indicator that wall heat loss is considered or otherwise
NI	Pointer to current integration level storage
NMUZBL	Indicator that blowdown is to be computed or otherwise
NP	Pointer to previous integration level storage

NPRC	Indicator that propellant is treated as continuum or otherwise
NPRO	Print option indicator. See File 2.
NWFR	Indicator of representation of friction between solid propellant and tube. If positive, number of entries in tabular description of coefficient of friction as a function of velocity of propellant
P(100)	Array of values of pressure
PBRF	Value of breech pressure at which blowdown computation is terminated
PDIA	Value of pressure which must be exceeded in breech prior to onset of permeability
PRM	Projectile mass
PRMB	Projectile mass ahead of midpoint of obturator
PST	Initial pressure of gas
QORF(100)	Array of values of heat loss, if mesh point corresponds to gas, and wall friction, if point corresponds to propellant
RDOT	Rate of regression of interface relative to unreacted propellant
RHO(100)	Array of values of density
RHOP	Initial density of propellant at zero pressure
SIG	Value of pressure on unreacted side of gas/propellant interface
SIGMAX	Maximum allowable value of SIG
SSTART	Shot start pressure
T(100)	Array of values of temperature
U(100)	Array of values of velocity
XB	Length of gas column
XBB	Length of propellant column

XI1	$\frac{\gamma}{\gamma - 1} \frac{P_o}{\rho_p}$
XI2	$e_p - \frac{P_o}{\gamma - 1} \left( \frac{1}{\rho_p} - b \right)$
XLPRI	Initial length of propellant column
XPR	Projectile travel
XPROP	Initial position of base of projectile relative to breech
ZR(20)	Array of values of mass fraction of propellant for tabular description of burn rate coefficients

Table B.3 Description of Input Files

---

File 1: One Card (20A4)      Mandatory

---

ITIT                      Problem title. Up to 80 alphanumeric characters

---

File 2: One Card (16I5)      Mandatory

---

IDEALI                      Propellant burn rate indicator  
0 - Measured burn rate data. File 6 required.  
1 - Langweiler ideal burning  
2 - Ideal burning with prespecified value of pressure on unreacted side of gas/propellant interface or of projectile acceleration. Note the discussion of SIGMAX, MACH, APMAX in File 4.  
3 - Like 2 except that APMAX is deduced from SIGMAX according to initial propellant mass. Option used for parametric studies in which SIGMAX is to be constant while charge-to-projectile mass ratio varies.  
4 - Like 2 except that PSTI (File 4) and SIGMAX are computed from APMAX according to initial propellant mass. Option used for parametric studies in which APMAX is to be held constant while charge-to-projectile mass ratio varies.

NPRC                      0 - Propellant treated as rigid  
1 - Propellant treated as continuum. File 7 required.

NPRO                      Print Option for logout other than summary data  
0 - Detailed print including flow profiles  
1 - One line summary at each logout step  
2 - Energy trajectory printed  
3 - Interior ballistic data and % energy trajectory printed  
4 - No print other than summary

NDSK                      Disc read/write parameter. If active, unit 8 must be defined.  
0 - Neither read nor write  
1 - Write only  
2 - Read only  
3 - Read and write

NDSKID                      Problem identifier if multiple storage on unit 8

NDSKDT                      Time step for restart of problem if NDSK = 2 or 3

NPAR                      Number of parametric cases. If NPAR > 0, File 17 is required.

NBR                      Number of entries in burning rate table, File 6.  
Default value is NBR = 1 (Maximum of 20)

NWFR	Propellant Wall Friction Parameter 0 - Friction between propellant and tube not considered -1 - Friction due to gas film. File 8 required. >0 - Number of entries in velocity dependent coefficient of friction table. (Maximum of 10). File 9 required.
NBRES1	0 - Obturator resistance not given as table >0 - Number of entries in table of resistive pressure versus travel (Maximum of 10). File 10 required.
NBRES2	0 - Resistance due to shocked air not considered 1 - Resistance due to shocked air considered. File 11 required.
NBRES3	0 - Obturator resistance not proportional to setback pressure. >0 - Number of entries in table of velocity dependent coefficient of friction of obturator. (Maximum of 10). Files 12 and 13 required.
NHTW	0 - Heat loss to wall not considered. 1 - Heat loss considered. File 14 required.
NMUZBL	0 - Tube blowdown after muzzle exit not considered. 1 - Blowdown considered. File 15 required.
NBRV	0 - Breech closed. 1 - Breech gas-permeable. File 16 required.

---

File 3: One Card (4I5, 5F10.0)      Mandatory

---

NSTOP	Number of integration steps before termination. If NSTOP = 99999, number is unbounded.
MAXDIM	Maximum number of mesh points to be used in continuum representations. ( $\leq 100$ )
NCY1	Following step NCY1, NPRO will default internally to 0 to yield detailed printing.
NCY2	Following step NCY2, NPRO resumes the value specified in File 2.
TINOM	Time interval for printing (See NPRO, File 2) and disc storage (See NDSK, File 2). (msec)
TISTOP	Time at which computation is to be terminated (msec)
XSTOP	Projectile travel at which computation is to be terminated (ins)

SAFE            Safety factor by which C-F-L time step is divided.  
                  Must be at least one.

DXMIN           Minimum mesh size for continuum representation (ins).

---

File 4: One Card 8F10.0)      Mandatory

---

DB              Diameter of tube (ins)

XIB              Initial length of gas column (ins)

PRM              Mass of projectile

SSI              Shot start pressure (psi)

PSTI             Initial pressure of gas (psi)

SIGMAX           Maximum value of pressure on unreacted side of  
                  gas/propellant interface. If SIGMAX = 0, no  
                  restriction is considered. (psi)

MACH             Maximum value of Mach number of reactants relative  
                  to regressing surface. If MACH = 0, no restriction  
                  is considered.

APMAX            Maximum value of acceleration of projectile.  
                  If APMAX = 0, no restriction is considered. (gravities)

---

File 5: One Card (8F10.0)      Mandatory

---

GAM              Ratio of specific heats of gas (-)

BV               Covolume ( $\text{in}^3/\text{lbm}$ )

MOL               Molecular weight ( $\text{lbm}/\text{lbmol}$ )

ECHEM            Chemical energy of propellant ( $\text{lb-f-in}/\text{lbm}$ )

RHOP              Density of solid propellant at zero pressure ( $\text{lbm}/\text{in}^3$ )

CM                Mass of propellant (lbm)

ALDEN            Loading density ( $\text{lbm}/\text{in}^3$ )

---

File 6: NBR Cards (4F10.0)      Required if and only if IDEALI = 0 or  
                  if NBR is read as a positive number.  
                  See File 2.

---

B1(1)	Burn rate additive constant for 1 <sup>st</sup> increment of propellant (in/sec)
B2(1)	Burn rate pre-exponential coefficient for 1 <sup>st</sup> increment of propellant (in/sec - psi <sup>BN</sup> )
BN(1)	Burn rate exponent for 1 <sup>st</sup> increment of propellant (-)
ZR(1)	Mass fraction defined by end of first increment (-)
B1(2)	Like B1(1) but for 2 <sup>nd</sup> increment. (New Card)
.	
.	
ZR(NBR)	Mass fraction defined by end of last increment, including contributions of all preceding increments (-)

---

File 7: One Card (2F10.0)      Required if and only if NPRC  $\neq$  0.  
See File 2.

---

AUP	Compressive wave speed in propellant at ambient conditions (in/sec)
ADWN	Unloading/Reloading wave speed (in/sec). If ADWN is entered so that it is less than the nominal loading wave speed, the loading value is used. By entering ADWN = 0 a reversible law is defined.

---

File 8: One Card (2F10.0)      Required if and only if NWFR < 0.  
See File 2.

---

VISLYR	Viscosity of gas film used to lubricate propellant (lbm/in-sec)
DELYR	Thickness of film (ins)

---

File 9: One to three Cards (8F10.0)      Required if and only if  
NWFR > 0. See File 2.

---

AMUV(1)	First value of velocity of propellant (in/sec)
AMU(1)	Corresponding coefficient of friction on tube (-)
.	
.	
AMUV(NWFR)	Last value of velocity (in/sec)
AMU(NWFR)	Corresponding coefficient of friction (-)



---

File 10: One to three Cards (8F10.0)	Required if and only if NBRES1 $\neq$ 0. See File 2.
--------------------------------------	---

---

BRX(1)	First value of projectile travel (ins)
BR(1)	Corresponding value of resistive pressure due to obturator (psi)
BRX(NBRES1)	Last value of projectile travel (ins)
BR(NBRES1)	Corresponding value of resistive pressure (psi)

---

File 11: One Card (4F10.0)	Required if and only if NBRES2 $\neq$ 0. See File 2.
----------------------------	---

---

AIRGAM	Ratio of specific heats of air (-)
AIRPO	Pressure of air in barrel (psi)
AIRTO	Temperature of air in barrel ( $^{\circ}$ R)
AIRMW	Molecular weight of air in barrel (lbm/lbmol)

---

File 12: One Card (3F10.0)	Required if and only if NBRES3 $\neq$ 0. See File 2.
----------------------------	---

---

PRMB	Mass of projectile ahead of midpoint of obturating band (lbm)
ELB	Length of bearing section of obturating band (ins)
ANU	Poisson's ratio of obturating band (-)

---

File 13: One to three Cards (8F10.0)	Required if and only if NBRES3 $\neq$ 0. See File 2.
--------------------------------------	---

---

BMUV(1)	First value of velocity of projectile (in/sec)
BMU(1)	Corresponding value of coefficient of friction between obturator and tube (-)
BMUV(NBRES3)	Last value of velocity of projectile (in/sec)
BMU(NBRES3)	Corresponding coefficient of friction (-)

---

---

File 14: One Card (4F10.0)      Required if and only if NHTW  $\neq$  0.  
See File 2.

---

TWALO      Temperature of tube ( $^{\circ}$ R)

CHTW      Coefficient of heat transfer correlation (-)  
Default value is 0.092.

VISG      Viscosity of gas (lbm/in-sec)  
Default value is  $10^{-5}$ .

PRNO      Prandtl number of gas (-)  
Default value is 0.7.

---

File 15: One Card (2F10.0)      Required if and only if NMUZBL  $\neq$  0.  
See File 2.

---

PBRF      Value of breech pressure at which blowdown calculation  
is to be terminated (psi)

CDMUZ      Discharge coefficient for efflux from muzzle (-)

---

File 16: One Card (4F10.0)      Required if and only if NBRV  $\neq$  0.  
See File 2.

---

ASBR      Throat area of discharge nozzle in breech (in<sup>2</sup>)

CDBR      Discharge coefficient for nozzle (-)

PDIA      Rupture pressure which must be exceeded before  
breech becomes permeable to gas (psi)

---

File 17: One or two Cards (8F10.0)      Required if and only if  
NPAR  $\neq$  0. See File 2.

---

COM(1)      Value of charge-to-projectile mass ratio for first case (-).  
.  
.  
.  
COM(NPAR)      Value for last case (-)

---

PROGRAM TO STUDY END BURNING TRAVELING CHARGE

VERSION CREATED FEB 1 1980.

IMPLICIT REAL\*8(A-H,O-Z)

REAL\*8 MOL, K, MACH

COMMON /BARA/ GS1(100,3), GS2(100,3), GS3(100,3)

COMMON /BAR3/ RHQ(100), P(100), E(100), T(100), U(100), ETA(100)

COMMON /BARC/ NDT, NI, NF, NP, INT, NDIM, MAXDIM

COMMON /BARD/ DXMIN, DELTAX

COMMON /BARE/ GAM, BV, MOL, ECHEM, RHOP, B1(20), B2(20), BN(20),  
1 CV, ZR(20)

COMMON /BARF/ XPR, VPR, CM, XB, VB, AB, PRM, RDOT, SIG, SSTART

COMMON /BAR3/ XBR, DELTBX, NPFC, NDIM1, NDIM2

COMMON /BARH/ AUP, ADWN, VISLYR, DELYR, AMUV(10), AMU(10), DB,  
\* 3RX(10), BR(10), AIRGAM, AIRPO, AIRTO, AIRMW, TWALO,  
\* PBRF, COMUZ, ASBR, CDBR, PDIA, CHTW, DRHO(2)

COMMON /BARH2/ PRMB, ELB, ANU, BMUV(10), BMU(10), NBRES3

COMMON /BARH3/ PRND, VISS

COMMON /BARH4/ RESAIR, RESOR

COMMON /BARI/ NWFR, NBRRES1, NBRRES2, NHTW, NMUZBL, NBRV

COMMON /BARCJ2/ PST, SIGMAX, MACH, APMAX, XII, XII2, NCJ, IDEAL

COMMON /BARJ/ QORF(100), PRPRES

COMMON /BERG/ K(4,2)

COMMON /LPRO/ NPRD

COMMON /BRVAR/ XLPRI, XPROP, NBR

DIMENSION DT1(5), SAVE(5), POS(100), NBC(2)

DIMENSION CCM(10), ITIT(20)

DIMENSION SEGW(100), SEGE(100), SEGKE(100)

EQUIVALENCE (DT1(1), XPR)

DATA R, G /19550.00, 385.1600/

READ TITLE LINE

20 READ (5,450,END=410) (ITIT(I), I=1,20)

READ AND PRINT INPUT DATA

READ(5,490) IDEALI, NPFC, NPRD, NDSK, NDSKID, NDSKDT, NPAR, NBR,  
\* NWFR, NBRRES1, NBRRES2, NBRRES3, NHTW, NMUZBL, NBRV

READ(5,495) NSTOP, MAXDIM, NCY1, NCY2, TINOM, TISTOP,  
\* XSTOP, SAFE, DXMIN

NPROI=NPRD

IDEAL=IDEALI

READ IN SINGLE SET OF VALUES IF C/M DOES NOT VARY.

```

READ (5,500) DB,XIB,PRM,SSI,PSTI,SIGMAX,MACH,APMAX
READ (5,500) GAM,BV,MOL,ECHM,RHOP,CM,ALDEN
IF (IDEALI.NE.0) GO TO 40
NBRA=1
IF (NBR.GT.0) NBRA=NBR
DO 30 I=1,NBRA
READ (5,500) B1(I),B2(I),BN(I),ZR(I)
30 CONTINUE
40 IF (NPRC.NE.0) READ (5,500) AUP,ADWN
IF (NWFR.LT.0) READ (5,500) VISLYR,DELYR
IF (NWFR.GT.0) READ (5,500) (AMUV(I),AMU(I),I=1,NWFR)
IF (NBRES1.NE.0) READ (5,500) (BRX(I),BR(I),I=1,NBRES1)
IF (NBRES2.NE.0) READ (5,500) AIRGAM,AIRPO,AIRTO,AIRMW
IF (NBRES3.EQ.0) GO TO 45
READ (5,500) PRMB,ELB,ANU
READ (5,500) (BMUV(I),BMU(I),I=1,NBRES3)
45 IF (NHTW.NE.0) READ (5,500) TWALO,CHTW,VISG,PRND
IF (VISG.LT.1.D-10) VISG=1.D-5
IF (PRND.LT.1.D-10) PRND=0.700
IF (CHTW.LT.1.D-10) CHTW=0.09200
IF (NMUZ3L.NE.0) READ (5,500) PBRF,COMUZ
IF (NBRV.NE.0) READ (5,500) ASBR,CDBR,PDIA
NPR=1
FOR=ECHEM*(GAM-1.00)
AB=3.141592600/4.00*DB*DB
VI=AB*XIB
CMI=CM
CT=CM+VI*PSTI/(FOR+PSTI*BV)
IF (NPAR.EQ.0) GO TO 80
READ (5,500) (COM(I),I=1,NPAR)
60 CT=COM(NPR)*PRM

      COMPUTE SIGMAX AND PSTI BASED ON APMAX
IF (IDEALI.EQ.4) IDEAL=2
IF (IDEALI.NE.4) GO TO 70
CPR=APMAX*(PRM+CT)/AB
TP1=VI*APMAX/AB+FOR-CPR*BV
TPSQ=TP1*TP1
TP2=4.00*BV*CPR*FOR
PSTI=(-TP1+DSQRT(TPSQ+TP2))/(2.00*BV)
SIGMAX=PSTI
70 CI=PSTI*VI/(FOR+PSTI*BV)
VC=CT/ALDEN
CM=CT-CI
RHOP=CM/(VC-VI)
CMI=CM
80 PST=PSTI
CTOT=CT
FTOT=CT*ECHEM

```

C  
C  
C

```

90. WRITE (6,460) (ITIT(I),I=1,20)
   WRITE(6,520) IDEALI,NPRC,NPRO,NDSK,NDSKID,NDSKOT,VPAR,NBR,
*   NWER,NBRES1,NBRES2,NBRES3,NHTW,NMUZBL,NBRV
   WRITE(6,525) NSTOP,MAXDIM,NCY1,NCY2,TINQM,TISTOP,
*   XSTOP,SAFE,DXMIN

   COMPUTE APMAX BASED ON SIGMAX

   IF (IDEALI.EQ.3) IDEAL=2
   IF (IDEALI.EQ.3) APMAX=SIGMAX*AB/(PRM+CM)
   WRITE (6,530) DB,XIB,PRM,CM,PST,SIGMAX,MACH,APMAX,COM(NPR),VC,
1  ALDEN,SSI
   WRITE(6,460) (ITIT(I),I=1,20)

   INITIALIZE CONSTANTS

   TNOM=1.0-3*TINQM
   TSTOP=1.0-3*TISTOP
   LINE=0
   NSTEP=0
   SSTART=SSI
   NPRT=0
   NEXIT=0
   DUM=0.00
   PMAX=PST
   PMAXA=PST
   NBRT=0
   YP=XIB
   NBC(1)=0
   NPC(2)=0
   IF (CM.LT.1.0-10) NPRT=2
   IF (MOL.LT.1.0-10) MOL=25.00
   CV=R/MOL/(GA4-1.00)
   TIME=0.00
   TPRT=0.00
   EDOT=0.00
   SIG=0.00
   VB=0.00
   XPR=0.00
   VPR=0.00
   QLOSS=0.00
   RESLS1=0.00
   RESLS2=0.00
   PRPRES=0.00
   STMAX=0.00
   AKGMAX=0.00
   PPMAX=0.00
   NNPRC=NPRC
   NNBC2=0
   RESAIR=0.00

```

```

RESOB=0.00
DPMAX=0.00
DPMIN=0.00
CTDELM=0.00
ETDELM=0.00
DRHO(1)=0.00
DRHO(2)=0.00
DO 94 I=1,8
94 K(I,1)=0.00
DO 95 I=1,100
95 QORF(I)=0.00
XI1=GAM/(GAM-1.00)*PST/RHOP
XI2=ECHEM-PST/(GAM-1.00)*(1.00/RHOP-BV)
XLPRI=CM/(RHOP*AB)
XBB=XLPRI
XPROP=CM/RHOP/AB+XB
IF(NBRES2.NE.0) WRITE(6,840) AIRGAM,AIRPO,AIRTO,AIRMW
IF(NHTW.NE.0) WRITE(6,850) TWALO,CHTW,VISG,PRNO
IF(NMUZBL.NE.0) WRITE(6,860) PBRF,CDMUZ
IF(NBRV.NE.0) WRITE(6,870) ASBR,CDBR,PDIA
IF(NBRES1.NE.0) WRITE(6,830) (BRX(I),BR(I),I=1,NBRES1)
IF(NBRES3.NE.0) WRITE(6,845) PRMB,ELB,ANU,(BMUV(I),BMU(I),
* I=1,NBRES3)
WRITE(6,540) GAM,BV,MOL,ECHEM,RHOP,B1(1),B2(1),BN(1),XLPRI,XPROP
IF(NPRC.NE.0) WRITE(6,800) AUP,ADWN
IF(NWFR.LT.0) WRITE(6,810) VISLYR,DELYR
IF(NWFR.GT.0) WRITE(6,820) (AMUV(I),AMU(I),I=1,NWFR)
IF(NBR.EQ.0) GO TO 110
WRITE(6,690)
DO 100 I=1,NBR
100 WRITE(6,700) I,B1(I),B2(I),BN(I),ZR(I)
CONTINUE
110 WRITE(6,550)
WRITE(6,470) (ITIT(I),I=1,20)
IPRT=1
IF(NPRO.EQ.1) WRITE(6,570)
IF(NPRO.EQ.2) WRITE(6,630)
IF(NPRO.EQ.3) WRITE(6,610)
IF(NDSK.EQ.0) GO TO 129
REWIND 8
IF(NDSK.LT.2) GO TO 123

RESTART OF MOST RECENT CASE

121 READ(8,END=122) MDSKID,MDSKDT,MPRC,MDIM,MDIM2
IF(MDSKID.EQ.NDSKID.AND.MDSKDT.EQ.NDSKDT) GO TO 125
GO TO 121
122 WRITE(6,790) NDSKID,NDSK
CALL EXIT
123 IF(NDSKID.LE.1) GO TO 129

```

```

124 READ(8,END=122) MDSKID
   IF(MDSKID.NE.99999) GO TO 124
   BACKSPACE 8
   GO TO 129
125 BACKSPACE 8
   CALL REFIT(0,1)
   IEND=MDIM
   IF(MPRC.EQ.1) IEND=MDIM2
   READ(8) MDSKID,NSTEP,NPRC,NDIM,NDIM2,NDT,NI,NP,NF,NDIM1,NBC,
   *      NPRT,NBRT,SSTART,PDIA,PMAX,PMAXA,STMAX,AKGMAX,
   *      DELTAX,DELTEX,DT1,TIME,RDPT,SIG,XB8,XLPRI,XPROP,
   *      PPMAX,(GS1(I,NF),GS2(I,NF),GS3(I,NF),I=1,IEND)
   TPRT=TIME
   NNPRC=NPRC
   SAVE(4)=XB
   BACKSPACE 8
   GO TO 130
129 CALL BAR1
   NF=1

   PRINT

130 NDIMM=NDIM
   IF(NPRC.EQ.1) NDIMM=NDIM2
   CALL BAR2(1,NDIMM,NF,XB)
   IF(NBRV.EQ.0) GO TO 135
   IF(P(1).GE.PDIA) NBC(1)=1

   PRINT AT BURNOUT AND AT EXTREMA OF PRESSURE

135 AO=DSQRT(G*GAM*P(NDIM)/RHO(NDIM)/(1.00-BV*RHO(NDIM)))
   AMACH=DABS(U(NDIM)-VB)/AO

   COMPUTE PROJECTILE ACCELERATION IN KILO-G:S

   IF (NBC(2).EQ.1) GO TO 138
   AKG=0.00
   IF(NDT.GT.0) AKG=K(2,2)/G/1000.00
138 MAND=0
   IF(NNPRC.NE.NPRC) MAND=1
   NNPRC=NPRC
   IF (NNBC2.NE.NBC(2)) MAND=1
   NNBC2=NBC(2)
   IF (NBRT.GT.1) GO TO 150
   IF (CM.LE.1.0-10) GO TO 140
   GO TO 150
140 NBRT=NBRT+1
   PRR80=P(1)
   PBB0=P(NDIM)

```

```

STRBO=SIG
XBO=XPR
TBO=TIME*1.D3
VBO=DT1(2)/12.D0
NSTBO=NSTEP
AKGBO=AKG
AMBO=AMACH
150 IF (NBRT.EQ.1) MAND=1
PBITA=0.D0
DO 160 I=1,NDIM
IF (P(I).GT.PBITA) PBITA=P(I)
160 CONTINUE
IPBIT=PBITA
PBIT=IPBIT
PMAXA=PMAX
PMAX=PBIT
IF (PBITA.GT.PPMAX) GO TO 170
GO TO 180
170 PPMAX=PBITA
PBMAX=P(NDIM)
PBRMAX=P(1)
STRMAX=SIG
XPMAX=XPR
TPMAX=TIME*1.D3
VPMAX=DT1(2)/12.D0
NSPMAX=NSTEP
ZPMAX=1.D0-DT1(3)/CMI
AKGPM=AKG
AMPM=AMACH
180 DPMAXA=P(1)-P(NDIM)
IF(DPMAXA.LT.DPMAX) GO TO 182
DPMAX=DPMAXA
PBPMPX=P(NDIM)
PBRPMX=P(1)
STRPMX=SIG
XPPMX=XPR
TPPMX=TIME*1.D3
VPPMX=DT1(2)/12.D0
NPMX=NSTEP
ZPMX=1.D0-DT1(3)/CMI
AKGPMX=AKG
AMPMX=AMACH
182 IF(DPMAXA.GE.DPMIN) GO TO 184
DPMIN=DPMAXA
PBPMPY=P(NDIM)
PBRPMY=P(1)
STRPMY=SIG
YPPMY=XPR
TPPMY=TIME*1.D3
VPPMY=DT1(2)/12.D0

```



```

      NPMY=NSTEP
      ZPMY=1.DO-DT1(3)/CMI
      AKGPMY=AKG
      AMPMY=AMACH
184  IF (AKG.GT.AKSMAX) GO TO 190
      GO TO 200
190  AKGMAX=AKG
      PBRAM=P(1)
      PRAM=P(NDIM)
      STRAM=SIG
      XAM=XPR
      TAME=TIME*1.D3
      VPAM=DT1(2)/12.DO
      ZAM=1.DO-DT1(3)/CMI
      NSAM=NSTEP
      AMAM=AMACH
200  TAME=TIME*1.D3
      IF (NBC(2).EQ.1) GO TO 205
      VELF=DT1(2)/12.DO
      Z=1.DO-DT1(3)/CMI
205  IF (SIG.GT.STMAX) GO TO 210
      GO TO 220
210  ASTMAX=AKG
      PBRSTM=P(1)
      PBSTM=P(NDIM)
      STMAX=SIG
      XSTM=XPR
      TSTM=TIME*1.D3
      VPSTM=DT1(2)/12.DO
      ZSTM=1.DO-DT1(3)/CMI
      NSTM=NSTEP
      AMSTM=AMACH
220  IF (NPRO.EQ.4) GO TO 310
      IF (NSTEP.GT.NCY1) NPRO=0
      IF (NSTEP.GT.NCY2) NPRO=NPRO1
      IF (DABS(TIME-TPRT).LE.1.D-10) GO TO 230
      IF (MAND.EQ.0) GO TO 335
230  LINE=LINE+NDIM+18
      IF (LINE.LT.55) GO TO 240
      LINE=NDIM+18
      IF (NPRO.GT.0) GO TO 240
      WRITE (5,550)
      C
      C
      C
      COMPUTE SEGMENT VOLUME
240  FAC=AB*XB*DELTAX
      SEGW(1)=FAC*.5D0*RHO(1)
      SEGW(NDIM)=FAC*.5D0*RHO(NDIM)
      SEGE(1)=FAC*.5D0*RHO(1)*E(1)
      SEGE(NDIM)=FAC*.5D0*RHO(NDIM)*E(NDIM)

```

```

SEGKE(1)=FAC*.5D0*RHO(1)*U(1)**2/(2.D0*G)
SEGKE(NDIM)=FAC*.5D0*RHO(NDIM)*J(NDIM)**2/(2.D0*G)
TSEGW=SEGW(1)+SEGW(NDIM)
TSEGIE=SEGE(1)+SEGE(NDIM)
TSEGKE=SEGKE(1)+SEGKE(NDIM)
KDIM=NDIM-1
DO 250 KK=2,KDIM

```

SEGMENT MASS

```

SEGW(KK)=FAC*RHO(KK)
TSEGW=TSEGW+SEGW(KK)

```

SEGMENT INTERNAL ENERGY

```

SEGE(KK)=FAC*RHO(KK)*E(KK)
TSEGIE=TSEGIE+SEGE(KK)

```

SEGMENT KINETIC ENERGY

```

SEGKE(KK)=FAC*RHO(KK)*U(KK)**2/(2.D0*G)
TSEGKE=TSEGKE+SEGKE(KK)

```

250 CONTINUE

CHEMICAL AND KINETIC ENERGY OF UNBURNT PROPELLANT

```

CHEUPR=CM*ECHEM
AKEUPR=CM*VPR**2/(2.D0*G)

```

PROJECTILE KINETIC ENERGY

```

PRKE=PRM*VPR**2/(2.D0*G)

```

TOTAL MASS

```

TMASS=TSEGW+CM
CTDEL=100.D0*(1.D0-TMASS/CTOT)
IF(DABS(CTDEL).GT.DABS(CTDELM)) CTDELM=CTDEL

```

TOTAL ENERGY

```

TENG=TSEGIE+TSEGKE+CHEUPR+AKEUPR+PRKE
ETDEL=100.D0*(1.D0-TENG/ETOT)
IF(DABS(ETDEL).GT.DABS(ETDELM)) ETDELM=ETDEL

```

COMPUTE PERCENTAGE ENERGY BALANCE

```

PIE=TSEGIE*100.D0/TENG
PKE=TSEGKE*100.D0/TENG
PCUPR=CHEUPR*100.D0/TENG

```

```

PKEUPR=AKEUPR*100.DO/TENG
PPRKE=PRKE*100.DO/TENG
PITT=PIE+PKE+PCUPR+PKEUPR+PPRKE
BIT=DAPS(U(NDIM)-VB)
BIT=BIT/DSQRT(G*GAM*P(NDIM)/RHO(NDIM)/(1.DO-BV*RHO(NDIM)))
DO 260 I=1,NDIM
260 POS(I)=DFLOAT(I-1)*XB*DELTAX
IF(NPRC.EQ.0) GO TO 256
DO 265 I=NDIM1,NDIM2
265 POS(I)=XB+DFLOAT(I-NDIM1)*XBB*DELTBX
CHECK OUTPUT OPTIONS
266 IF (NPRO.GT.0) GO TO 270
PROFILE DISTRIBUTION OUTPUT
WRITE (6,560) NSTEP,TAME,DT1,RDOT,SIG,BIT,AKG,RESAIR,RESOB
WRITE (6,570) TMASS,TSEGW,CM
WRITE (6,580) TENG,TSEGIE,TSEGKE,CHEUPR,AKEUPR,PRKE,PITT,PIE,PKE,
1 PCUPR,PKEUPR,PPRKE
WRITE (6,590)
WRITE (6,600) (POS(I),RHO(I),P(I),T(I),U(I),SEGKE(I),SEGE(I),
1 SEGW(I)),I=1,NDIM)
IF(NPRC.EQ.1) WRITE(6,601) (POS(I),RHO(I),P(I),U(I),I=NDIM1,NDIM2)
GO TO 310
270 IF (NPRO.EQ.1) GO TO 290
IF (NPRO.EQ.2) GO TO 280
ONE LINE IB DATA + ( ENERGY PRINTED
PBR=P(1)/1000.DO
PBASE=P(NDIM)/1000.DO
STRESS=SIG/1000.DO
WRITE (6,620) TAME,XPR,VELF,AKG,PBR,PBASE,STRESS,Z,DT1(4),RDOT,BIT
1 ,PIE,PKE,PCUPR,PKEUPR,PPRKE,NSTEP
GO TO 300
ONE LINE ENERGY TRAJECTORY
280 WRITE (6,640) TAME,XPR,VELF,TENG,TSEGIE,TSEGKE,CHEUPR,AKEUPR,PRKE,
1 PITT,PIE,PKE,PCUPR,PKEUPR,PPRKE
GO TO 300
290 WRITE (6,680) TAME,XPR,VELF,P(1),P(NDIM),DT1(3),Z,DT1(4),DT1(5),
1 RDOT,SIG,BIT,NSTEP
PRINT TITLE LINE AFTER 50 TIME STEPS
300 IPRT=IPRT+1
IF (IPRT.LT.50) GO TO 310

```



```

IF (CM.LT.1.D-10) CM=0.D0
IF (CM.LT.1.D-10) SAVE(3)=0.D0
IF (XB.GT.XPR+XPROP-1.D-6) XB=XPR+XPROP
365 CALL BAR3 (1,SAVE(4),VB,XBBP,VPR,DT)
IF (NBC(1).EQ.0) CALL BREECH (SAVE(4),XB,DT)
IF (NBC(1).EQ.1) CALL OUTFLO(1,SAVE(4),XB,DT,1.D0)
IF (NPRC.EQ.1) CALL BASEPR(XBBP,DT)
IER2=0
IF (NBC(2).EQ.0) CALL BASE (SAVE(4),XB,XBBP,DT,IER2)
IF (NBC(2).EQ.1) CALL OUTFLO(NDIM,SAVE(4),XB,DT,-1.D0)
IF (IER2.EQ.1) GO TO 420
IF (NCJ.EQ.1) GO TO 390
IF (NPRC.EQ.1) CALL SIGCHK
IF (NWFR.NE.0.AND.NPRC.EQ.1) CALL VELCHK
IF (NBC(2).EQ.1) GO TO 366
CALL GETK (2)
366 CALL BAR3 (2,XB,VB,XBB,VPR,DT)
IF (NBC(2).EQ.1) GO TO 375
DO 370 I=1,4
370 DT1(I)=SAVE(I)+0.5DO*(K(I,1)+K(I,2))*DT
XBB=XPR-XB+XIB+XLPRI
IF (CM.LT.1.D-10) CM=0.D0
IF (CM.LT.1.D-10) SAVE(3)=0.D0
IF (XB.GT.XPR+XPROP-1.D-6) XB=XPR+XPROP
375 IF (NBC(1).EQ.0) CALL BREECH (SAVE(4),XB,DT)
IF (NBC(1).EQ.1) CALL OUTFLO(1,SAVE(4),XB,DT,1.D0)
IF (NPRC.EQ.1) CALL BASEPR(XBBP,DT)
IF (NBC(2).EQ.0) CALL BASE (SAVE(4),XB,XBBP,DT,IER2)
IF (NBC(2).EQ.1) CALL OUTFLO(NDIM,SAVE(4),XB,DT,-1.D0)
IF (IER2.EQ.1) GO TO 420
IF (NCJ.EQ.1) GO TO 390
IF (NPRC.EQ.1) CALL SIGCHK
IF (NWFR.NE.0.AND.NPRC.EQ.1) CALL VELCHK
QLOS=(QDRF(1)+QDRF(NDIM))*0.500
NDIML=NDIM-1
DO 376 I=2,NDIML
QLOS=QLOS+QDRF(I)
376 CONTINUE
QLOSS=QLOS*AB*DT*XB*DELTAX+GLOSS
RESLS1=RESLS1+(RESAIR+RESOR)*AB*DT*VPR
IF (NPRC.EQ.0) GO TO 378
RESLS=(U(NDIM1)*QDRF(NDIM1)+U(NDIM2)*QDRF(NDIM2))*0.500
NDIML=NDIM1+1
NDIMR=NDIM2-1
DO 377 I=NDIML,NDIMR
RESLS=RESLS+U(I)*QDRF(I)
377 CONTINUE
RESLS2=RESLS2-RESLS*AB*DT*XB*DELTAX
GO TO 379
379 RESLS2=RESLS2-PPRFS*AB*DT*XB*VPR

```

379 IF(NBC(2).EQ.0) CALL REFIT (1,NF)  
 NSTEP=NSTEP+1  
 TIME=TIME+DT

C  
C  
C

TEST FOR TERMINATION

IF (NSTOP.EQ.99999) GO TO 380  
 IF (NSTEP.GE.NSTOP) NEXIT=1  
 380 IF (TIME.GE.TSTOP) NEXIT=1  
 IF(NBC(2).EQ.1) GO TO 383  
 IF (XPR.LT.XSTOP-1.0-3) GO TO 385  
 IF(NMUZBL.EQ.0) GO TO 384

CM=0.00  
 VPR=0.00  
 T1MZ=TAME  
 P1MZ=P(1)  
 PNMZ=P(NDIM)  
 SIGMZ=SIG  
 AMACHZ=AMACH  
 NSTEPZ=NSTEP  
 WRITE (6,885)  
 XB=XPR+XI8+XLPR1  
 SAVE(4)=XB  
 VB=0.00  
 NPROC=0

NBC(2)=1  
 383 IF(P(1).GT.PBRF) GO TO 385  
 384 NEXIT=1  
 385 IF (NEXIT.EQ.1) TPRT=TIME  
 GO TO 130

390 NEXIT=1  
 TPRT=TIME  
 IF (NCJ.NE.1) GO TO 130  
 NF=NI

IF (INT.EQ.0) NF=NP  
 DO 400 I=1,5  
 400 DT1(I)=SAVE(I)  
 RDOT=VB-VPR  
 IF(NPROC.EQ.1) RDOT=VB-GS2(NDIM1,NF)/GS1(NDIM1,NF)  
 XBR=XPR-XB+XI3+XLPR1  
 GO TO 130

410 CALL EXIT

C  
C  
C  
C  
C

PRINT OUT SUMMARY DATA

420 IF (PPMAX.GT.PSTI) GO TO 430

SET MAX. PRESSURE TO INITIAL CONDITIONS

STRMAX=PSTI

```

PBMAX=PSTI
PBRMAX=PSTI
PPMAX=PSTI
AMPX=0.00
ZPMAX=0.00
VPMAX=0.00
XPMAX=0.00
TPMAX=0.00
NSPMAX=0
AKGPM=PSTI*AB/((PRM+CMI)*1000.00)
430 WRITE (6,710)
WRITE (6,470) (ITIT(I),I=1,20)
WRITE (6,480) VELF,PPMAX,AKGMAX,STMAX
WRITE (6,720)
WRITE (6,770)
WRITE (6,780) TBO,XBO,VBO,AKGBO,DUM,PBRBO,PBBO,STRBO,Z,AMBO,NSTBO
WRITE (6,730)
WRITE (6,770)
WRITE (6,780) TPMAX,XPMAX,VPMAX,AKGPM,PPMAX,PBRMAX,PBMAX,STRMAX,
1 ZPMAX,AMPX,NSPMAX
WRITE (6,740)
WRITE (6,770)
WRITE (6,780) TAM,XAM,VPAM,AKGMAX,DUM,PBRAM,PBAM,STRAM,ZAM,AMAM,
1 NSAM
WRITE (6,750)
WRITE (6,770)
WRITE (6,780) TSTM,XSTM,VPSTM,ASTMAX,DUM,PBRSTM,PBSTM,STMAX,ZSTM,
1 AMSTM,NSTM
WRITE (6,760)
WRITE (6,770)
IF (NDC(2).EQ.1) GO TO 435
P1MZ=P(1)
PNMZ=P(NDIM)
TIMZ=TAME
SIGMZ=SIC
AMACHZ=AMACH
NSTEPZ=NSTEP
435 WRITE (6,780) TIMZ,XPR,VELF,AKG,DUM,P1MZ,PNMZ,SIGMZ,Z,AMACHZ,
* NSTEPZ
WRITE (6,764)
WRITE (6,770)
WRITE (6,780) TPRMX,YPRMX,VPRMX,AKGPMX,DUM,PBRPMX,PBPMX,STRPMX,
* ZPMX,AMPX,NPMX
WRITE (6,766)
WRITE (6,770)
WRITE (6,780) TPRMY,YPRMY,VPRMY,AKGPMY,DUM,PBRPMY,PBPMY,STRPMY,
* ZPMY,AMPY,NPMY
WRITE (6,800) CTDEL,CTDELM,ETDEL,ETDELM,OLSS,RESLS1,RESLS2
NENDOF=9999
IF (NDSK.EQ.1.OR.NDSK.EQ.3) WRITE (8) NENDOF

```

C  
C  
C

# SWITCHES FOR VARYING C/M PARAMETRICALLY

```

IF (NPAR.EQ.0) GO TO 20
NPR=NPR+1
IF (NPR.EQ.NPAR+1) GO TO 20
NDSKID=NDSKID+1
GO TO 60
440 WRITE (6,510)
GO TO 420

C
C
C
450 FORMAT (20A4)
460 FORMAT (1H1,10X,42H SIMULATION OF END BURNING TRAVELING CHARGE,10X,
120H VERSION (FEB 1 1980)//1X,20A4/)
470 FORMAT (1X,20A4/)
480 FORMAT (20X,15H MUZZLE VELOCITY,6X,5H (F/S),3X,F7.0/20X,16H MAXIMUM P
1RESSURE,5X,5H (PSI),1X,F9.0/20X,26H MAXIMUM ACCELERATION (K-G),3X,F7
2.0/20X,14H MAXIMUM STRESS,7X,5H (PSI),1X,F9.0/)
490 FORMAT(16I5)
495 FORMAT(4I5,6F10.0)
500 FORMAT (8F10.0)
510 FORMAT (31H NEG. SQUARE ROOT ERROR IN BAR4)
520 FORMAT(10X,12H CONTROL DATA//
*42H IDEAL BURN RATE LAW ,I5/
*42H CONTINUUM MODEL OF UNREACTED PROPELLANT ,I5/
*42H PRINT OPTION ,I5/
*42H DISC READ/WRITE PARAMETER ,I5/
*42H PROBLEM ID FOR DISC READ/WRITE ,I5/
*42H INTEGRATION STEP FOR DISC RESTART ,I5/
*42H NUMBER OF PARAMETRIC CASES ,I5/
*42H NUMBER OF BURN RATE PARAMETERS ,I5/
*42H PROPELLANT WALL FRICTION PARAMETER ,I5/
*42H NUMBER OF ENTRIES IN PROJECTILE BORE /
*42H RESISTANCE TABLE ,I5/
*42H INDICATOR FOR AIR RESISTANCE ,I5/
*42H NUMBER OF ENTRIES IN ORBITATOR FRICTION /
*42H TABLE ,I5/
*42H WALL HEAT LOSS OPTION ,I5/
*42H TUBE BLOW-DOWN OPTION ,I5/
*42H RECOILLESS TUBE OPTION ,I5//)
525 FORMAT(5X,22H INTEGRATION PARAMETERS//
*42H MAXIMUM NUMBER OF STEPS ,I5/
*42H MAXIMUM NUMBER OF MESH POINTS ,I5/
*42H FIRST CYCLE TO BE PRINTED WITH AXIAL /
*42H DISTRIBUTION ,I5/
*42H LAST CYCLE TO BE PRINTED WITH AXIAL /
*42H DISTRIBUTION ,I5/
*42H TIME STEP FOR LOGOUT CYCLE (MSEC) ,F10.4/

```



```

*42H PROBLEM TERMINATION TIME (MSEC) ,F10.3/
*42H MAXIMUM PROJECTILE TRAVEL (INS) ,F10.3/
*42H STABILITY SAFETY FACTOR ,F10.3/
*42H MINIMUM MESH SIZE (INS) ,F10.3//)
530 FORMAT (11X,37HTUBE,PROJECTILE AND CHARGE PROPERTIES//42H BORE DIA
1METER (INS) ,F10.3/42H INITIAL POSITION OF RE
2AR FACE OF ,/42H PROPELLANT (INS)
3,F10.3/42H PROJECTILE MASS (LBM) ,F10.5/42H CHA
4RGE MASS (LBM) ,F10.3/42H INITIAL PRESSURE
5(Psi) ,F10.0/41H MAXIMUM PRESSURE IN UNREACTED P
6ROPELLANT,/42H (Psi), IF IDEAL=2 ,F10.0/42H
7 MAXIMUM MACH NUMBER OF REACTION PRODUCTS ,F10.3/42H MAXIMUM ACCEL
8ERATION OF PROJECTILE(GRAV) ,F10.0/42H C/M
9 ,F10.2/42H CHAMBER VOLUME (IN**3)
A,F10.5/42H LOADING DENSITY(LB/IN**3) ,F7.5/42H SHOT
B-START PRESSURE (Psi) ,F10.0//)
540 FORMAT (11X,24HPROPERTIES OF PROPELLANT//42H RATIO OF SPECIFIC HEA
1TS (-) ,F10.3/42H COVOLUME (IN**3/LBM)
2 ,F10.3/42H MOLECULAR WEIGHT (LBM/LBMOL) ,F10.3/4
33H CHEMICAL ENERGY OF PROPELLANT (LBF-IN/LBM),F10.0/42H DENSITY OF
4 PROPELLANT (LBM/IN**3) ,F10.4/42H BURNING RATE ADDITIVE CO
5NSTANT (IN/SEC) ,F10.4/42H BURNING RATE PRE-EXPONENTIAL FACTOR
6 /42H (IN/SEC-PSI**BN) ,F10.6/42H BURNIN
7G RATE EXPONENT (-) ,F10.4/42H TC GRAIN LENGTH (IN)
8 ,F10.3/42H LENGTH BREECH TO PROJECTILE BASE (
9IN) ,F10.3//)
550 FORMAT (11H)
560 FORMAT (1H0,10X,16HSOLUTION AT STEP,15,5X,12HTIME(MSEC) =,F7.3//50
1H PROJECTILE TRAVEL(INS) ,F10.3/50H PROJ
2ECTILE VELOCITY(INS/SEC) ,F10.0/50H UNREACTED
3PROPELLANT MASS(LBM) ,F10.4/50H POSITION OF PROP
4ELLANT BOUNDARY(INS) ,F10.3/50H VELOCITY OF PROPELLANT
5 BOUNDARY(INS/SEC) ,F10.0/50H PROPELLANT REGRESSION RATE(I
6NS/SEC) ,F10.2/50H STRESS ON UNREACTED SIDE OF FLAME(
7PSI) ,F10.0/50H MACH NUMBER OF REACTION PRODUCTS(-)
8 ,F10.3/
*50H PROJECTILE ACCELERATION (KG) ,F10.3/
*50H RESISTANCE DUE TO SHOCKED AIR (PSI) ,F10.0/
*50H RESISTANCE DUE TO OBTURATOR (PSI) ,F10.0//)
570 FORMAT (11X,5HTOTAL,6X,3HGAS,3X,19HUNBURNED PROPELLANT/10H MASS(LB
1):,F8.4,1X,F8.4,6X,F8.4//)
580 FORMAT (20X,5HTOTAL,6X,8HINTERNAL,2X,11HGAS KINETIC,1X,13HUNBURN
1PROP.,1X,17HCHE UNBURN PROP.,1X,2HKE,2X,13HPROJECTILE KE/1X,14HEN
2ERGY(IN-LB):,3E12.6,3X,E12.6,6X,E12.6,5X,E12.6/2X,13H % ENERGY :
3,3(4X,F7.2),7X,F7.2,2(10X,F7.2))
590 FORMAT (40X,32HDISTRIBUTIONS OF STATE VARIABLES//40H POSITION DENS
1ITY PRESSURE TEMPERATURE,40H VELOCITY KINETIC ENERGY INTERNAL EN
2ERGY,3X,4HMASS/3X,3HINS,4X,8HLB/IN**3,3X,3HPSI,8X,5HDEG-R,6X,3HI/S
3,6X,5HIN/LB,11X,5HIN/LB,10X,2HLB/)
600 FORMAT (1X,F7.3,1X,F9.6,1X,F9.0,2X,F6.0,4X,F9.1,1X,E12.6,4X,E12.6,

```

```

13X,F9.6)
601 FORMAT(1X,F7.3,F10.6,1X,F9.0,12X,F9.1)
610 FORMAT(75X,21(1H*),8H( ENERGY,18(1H*)/3X,4HTIME,3X,12HTRAVEL VEL
1.,2X,6HACCEL.,3X,15HPRESSURE (KPSI),7X,1HZ,6X,2HXB,5X,1HR,5X,14HMA
2CH INTERNAL,4X,3HGAS,4X,27HUNBJRNT UNBURNT PROJECTILE,1X,4HSTEP/
34X,2HMS,6X,2HIN,4X,3HF/S,4X,3HK-G,3X,6HBREECH,2X,4HBASE,3X,6HSTRES
4S10X,2HIN,6X,3HI/S,20X,7HKINETIC,2X,25HCHEMICAL KINETIC KINETIC/)
620 FORMAT(1X,F7.2,F8.2,F7.0,F7.1,2F7.2,F8.2,F6.3,F7.1,F8.0,F7.3,5(1X
1,F8.3),2X,15)
630 FORMAT(5H TIME,4X,6HTRAVEL,2X,8HVELOCITY,2X,43H-----
1--ENERGY(IN-LB)-----,36H-----***** % ENERGY,
218H*****/4H MS,7X,2HIN,7X,3HF/S,5X,5HTOTAL,5X,8HINTE
3RNAL,3X,6HGAS KE,6X,7HUBP CHE,4X,6HUBP KE,3X,7HPROJ.KE,3X,11HTOTAL
4 INT,25H GAS KE UB CE UB KE PR KE/)
640 FORMAT(1X,F7.2,F9.2,F8.1,6G11.5,6F6.1)
660 FORMAT(54H WARNING. IDEAL CASE REQUIRES STRONG DEFLAGRATION WAVE)
670 FORMAT(49H TIME TRAVEL VELOCITY PBREECH P BASE P-MASS,40H
1 Z X8 XBDOT R P-STRESS,13H MACH STEP/)
680 FORMAT(1X,F8.3,F9.2,F8.1,2F8.0,F7.3,F7.4,F7.1,2F8.0,F9.0,F7.3,16)
690 FORMAT(11X,23H VARIABLE BURN RATE DATA/43H STEP INTERCEPT COEFFIC
1IENT EXPONENT Z)
700 FORMAT(1X,13,3X,F8.3,1X,G12.6,1X,F8.4,2X,F7.4)
710 FORMAT(1H1,27X,14H SUMMARY OUTPUT//)
720 FORMAT(31X,7HBURNDUT)
730 FORMAT(27X,15H MAXIMUM PRESSURE)
740 FORMAT(27X,20H MAXIMUM ACCELERATION)
750 FORMAT(27X,14H MAXIMUM STRESS)
760 FORMAT(32X,6HMUZZLE)
764 FORMAT(26X,21H MAX. FORWARD GRADIENT)
766 FORMAT(26X,21H MAX. REVERSE GRADIENT)
770 FORMAT(3X,4HTIME,3X,22H TRAVEL VELOCITY ACCEL,1X,7(1H-),14HPRESSU
1RE (PSI),12(1H-),3X,1HZ,5X,10HMACH NSTEP/4X,2HMS,6X,2HIN,5X,3HF/S,
26X,2HKG,4X,21H MAXIMUM BREECH BASE,4X,6HSTRESS,11X,2HND)
780 FORMAT(1X,F7.2,F8.2,1X,F8.1,F8.2,3F8.0,F9.0,F7.4,F7.4,15/)
790 FORMAT(22H RESTART WITH NDSKID =,110,11H AND NDSK =,110,
*20H FAILS. TERMINATING.)
800 FORMAT(
*42H COMPRESSION WAVE SPEED IN PROPELLANT /
*42H (IN/SEC) ,F10.0/
*42H EXPANSION WAVE SPEED IN PROPELLANT /
*42H (IN/SEC) ,F10.0//)
810 FORMAT(
*42H VISCOSITY OF LUBRICATING FILM /
*42H (LBM/IN-SEC) ,E10.3/
*42H THICKNESS OF LUBRICATING FILM (INS) ,F10.4//)
820 FORMAT(1H0, 8X,36H FRICTION BETWEEN PROPELLANT AND TUBE//
*44H VELOCITY FRICTION COEFFICIENT/
*44H (IN/SEC) (-) /
*(1H ,F15.1,10X,F10.3))
830 FORMAT(1H0, 8X,35H RESISTIVE PRESSURE DUE TO OBSTURATOR//

```

```

*44H          TRAVEL          RESISTIVE PRESSURE /
*44H          (INS)          (PSI) /
*(1H ,F15.3,10X,F10.0))
840 FORMAT(
*42H RATIO OF SPECIFIC HEATS OF AIR (-)          ,F10.4/
*42H PPESSURE OF AIR IN BARREL (PSI)          ,F10.3/
*42H TEMPERATURE OF AIR IN BARREL (DEG.R)          ,F10.1/
*42H MOLECULAR WEIGHT OF AIR IN BARREL          /
*42H          (LBM/LBMDL)          ,F10.4//)
845 FORMAT(
*42H MASS OF PROJECTILE AHEAD OF DBTURATOR          /
*42H          (LBM)          ,F10.5/
*42H LENGTH OF DBTURATOR (INS)          ,F10.3/
*42H POISSON RATIO OF PROJECTILE (-)          ,F10.3//
* 8X,35H FRICTION BETWEEN DBTURATOR AND TUBE//
*44H          VELOCITY          FRICTION COEFFICIENT/
*44H          (IN/SEC)          (-) /
*(1H ,F15.1,10X,F10.3))
850 FORMAT(
*42H TEMPERATURE OF TUBE WALL (DEG.R)          ,F10.1/
*42H COEFFICIENT IN HEAT TRANSFER CORRELATION          ,F10.4/
*42H VISCOSITY OF GAS (LBM/IN-SEC)          ,F10.3/
*42H PRANDTL NUMBER OF GAS (-)          ,F10.3//)
860 FORMAT(
*42H BLOWDOWN TERMINATION PRESSURE (PSI)          ,F10.1/
*42H DISCHARGE COEFFICIENT FOR MUZZLE (-)          ,F10.3//)
870 FORMAT(
*42H THROAT AREA OF BREECH NOZZLE (IN**2)          ,F10.4/
*42H DISCHARGE COEFFICIENT OF BREECH NOZZLE(-)          ,F10.3/
*42H RUPTURE PRESSURE FOR BREECH DIAPHRAGM          /
*42H          (PSI)          ,F10.1//)
880 FORMAT(1H0,24X,21HGLOBAL BALANCE CHECKS/
*20X,20HFINAL MASS DEFECT(%),4X,F10.3/
*20X,22HMAXIMUM MASS DEFECT(%),2X,F10.3/
*20X,22HFINAL ENERGY DEFECT(%),2X,F10.3/
*20X,24HMAXIMUM ENERGY DEFECT(%),F10.3//
*20X, 'TOTAL HEAT LOSS TO TUBE (LBF-IN)',F10.0/
*20X, 'LOSS DUE TO PROJECTILE RESISTANCE (LBF-IN)',F10.0/
*20X, 'LOSS DUE TO PROPELLANT RESISTANCE (LBF-IN)',F10.0//)
885 FORMAT(' MUZZLE EXIT HAS OCCURRED, PROCEEDING WITH BLOWDOWN',
1 ' ANALYSIS')
END

```

# SUBROUTINE BAR1

INITIALIZES COMPUTATIONAL ARRAYS. THIS ROUTINE MUST BE CALLED  
AT OUTSET OF INTEGRATION PROCEDURE.

IMPLICIT REAL\*8(A-H,O-Z)  
REAL\*8 MDL, MACH

COMMON /BARA/ GS1(100,3), GS2(100,3), GS3(100,3)  
COMMON /BARC/ NDT, NI, NF, NP, INT, NDIM, MAXDIM  
COMMON /BARE/ GAM, BV, MDL, ECHEM, RHOP, B1(20), B2(20), BN(20),  
1 CV, ZR(20)  
COMMON /BARF/ XPR, VPR, CM, XB, VB, AB, PRM, RDOT, SIG, SSTART  
COMMON /BARG/ XPB, DELTBX, NPRC, NDIM1, NDIM2  
COMMON /BARH/ AUP, ADWN, VISLYR, DELYR, AMUV(10), AMU(10), DB,  
\* BRX(10), BR(10), AIRGAM, AIRPO, AIRTO, AIRMW, TWALO,  
\* PBRF, CDMUZ, ASBR, CDBR, PDIA, CHTW, DRHO(2)  
COMMON /BARI/ NWFR, NBRES1, NBRES2, NHTW, NMUZBL, NBRV  
COMMON /BARCJ2/ PST, SIGMAX, MACH, APMAX, XI1, XI2, NCJ, IDEAL  
COMMON /BRVAR/ XLPP1, XPROP, NBR  
DATA G /386.16D0/

NDT=0  
DO 10 I=1,900  
10 GS1(I,1)=0.00  
CALL REFIT(0,1)  
IF (CM.GT.0.00.AND.IDEAL.EQ.0) GO TO 30  
IF (CM.GT.0.00.AND.IDEAL.EQ.2) GO TO 80  
20 RHOST=1.00/(BV+(GAM-1.00)\*ECHEM/PST)  
DUB=0.00  
ESTA=ECHEM  
SIG=PST  
RDOT=0.00  
GO TO 50  
30 CALL BURN(PST,RDOT,RDOTPR)  
X1=2.00\*G/RDOT\*(PST/RHOP\*GAM/(GAM-1.00)-RDOT\*RDOT/G)  
X2=RDOT\*RDOT-2.00\*G\*(ECHEM+BV\*PST/(GAM-1.00)+PST/RHOP)  
X3=X1\*X1-4.00\*X2  
IF (X3.LT.0.00) GO TO 70  
X3=DSQRT(X3)  
IF (X1.LT.0.00) X3=-X3  
X3=(-X1+X3)\*0.500  
UB=RDOT+VPR-X3  
RHOST=RDOT\*RHOP/X3  
GO TO 105  
40 ESTA=PST\*(1.00-BV\*RHOST)/RHOST/(GAM-1.00)  
SIG=PST+RHOP/G\*RDOT\*RDOT\*(RHOP/RHOST-1.00)  
DUB=UB/DFLOAT(NDIM-1)  
50 A=RHOST\*XB

```

DO 60 J=1,3
DO 60 I=1,NDIM
GS1(I,J)=A
B=DFLOAT(I-1)*DUB
GS2(I,J)=A*B
60 GS3(I,J)=A*(ESTA+B*R*.5DO/G)
VR=RDOT
IF(NPRC.EQ.0) RETURN

```

C  
C  
C

# DISTRIBUTIONS IN CONTINUUM PROPELLANT

```

IF(NWFR.GT.0) GO TO 62
A=RNDM(SIG)
XLPRI=CM/A/AB
XPPDP=XLPRI+X3
XBB=XLPRI
DO 61 J=1,3
DO 61 I=NDIM1,NDIM2
GS1(I,J)=A
GS3(I,J)=SIG
61 CONTINUE
RETURN
62 ITER=0
SUMA=CM/AB
XBBL=0.00
XBBH=XBB
63 XBB=0.500*(XBBL+XBBH)
BIT=-4.00/D3*AMU(1)*DELTBX*XBB
SUM=0.00
DO 65 I=NDIM1,NDIM2
SIGIJ=SIG*DEXP(BIT*DFLOAT(I-NDIM1))
GS3(I,1)=SIGIJ
RIJ=RNDM(SIGIJ)
GS1(I,1)=RIJ
FAC=1.00
IF((I-NDIM1)*(I-NDIM2).EQ.0) FAC=0.500
SUM=SUM+RIJ*FAC
65 CONTINUE
SUM=SUM*DELTBX
IF(DABS(SUM-SUMA/XBB).LT.1.D-6) GO TO 68
ITER=ITER+1
IF(ITER.LT.50) GO TO 66
WRITE(6,120)
CALL EXIT
66 IF(SUM.GT.SUMA/XBB) GO TO 67
XBBL=XBB
GO TO 63
67 XBBH=XBB
GO TO 63
68 DO 69 J=2,3

```

```

DO 69 I=NDIM1,NDIM2
GS1(I,J)=GS1(I,1)
GS3(I,J)=GS3(I,1)
69 CONTINUE
XLPRI=XBB
XPROP=XLPRI+XB
RETURN
70 WRITE (6,110)
CALL EXIT
80 TEST1=SIGMAX
IF (APMAX.LT.1.D-10) GO TO 90
TEST1A=RESP(XPR,VPR,AFAX)
TEST1=APMAX*(PRM+CM)/AB+TEST1A+AFAX*APMAX*G
IF (SIGMAX.LT.1.D-10) GO TO 90
IF (SIGMAX.LT.TEST1) TEST1=SIGMAX
90 IF (PST.GE.TEST1-1.D-10) GO TO 20
BIT=G/RHOP/RHOP/2.DO
NWAY=1
BIT=G/RHOP/RHOP/2.DO
BIT=BIT*(TEST1-PST)*(TEST1+(GAM+1.DO)/(GAM-1.DO)*PST)
BIT=BIT/(ECHEM+(BV-1.DO/RHOP)*PST/(GAM-1.DO))
RHOST=RHOP/(1.DO+(TEST1-PST)*G/RHOP/BIT)
100 RDOT=DSQRT(BIT)
UB=RDOT*(1.DO-RHOP/RHOST)
IF (NWAY.EQ.2) GO TO 40

C
C
CHECK MACH NUMBER
105 IF (MACH.LT.1.D-10) GO TO 40
BITM=DABS(UB-RDOT)/DSQRT(G*GAM*PST/RHOST/(1.DO-BV*RHOST))
IF (BITM.LE.MACH) GO TO 40
IF (MACH.LT.1.DO) GO TO 107
BITN=ECHEM+TEST1/RHOP-BV*PST/(GAM-1.DO)*(1.DO+(GAM-1.DO)*GAM*MACH
1 *MACH)
BITNN=RHOP*BV
BITNN=BITNN*BITNN-1.DO
BITL=BITNN*(GAM*PST*MACH/RHOP)**2*(MACH*MACH+2.DO/(GAM-1.DO))
106 DIS=BITN*BITN-BITL
IF (DIS.LT.0.DO) GO TO 70
BIT=(BITN-DSQRT(DIS))*G/BITNN
RHOST=1.DO/(BV+GAM*MACH*MACH*G*PST/RHOP/RHOP/BIT)
NWAY=2
GO TO 100
107 BITNN=1.DO-BV*RHOP
BITMM=1.DO+GAM*MACH*MACH
BITN=ECHEM+BITNN*BITMM*PST/RHOP
BITL=BITNN*GAM*PST*MACH/RHOP
BITL=2.DO/(GAM-1.DO)*BITL*BITL*(1.DO+(GAM-1.DO)/2.DO*MACH*MACH)
BITNN=BITNN*BITNN
GO TO 106

```

C

110 FORMAT (43H NEGATIVE DISCRIMINANT IN BAR1. TERMINATING)  
120 FORMAT(53H EXCESSIVE ITERATIONS TO DETERMINE PROPELLANT LENGTH.)  
END

SUBROUTINE BAR2 (I,J,K,XBP)

TRANSFORMS COMPUTATIONAL ARRAYS FOR LEVEL K INTO CUSTOMARY  
STATE VARIABLES FOR MESH RANGE I TO J  
ARGUMENT XBP IS THE POSITION OF THE PROPELLANT AT LEVEL K.

IMPLICIT REAL\*8(A-H,D-Z)

REAL\*8 MOL

COMMON /BARA/ GS1(100,3), GS2(100,3), GS3(100,3)

COMMON /BARB/ RHO(100), P(100), E(100), T(100), U(100), ETA(100)

COMMON /BARC/ NDT, NI, NF, NP, INT, NDIM, MAXDIM

COMMON /BARE/ GAM, BV, MOL, ECHM, RHOP, B1(20), B2(20), BN(20),

1 CV, ZR(20)

COMMON /BARG/ XBB, DELTBX, NPRC, NDIM1, NDIM2

DATA G /386.1600/

II=I

JJ=J

IF(I.GT.NDIM) GO TO 15

IF(J.GT.NDIM) JJ=NDIM

DO 10 L=I, JJ

RHO(L)=GS1(L,K)/XBP

U(L)=GS2(L,K)/GS1(L,K)

E(L)=GS3(L,K)/GS1(L,K)-U(L)\*U(L)\*0.5D0/G

P(L)=(GAM-1.D0)\*RHO(L)\*E(L)/(1.D0-BV\*RHO(L))

10 T(L)=E(L)/CV

IF(J.LE.NDIM) RETURN

II=NDIM1

JJ=J

15 IF(NPRC.EQ.0) GO TO 20

DO 16 L=II, JJ

RHO(L)=GS1(L,K)

U(L)=GS2(L,K)

16 P(L)=GS3(L,K)

RETURN

20 WRITE (6,30) I,J,NDIM

CALL EXIT

30 FORMAT (40H BAR2 CALLED WITH ILLEGAL ARGUMENTS, I =,I10,4H J =,I10

1,7H NDIM =,I10,12H TERMINATING)

END



SUBROUTINE BAR3 (JNT,XBP,VBP,XBBP,VBBP,DT)

UPDATES COMPUTATIONAL ARRAYS USING A TWO-LEVEL EXPLICIT MARCHING SCHEME. ROUTINE MUST BE CALLED TWICE PER UPDATE CYCLE, ONCE WITH JNT = 1 (PREDICTOR STEP) AND THEN WITH JNT = 0 (CORRECTOR STEP). ONLY THE INTERIOR MESH POINT VALUES ARE UPDATED; THE BOUNDARY VALUES ARE TREATED EXTERNALLY. ARGUMENTS XBP AND VBP ARE THE POSITION AND VELOCITY OF THE PROPELLANT AT THE PRESENT LEVEL. ARGUMENT XBBP IS THE LENGTH OF THE PROPELLANT AT THE PRESENT LEVEL AND VBBP IS THE VELOCITY OF THE PROJECTILE. ARGUMENT DT IS THE TIME STEP OVER WHICH THE SOLUTION IS BEING INCREMENTED.

IMPLICIT REAL\*8(A-H,O-Z)

COMMON /BARA/ GS1(100,3), GS2(100,3), GS3(100,3)  
COMMON /BAR3/ RHO(100), P(100), E(100), T(100), U(100), ETA(100)  
COMMON /BARC/ NDT, NI, NF, NP, INT, NDIM, MAXDIM  
COMMON /BARD/ DXMIN, DELTAX  
COMMON /BARG/ XBB, DELTBX, NPROC, NDIM1, NDIM2  
COMMON /BARI/ NWFR, NBRES1, NBRES2, NHTW, NMJZBL, NBRV  
COMMON /BARJ/ QORF(100), PRPRES

DIMENSION GS(100,3,3)  
EQUIVALENCE (GS(1,1,1),GS1(1,1))  
DATA G /386.15D0/

NI=MOD(NDT,3)+1  
NF=MOD(NDT+1,3)+1  
NP=MOD(NDT+2,3)+1  
NDIM=NDIM  
IF(NPROC.EQ.1) NDIM=NDIM2  
INT=MOD(NDT+1,2)  
DO 5 I=1,NDIM  
5 QORF(I)=0.00  
CALL BAR2 (1,NDIM,NI,XBP)  
IF(NWFR.NE.0.AND.NPROC.EQ.1) CALL WFR  
IF(NHTW.NE.0) CALL HTW  
DO 10 I=1,NDIM  
10 ETA(I)=U(I)-DFLOAT(I-1)\*VBP\*DELTAX  
DX=DELTAX\*XBP  
DELTAX=DELTAX  
IL=2  
IR=NDIM-1  
IF(NPROC.EQ.0) GO TO 15  
DO 14 I=NDIM1,NDIM2  
14 ETA(I)=U(I)-(DFLOAT(I-NDIM1)\*DELTBX\*(VBBP-VBP)+VBP)  
15 IF (INT.EQ.0) GO TO 20  
IP=1

```

IM=0
GO TO 25
20 IP=0
IM=1
25 DO 70 I=IL,IR
IF(I.GT.NDI4) GO TO 25
I2=I+IP
I1=I-IM
GS1(I,NF)=(GS1(I1,NI)*ETA(I1)-GS1(I2,NI)*ETA(I2))/DX
GS2(I,NF)=(GS2(I1,NI)*ETA(I1)-GS2(I2,NI)*ETA(I2))/DX+
*(P(I1)-P(I2))/DELTX*G
GS3(I,NF)=(GS3(I1,NI)*ETA(I1)-GS3(I2,NI)*ETA(I2))/DX+(P(I1)*U(I1)
1 -P(I2)*U(I2))/DELTX-QORF(I)*XBP
GO TO 35
26 X=RHO(I)
JL=I
IF(ETA(I).GT.0.D0) JL=I-1
JR=JL+1
XD=-X*(U(I+1)-U(I-1))/DX2
GS1(I,NF)=-ETA(I)*(RHO(JR)-RHO(JL))/DX+XD
AP=DSDR(X,XD,P(I))
GS3(I,NF)=-ETA(I)*(P(JR)-P(JL))/DX+AP*AP/G*XD
DPDX=(P(I-1)-P(I+1))/DX2
IF(DABS(QORF(I)).LT.1.D-10) GO TO 34
IF(DABS(U(I)).GT.1.D-3) GO TO 33

CHECK FOR LOCKING DUE TO FRICTION

IF(DPDX.GT.0.D0) GO TO 32
DPDX=DPDX-QORF(I)
IF(DPDX.GT.0.D0) DPDX=0.D0
GO TO 34
32 DPDX=DPDX+QORF(I)
IF(DPDX.LT.0.D0) DPDX=0.D0
GO TO 34
33 DPDX=DPDX+QORF(I)
34 GS2(I,NF)=-ETA(I)*(U(JR)-U(JL))/DX+G*DPDX/X
35 IF (INT.EQ.0) GO TO 50

PREDICTOR STEP

DO 40 K=1,3
40 GS(I,NF,K)=GS(I,NI,K)+GS(I,NF,K)*DT
GO TO 70

CORRECTOR STEP

50 DO 60 K=1,3
60 GS(I,NF,K)=0.5D0*(GS(I,NP,K)+GS(I,NI,K)+GS(I,NF,K)*DT)
70 CONTINUE

```

```
IF(NPRC.EQ.0.JR.IR.GT.NDIM) GO TO 80
IL=NDIM1+1
IR=NDIM2-1
DX=DELTSX*XBSP
DX2=2.00*DX
GO TO 25
80 NDI=NDI+1
RETURN
END
```

SUBROUTINE BAR4 (TSET,XB,XBB,SAFE,IER)

COURANT STABILITY CONDITION FOR FLOW.

TSET IS THE MAXIMUM VALUE WHICH THE TIME STEP MAY HAVE FOR  
STABLE INTEGRATION OF THE BALANCE EQUATIONS FOR THE FLOW.  
ARGUMENT XB IS THE PRESENT VALUE OF THE GAS/PROPELLANT  
INTERFACE AND XBB IS THE PRESENT LENGTH OF THE PROPELLANT.  
ARGUMENT SAFE IS A VALUE LARGER THAN ONE AND IS USED TO RESTRICT  
THE TIME STEP MORE STRINGENTLY THAN THE BASIC COURANT CONDITION.

IMPLICIT REAL\*8(A-H,O-Z)  
REAL\*8 MOL

COMMON /BARB/ RHO(100), P(100), E(100), T(100), U(100), ETA(100)  
COMMON /BARC/ NDT, NI, NF, NP, INT, NDIM, MAXDIM  
COMMON /BARD/ DXMIN, DELTAX  
COMMON /BARE/ GAM, BV, MOL, ECHEM, RHOP, B1(20), B2(20), BN(20),  
1 CV, ZR(20)  
COMMON /BARG/ YBB, DELTBX, NPROC, NDIM1, NDIM2  
DATA G /386.1600/

120  
C  
TSET=0.00  
DO 10 I=1,NDIM  
TCON=(GAM\*G\*P(I)/RHO(I)/(1.00-BV\*RHO(I)))  
IF (TCON.LT.0.00) GO TO 20  
C=DSQRT(GAM\*G\*P(I)/RHO(I)/(1.00-BV\*RHO(I)))  
BIT=DABS(U(I)-ETA(I))+C  
IF (BIT.GT.TSET) TSET=BIT  
10 CONTINUE  
TSET=XB\*DELTAX/TSET/SAFE  
IF(NPROC.EQ.0) RETURN  
TSET1=0.00  
DO 15 I=NDIM1,NDIM2  
AP=DSQR(RHO(I),1.00,P(I))  
APA=DSQR(RHO(I),-1.00,P(I))  
IF(APA.GT.AP) AP=APA  
BIT=DABS(U(I)-ETA(I))+AP  
IF(BIT.GT.TSET1) TSET1=BIT  
15 CONTINUE  
TSET1=XBB\*DELTBX/TSET1/SAFE  
IF(TSET1.LT.TSET) TSET=TSET1  
RETURN  
20 I=1  
IER=1  
RETURN  
END

SUBROUTINE BASE (XBP,XBF,XBBP,DT,IER)

UPDATES BOUNDARY VALUES AT GAS/PROPELLANT INTERFACE

ARGUMENTS XBP AND XBF ARE RESPECTIVELY THE POSITIONS OF THE  
INTERFACE AT THE PRESENT AND FUTURE LEVELS. ARGUMENT DT IS  
THE TIME STEP OVER WHICH THE SOLUTION IS BEING UPDATED.  
ARGUMENT XBBP IS THE LENGTH OF THE PROPELLANT AT THE PRESENT LEVEL

IMPLICIT REAL\*8(A-H,O-Z)  
REAL\*8 MOL, MACH

COMMON /BARA/ GS1(100,3), GS2(100,3), GS3(100,3)  
COMMON /BARB/ PHO(100), P(100), E(100), T(100), U(100), ETA(100)  
COMMON /BARC/ NDT, NI, NF, NP, INT, NDIM, MAXDIM  
COMMON /BARE/ GAM, BV, MOL, ECHEM, RHOP, B1(20), B2(20), BN(20),  
1 CV, ZR(20)  
COMMON /BARF/ XPP, VPR, CM, XB, VB, AB, PRM, RDOT, SIG, SSTART  
COMMON /BARG/ XBB, DELTBX, NPRC, NDIM1, NDIM2  
COMMON /BARH/ AUP, ADWN, VISLYR, DELYR, AMUV(10), AMU(10), DB,  
\* BRX(10), BR(10), AIRGAM, AIRPO, AIRTO, AIRMW, TVALO,  
\* PBRF, CDMUZ, ASBR, CDBR, PDIA, CHTW, DRHO(2)  
COMMON /BARCJ2/ PST, SIGMAX, MACH, APMAX, XI1, XI2, NCJ, IDEAL  
COMMON /BARJ/ QDRF(100), PRPRES  
COMMON /CJCD/ ICJ  
DATA R, G /18550.00, 386.16D0/

NCJ=0  
NSUP=0  
JDEAL=0  
ITEPP=0  
VVPR=VPR  
RHOPP=RHOP  
IF(NPRC.EQ.0) GO TO 5  
VVPR=U(NDIM1)  
CALL CARAC (NDIM1,VVPR,SSIG,DSDV,XBP,XBBP,DT,+1.0D0,C,DRHO(1))  
DIFFB=(VB-VVPR)\*DT/XBBP/DELTBX  
DIFFA=1.0D0-DIFFB  
P2=P(NDIM1)\*DIFFA+P(NDIM1+1)\*DIFFB  
RH02=RH0(NDIM1)\*DIFFA+RH0(NDIM1+1)\*DIFFB  
C=0.5D0\*(C+DSDR(RH02,DRHO(1),P2))  
C2P=C\*C  
RHOPP=RH02+(SSIG-P2)\*G/C2P  
DRHO(1)=(RHOPP-RH02)/DT  
5 IF (NDT.EQ.1) NOUT=0  
IF (CM.GT.0.0D0) GO TO 20  
IF (NOUT.GE.10) GO TO 60

BOUNDARY VALUE OF PRESSURE FROM SIMPLE WAVE ANALYSIS FOR FIVE  
INTEGRATION CYCLES AFTER BURNOUT

C

```

IF (NOUT.NE.0) GO TO 10
PST=P(NDIM)
RHOST=RHO(NDIM)
UST=U(NDIM)
10 UNF=VVPR
WPR=VVPR-UST
TP=(1.00-(GAM-1.00)/2.00*WPR/DSQRT(G*GAM*PST*(1.00-BV*RHOST)/RHOST
1 ))
IF (TP.LT.0.00) GO TO 230
PNF=PST*TP*(2.00*GAM/(GAM-1.00))
NOUT=NOUT+1
RHONF=1.00/(BV+(PST/PNF)*(1.00/GAM)*(1.00/RHOST-BV))
ROOT=0.00
SIG=PNF
IF (PNF.GT..0500*PST) GO TO 200
NCJ=1
WRITE (6,270)
RETURN
20 IF (IDEAL.NE.1) GO TO 60
IF (U(NDIM).GT.1.0-10) GO TO 50

IDEAL BURN RATE LAW (IDEAL=0)

UNF=0.00
PNF=PST
BIT=X12-VVPR*VVPR/2.00/G
IF (BIT.GT.0.00) GO TO 30
WRITE (6,250)
NCJ=1
RETURN
30 ROOT=X11*VVPR/BIT
IF (ROOT.LE.1.0-10) GO TO 70
RHONF=RHO*ROOT/(ROOT+VVPR)
IF (RHONF.LT.1.00/BV) GO TO 40
IF (MACH.GT.1.0-10) GO TO 50
WRITE (6,260)
NCJ=1
RETURN

CHECK MACH NUMBER OF REACTION PRODUCTS

40 IF (MACH.LE.1.0-10) GO TO 190
BITARG=G*GAM*PNF/RHONF/(1.00-BV*RHONF)
IF (BITARG.LE.0.00) GO TO 50
BIT=DABS(UNF-VVPR-ROOT)/DSQRT(BITARG)
IF (BIT.GE.1.00) GO TO 50
IF (BIT.LE.MACH) GO TO 189
50 IDEAL=1
60 ITER=0

```

122

```

UNF=U(NDIM)
IF (CM.LE.0.00) UNF=VVPR
CALL CARAC (NDIM,UNF,PNF,XA,XBP,XBBP,DT,-1.00,C,0.00)
IF (CM.GT.0.00) GO TO 80
70 RDOT=0.00
SIG=PNF
C=0.500*(C+DSQRT(G*GAM*P(NDIM)/RHO(NDIM)/(1.00-BV*RHO(NDIM))))
C2=C*C
RHONF=RHO(NDIM)+G/C2*(PNF-P(NDIM)+QORF(NDIM)*(GAM-1.00)/
* (1.00-BV*RHO(NDIM))*DT)
GO TO 192
80 YB=PNF-UNF*XA
90 IF (JDEAL.EQ.0) GO TO 100
NRBIT=0
IF (MACH.GE.1.00) GO TO 95
BIT1=(PNF-YB)/XA-VVPR
BIT2=1.00-BV*RHOPP
BIT3=4.00*BIT2*MACH*MACH*GAM*G/RHOPP
TMP=BIT1**2+BIT3*PNF
IF (TMP.LT.0.00) GO TO 230
BIT4=DSQRT(TMP)
RDOT=(BIT1+BIT4)/BIT2*0.500
RDOTPR=(1.00/XA+0.500/BIT4*(2.00/XA*BIT1+BIT3))/BIT2*0.500
GO TO 140
95 IF (IDEAL.EQ.2) GO TO 96
NCJ=1
WRITE(6,240)
RETURN
96 RBIT=G/RHOPP*(TEST1-(1.00+GAM*MACH*MACH)*PNF)/(BV*RHOPP-1.00)
IF (PNF.GT.TEST1) PNF=TEST1
IF (RBIT.GT.0.00) GO TO 97
NRBIT=NRBIT+1
PNF=0.9500*PNF
IF (NRBIT.LT.10) GO TO 96
WRITE(6,245)
RETURN
97 RDOT=DSQRT(RBIT)
RDOTPR=-0.500*G/RHOPP/RDOT*(1.00+GAM*MACH*MACH)/(BV*RHOPP-1.00)
PSI=GAM*G*MACH*MACH/RHOPP/RDOT/RDOT
PSIPR=PSI*(1.00-2.00*PNF*RDOTPR/RDOT)
PSI=RHOPP*(BV+PNF*PSI/RHOPP)
NSUP=1
GO TO 145
100 IF (IDEAL.EQ.2) GO TO 110
IF (PNF.GT.0.00) GO TO 105
IF (MACH.GT.1.0-10) GO TO 50
NCJ=1
RETURN
105 CALL BURN (PNF,RDOT,RDOTPR)
GO TO 140

```

C  
C  
C

IDEAL CASE (IDEAL=2)

```
110 IF (APMAX.LT.1.D-10) GO TO 120
    TEST1A=RESP(XPR,VPR,AFAX)
    TEST1=APMAX*(PRM+CM)/AB+TEST1A+AFAX*APMAX*G
    IF (SIGMAX.LT.1.D-10) GO TO 130
    IF (SIGMAX.LT.TEST1) TEST1=SIGMAX
    GO TO 130
120 TEST1=SIGMAX
130 BIT1=TEST1*(GAM+1.DO)/(GAM-1.DO)*PNF
    BIT2=XA*VVPR+YB-PNF
    BIT2=BIT2*0.5DO/XA/RHOPP
    BIT3=ECHM+(BV-1.DO/RHOPP)*PNF/(GAM-1.DO)
    RDOT=BIT1*BIT2/BIT3
    RDOTPR=(GAM+1.DO)/(GAM-1.DO)*BIT2/BIT3-BIT1/BIT3*0.5DO/XA/RHOPP
    1 -BIT1*BIT2/BIT3/BIT3*(BV-1.DO/RHOPP)/(GAM-1.DO)
140 CONTINUE
    IF(RDOT.LE.1.D-10) GO TO 175
    PSI=(VVPR+RDOT-(PNF-YB)/XA)
    PSIPR=(RDOTPR-1.DO/XA)*RDOT-PSI*RDOTPR
    PSI=PSI/RDOT
    PSIPR=PSIPR/RDOT/RDOT
145 FP1=(GAM/(GAM-1.DO)*PSI-1.DO-BV*RHOPP/(GAM-1.DO))/RHOPP
    FP2=PSI-1.DO
    FP=PNF*FP1-ECHM+RDOT*RDOT*FP2*FP2/2.DO/G
    FPPR=FP1+PNF*GAM/(GAM-1.DO)/RHOPP*PSIPR+RDOT*RDOTPR*FP2*FP2/G
    * +RDOT
    1 *RDOT*FP2*PSIPR/G
    IF (DABS(FP).LT.1.DO) GO TO 170
    IF (ITER.LT.50) GO TO 150
    WRITE (6,280)
    GO TO 170
150 PNF=PNF-FP/FPPR
    ITER=ITER+1
    IF (JDEAL.EQ.1) GO TO 90
    GO TO 100
170 IF (IDEAL.EQ.0) GO TO 180
    IF (RDOT.GT.0.DO) GO TO 190
175 UNF=VVPR
    CALL CARAC (NDIM,UNF,PNF,XA,XBP,XBBP,DT,-1.DO,C,0.DO)
    GO TO 70
180 IF(NSUP.EQ.0) GO TO 185
    RHONF=RHOPP/PSI
    UNF=VVPR+(1.DO-PSI)*RDOT
    GO TO 188
185 UNF=(PNF-YB)/XA
    RHONF=RDOT*RHOPP/(VVPR+RDOT-UNF)
188 IF (IDEAL.NE.1.AND.JDEAL.EQ.0) GO TO 40
189 IF(IDEAL.NE.0) GO TO 190
```



```

IF(RHONF.LT.0.900/BV.AND.PNF.GT.0.00 ) GO TO 190
IF(JDEAL.EQ.1) GO TO 190
IF(MACH.GT.1.0-10.AND.MACH.LT.1.00) GO TO 50
WRITE(6,310)
RETURN
190 SIG=PNF+RHOPP*ROOT*ROOT/G*(RHOPP/RHONF-1.00)
192 IF(NPRC.EQ.0) GO TO 200
DSSIG=SIG-SSIG
IF(DABS(DSSIG).LT.1.0-3) GO TO 200
IF(ITERP.LT.50) GO TO 195
WRITE(6,300)
GO TO 200
195 ITERP=ITERP+1
VVPR=VVPR+DSSIG/DSDV
RHOPP=RHOPP+DSSIG*G/C2P
RHOPPP=RNDM(SIG)
IF(RHOPP.LT.RHOPPP) RHOPP=RHOPPP
SSIG=SIG
GO TO 20
200 ENF=PNF*(1.00-BV*RHONF)/(GAM-1.00)/RHONF
210 U(NDIM)=UNF
P(NDIM)=PNF
E(NDIM)=ENF
T(NDIM)=ENF/CV
RHO(NDIM)=RHONF
BIT=XBFB*RHONF
VB=VVPR+ROOT
GS1(NDIM,NF)=BIT
GS2(NDIM,NF)=BIT*JNF
GS3(NDIM,NF)=BIT*(ENF+UNF*UNF*0.500/G)
IF(NPRC.EQ.0) GO TO 220
U(NDIM1)=VVPR
P(NDIM1)=SIG
RHO(NDIM1)=RHOPP
GS1(NDIM1,NF)=RHOPP
GS2(NDIM1,NF)=VVPR
GS3(NDIM1,NF)=SIG
220 RETURN
C SET PNF ERROR CONDITION
230 WRITE (6,290)
IER=1
GO TO 220
C
240 FORMAT(42H ILLEGAL PARAMETERS FOR SUPERSONIC BURNING)
245 FORMAT(47H NEGATIVE SQUARE ROOT DURING SUPERSONIC BURNING)
250 FORMAT (39H IDEAL BURN RATE INFINITE. TERMINATING.)
260 FORMAT (54H IDEAL BURN RATE PRODUCES DENSITY LESS THAN RECIPROCAL/
126H OF COVOLUME. TERMINATING.)
270 FORMAT (53H BASE PRESSURE DROPS TO LESS THAN 5% OF INITIAL VALUE/3
12H FOLLOWING BURNOUT. TERMINATING.)

```

280 FORMAT (28H FAILURE TO CONVERGE IN BASE)  
290 FORMAT (29H PNF FUNCTION IN BASE<0--STOP)  
300 FORMAT(54H FAILURE TO CONVERGE IN BASE WITH CONTINUUM PROPELLANT)  
310 FORMAT(50H COVOLUME LIMIT APPROACHED WITH MEASURED BURN RATE)  
END

SUBROUTINE BASEPR (XBBP,DT)

UPDATES BOUNDARY VALUES AT INTERFACE BETWEEN PROJECTILE  
BASE AND CONTINUUM PROPELLANT.

ARGUMENT XBBP IS THE LENGTH OF THE PROPELLANT AT THE PRESENT  
LEVEL AND DT IS THE TIME STEP.

IMPLICIT REAL\*8(A-H,O-Z)  
REAL\*8 MOL

COMMON /BARA/ GS1(100,3), GS2(100,3), GS3(100,3)  
COMMON /BARB/ RHO(100), P(100), E(100), T(100), U(100), ETA(100)  
COMMON /BARC/ NDT, NI, NF, NP, INT, NDIM, MAXDIM  
COMMON /BARE/ GAM, BV, MOL, ECHM, RHOP, B1(20), B2(20), BN(20),  
1 CV, ZR(20)

COMMON /BARE/ XPR, VPR, CM, XB, VB, AB, PRM, RDOT, SIG, SSTART  
COMMON /BARG/ XBB, DELTBX, NPEC, NDIM1, NDIM2

COMMON /BARH/ AUP, ADWN, VISLYR, DELYR, AMUV(10), AMU(10), DB,  
\* BRX(10), BR(10), AIRGAM, AIRPO, AIRTO, AIRMW, TWALO,  
\* BPPF, CDMUZ, ASBR, CDBR, PDIA, CHTW, DRHO(2)  
DATA G /386.1600/

CALL CARAC(NDIM2, VPR, PNF, DPOU, 0.00, XBBP, DT, -1.00, C, DRHO(2))

U(NDIM2)=VPR

C=0.500\*(C+DSQR(RHO(NDIM2), DRHO(2), P(NDIM2)))

C2=C\*C

RHOPP=RNDM(PNF)

BIT=RHO(NDIM2)

RHO(NDIM2)=RHO(NDIM2)+G/C2\*(PNF-P(NDIM2))

IF(RHO(NDIM2).LT.RHOPP) RHO(NDIM2)=RHOPP

DRHO(2)=(RHO(NDIM2)-BIT)/DT

P(NDIM2)=PNF

GS1(NDIM2,NF)=RHO(NDIM2)

GS2(NDIM2,NF)=VPR

GS3(NDIM2,NF)=PNF

RETURN

END

SUBROUTINE BREECH (XBP,XBF,DT)

UPDATES BOUNDARY VALUES AT BREECH OF TUBE WHEN IMPERMEABLE  
ARGUMENTS XBP AND XBF ARE RESPECTIVELY THE POSITIONS OF THE  
PROPELLANT AT THE PRESENT AND FUTURE LEVELS.  
ARGUMENT DT IS THE TIME STEP OVER WHICH THE SOLUTION IS BEING  
INCREMENTED.

IMPLICIT REAL\*8(A-H,O-Z)  
REAL\*8 MDL

COMMON /BARA/ GS1(100,3), GS2(100,3), GS3(100,3)  
COMMON /BARB/ RHO(100), P(100), E(100), T(100), U(100), ETA(100)  
COMMON /BARC/ NDT, NI, NF, NP, INT, NDIM, MAXDIM  
COMMON /BARE/ GAM, BV, MDL, ECHM, RHOP, B1(20), B2(20), BN(20),  
1 CV, ZR(20)  
COMMON /BARJ/ QORF(100),PRPRES  
DATA G /386.1600/

CALL CARAC (1,0.00,PNF,DPDU,XBP,0.00,DT,1.00,C,0.00)  
U(1)=0.00  
C=0.500\*(C+DSQRT(G\*GAM\*P(1)/RHO(1)/(1.00-BV\*RHO(1))))  
C2=C\*C  
RHO(1)=RHO(1)+G/C2\*(PNF-P(1)+QORF(1)\*(GAM-1.00)/  
\*(1.00-BV\*RHO(1))\*DT)  
P(1)=PNF  
E(1)=P(1)/RHO(1)/(GAM-1.00)\*(1.00-BV\*RHO(1))  
T(1)=E(1)/CV  
BIT=XBF\*RHO(1)  
GS1(1,NF)=BIT  
GS2(1,NF)=0.00  
GS3(1,NF)=BIT\*E(1)  
RETURN  
END

SUBROUTINE BURN (PNF,RDOT,RDOTPR)

CALCULATES REGRESSION RATE (RDOT) AND DERIVATIVE WITH RESPECT  
TO PRESSURE (RDOTPR) AS A FUNCTION OF PRESSURE (PNF) FOR  
EXPONENTIAL BURN RATE LAW (IDEAL=0)  
SUBROUTINE ALLOWS FOR MULTIPLE BURN RATE FUNCTIONS WHICH CHANGE  
AS THE TC GRAIN BURNS.

IMPLICIT REAL\*8(A-H,O-Z)  
REAL\*8 MOL

COMMON /BARE/ GAM, BV, MOL, ECHM, RHOP, B1(20), B2(20), BN(20),  
1 CV, ZR(20)  
COMMON /BARE/ XPR, VPR, CM, XB, DUM(5)  
COMMON /BRVAR/ XLPRI, XPROP, NBR

CHECK FOR VARIATION OF BURN RATE FUNCTION.

IF (NBR.EQ.0) GO TO 20  
XLPR=XPROP+XPR-XB

COMPUTE FRACTION OF GRAIN MASS BURNED

ZP=1.00-CM/RHOP/XLPR  
IF (ZP.LT.0.00) GO TO 20  
DO 10 I=1,NBR

CHECK FOR FRACTION OF GRAIN MASS BURNED, IF EXCEEDED  
CHANGE BURN RATE FUNCTION.

IF (ZP.LT.ZR(I)) GO TO 30  
10 CONTINUE

B1I=B1(NBR)  
B2I=B2(NBR)  
BNI=BN(NBR)

GO TO 40

20 B1I=B1(1)  
B2I=B2(1)  
BNI=BN(1)

GO TO 40

30 B1I=B1(I)  
B2I=B2(I)  
BNI=BN(I)

I=1

40 CONTINUE

RDOT=B2I\*PNF\*\*BNI  
RDOTPR=RDOT\*BNI/PNF  
RDOT=RDOT+B1I  
RETURN  
END

SUBROUTINE CARAC (KK,UNF,PNF,DPDU,XBP,XBBP,DT,SGN,CR,DRHO)

USES CONDITIONS OF COMPATIBILITY ON ACOUSTIC CHARACTERISTICS  
TO DETERMINE BOUNDARY VALUES OF PRESSURE (PNF) CONSISTENT  
WITH VELOCITY (UNF) AT POINT KK. ALSO RETURNS DERIVATIVE  
OF PRESSURE WITH RESPECT TO VELOCITY (DPDU), SPEED OF SOUND  
(CR).

ARGUMENT XBP IS THE POSITION OF THE GAS/PROPELLANT INTERFACE  
AT THE PRESENT LEVEL AND XBBP IS THE LENGTH OF THE PROPELLANT.  
ARGUMENT DT IS THE TIME STEP OVER WHICH THE SOLUTION IS BEING  
INCREMENTED.

ARGUMENT SGN IS SET EQUAL TO 1 FOR A LEFT HAND BOUNDARY AND -1  
FOR A RIGHT HAND BOUNDARY. ARGUMENT DRHO IS THE TIME DERIVATIVE  
OF THE PROPELLANT DENSITY.

IMPLICIT REAL\*8(A-H,O-Z)  
REAL\*8 IZ, MOL, MACH

COMMON /BARB/ RHO(100), P(100), E(100), T(100), U(100), ETA(100)  
COMMON /BARC/ NDT, NI, NF, NP, INT, NDIM, MAXDIM  
COMMON /BARD/ DXMIN, DELTAX  
COMMON /BARE/ GAM, BV, MOL, ECHM, RHOP, B1(20), B2(20), BN(20),  
1 CV, ZR(20)  
COMMON /BARF/ XPR, VPR, CM, XB, VB, AB, PRM, RDOT, SIG, SSTART  
COMMON /BARG/ XBB, DELTBX, NPRC, NDIM1, NDIM2  
COMMON /BARI/ NWFR, NBRES1, NBRES2, NHTW, NMUZBL, NBRV  
COMMON /BARJ/ QORF(100), PRPRES  
COMMON /BARCJ2/ PST, SIGMAX, MACH, APMAX, XI1, XI2, NCJ, IDEAL  
COMMON /LPRD/ NPRO  
DATA G /386.15D0/

UREL=0.D0  
IF(KK.EQ.1) GO TO 2  
IF(NPRC.EQ.1.AND.KK.EQ.NDIM2) GO TO 2  
UREL=UNF-VB  
2 IF(SGN.LT.0.D0) GO TO 4  
IA=KK  
IB=KK+1  
GO TO 10  
4 IA=KK-1  
IB=KK  
10 IF(KK.LE.NDIM) GO TO 20  
C=DSQR(RHO(KK),DRHO,P(KK))  
I2=DFLOAT(NDIM1)+(-(SGN-1.D0)/2.D0-DT\*(-SGN\*C+UREL)/XBBP)  
\* /DELTBX  
GO TO 25  
20 C=DSQR(GAM\*P(KK)\*G/RHO(KK)/(1.D0-BV\*RHO(KK)))  
SGM=SGN  
IF(DABS(DRHO).LE.1.D-10) GO TO 24  
SGM=DRHO

```

IF(SGN.LT.0.D0) GO TO 22
IA=IA-1
IB=IB-1
GO TO 24
22 IA=IA+1
IB=IB+1
24 I2=1.D0+(-(SGM-1.D0)/2.D0-DT*(-SGN*C+UREL)/XBP)/DELTAX
25 IF (I2.GE.DFLJAT(IA).AND.I2.LE.DFLJAT(IB)) GO TO 40
IF (NPRO.GT.0) GO TO 30
IF (IDEAL.GT.0.AND.MACH.LT.1.D-10) GO TO 30
IF (IDEAL.GT.0.AND.MACH.GE.0.9900) GO TO 30
WRITE (6,50) KK,I2,C,UREL
30 CONTINUE
IF (I2.LT.DFLJAT(IA)) I2=DFLJAT(IA)
IF (I2.GT.DFLJAT(IB)) I2=DFLJAT(IB)
40 DIFFA=IB-I2
DIFFB=I2-IA
CR=C
NB=NI
IF (INT.EQ.0) NB=NP
RHO1=RHO(KK)
CALL BAR2 (IA,IB,NB,XBP)
U2=U(IA)*DIFFA+U(IB)*DIFFB
P2=P(IA)*DIFFA+P(IB)*DIFFB
RHO2=RHO(IA)*DIFFA+RHO(IB)*DIFFB
RHO2=0.5D0*(RHO2+RHO1)
BIT=(QORF(KK)+DIFFA*QORF(IA)+DIFFB*QORF(IB))*DT*0.5D0
IF (KK.GT.NDIM) GO TO 45
BIT=-BIT*(GAM-1.D0)/(1.D0-BV*RHO2)
C=0.5D0*(C+DSQR(GAM*P2*G/RHO2/(1.D0-BV*RHO2)))
44 PNF=P2-SGN*RHO2*C*(U2-UNF)/G+BIT
DPDU=SGN*RHO2*C/G
RETURN
45 C=0.5D0*(C+DSQR(RHO2,DRHO,P2))
IF (BIT*UNF.GT.0.D0) BIT=-BIT
BIT=-SGN*C*BIT
IF (NWFR.LE.0) GO TO 44
BIT=BIT/P(KK)
DPDU=SGN*RHO2*C/G/(1.D0-BIT)
IF (DABS(BIT).LT.1.D-10) GO TO 45
IF (DABS(U2).LT.1.D0.AND.DABS(UNF).LT.1.D0) GO TO 47
46 PNF=P2/(1.D0-BIT)-DPDU*(U2-UNF)
RETURN
47 PNF=P(KK)
RETURN
C
50 FORMAT (40H CHARACTERISTIC INTERCEPT OUT OF RANGE. WARNING.,4G20.6
1)
END

```

FUNCTION DSDR(X,XD,Y)

COMPUTES SMALL AMPLITUDE WAVE SPEED IN SOLID PROPELLANT AS  
A FUNCTION OF DENSITY (X), RATE-OF-CHANGE-OF-DENSITY (XD), AND  
PRESSURE (Y)

IMPLICIT REAL\*8(A-H,D-Z)

REAL\*8 MDL

COMMON /BARE/ GAM, BV, MDL, ECHM, RHOP, B1(20), B2(20), BN(20),

1 CV, ZR(20)

COMMON /BARH/ AUP,ADWN,VISLYR,DELYR,AMUV(10),AMU(10),  
\* BRX(10),BR(10),AIRGAM,AIRPO,AIRTO,AIRMW,TWALO,  
\* PBRF,CDMUZ,ASBR,CDBR,PDIA,CHTW,DRHO(2)

DSDR=AUP\*X/RHOP

IF(XD.LT.0.00) GO TO 10

YN=SNOM(X)

IF(Y.LT.YN-1.0-10) GO TO 10

RETURN

10 IF(ADWN.GT.DSDR) DSDR=ADWN

RETURN

END



SUBROUTINE GETK (I)

DERIVATIVES OF PROPELLANT AND PROJECTILE MOTION

GETK IS CALLED TWICE PER UPDATE CYCLE WITH I=1 FOR THE PREDICTOR  
STEP AND I=2 FOR THE CORRECTOR STEP.

IMPLICIT REAL\*8(A-H,O-Z)  
REAL\*8 MOL, K

COMMON /BARB/ RHO(100), P(100), E(100), T(100), U(100), ETA(100)  
COMMON /BARE/ GAM, BV, MOL, ECHEM, RHOP, B1(20), B2(20), BN(20),  
1 CV, ZR(20)  
COMMON /BARF/ XPR, VPR, CM, XB, VB, AB, PRM, RDOT, SIG, SSTART  
COMMON /BARG/ XPB, DELTEX, NPPC, NDIM1, NDIM2  
COMMON /BARH2/ PRMB, ELB, ANJ, BMUV(10), BMU(10), NBRES3  
COMMON /BARH4/ RESAIR, RESOR  
COMMON /BARJ/ QORF(100), PRPRES  
COMMON /BERG/ K(4,2)  
DATA G /386.16D0/

CHECK FOR SHOT-START CONDITION

IF (SIG.GT.SSTART) GO TO 10  
IF (NBRES3.NE.0) GO TO 10  
K(1,1)=0.00  
K(2,1)=0.00  
GO TO 20  
10 K(1,1)=VPR  
IF (NBRES3.EQ.0) SSTART=0.00  
IF (NPPC.EQ.1) GO TO 12  
SIGX=SIG-RESP(XPR,VPR,A)  
PRTOT=PRM+CM  
GO TO 14  
12 SIGX=P(NDIM2)-RESP(XPR,VPR,A)+PRPRES\*XBB  
PRTOT=PRM  
14 IF (SIGX.LT.0.00.AND.VPR.LE.0.00) SIGX=0.00  
K(2,1)=AB\*G\*SIGX/PRTOT/(1.00+A\*AB\*G/PRTOT)  
RESOR=RESOR+A\*K(2,1)  
20 K(3,1)=0.00  
RHOPX=RHOP  
IF (NPPC.EQ.1) RHOPX=RHO(NDIM1)  
IF (CM.GT.0.00) K(3,1)=-RDOT\*AB\*RHOPX  
K(4,1)=VB  
RETURN  
END

SUBROUTINE HTW

HEAT LOSS TO TUBE WALL FROM GAS

IMPLICIT REAL\*8(A-H,O-Z)  
REAL\*8 MOL

COMMON /BARB/ RHO(100), P(100), E(100), T(100), U(100), ETA(100)  
COMMON /BARC/ NDT, NI, NF, NP, INT, NDIM, MAXDIM  
COMMON /BARE/ GAM, RV, MOL, ECHEM, RHOP, B1(20), B2(20), BN(20),  
1 CV, ZR(20)

COMMON /BARG/ XBB, DELTBX, NPROC, NDIM1, NDIM2

COMMON /BARH/ AUP, ADWN, VISLYR, DELYR, AMUV(10), AMU(10), DB,  
\* BRX(10), BR(10), AIRGAM, AIRPO, AIRTO, AIRMW, TWALO,  
\* DBRF, COMUZ, ASBK, CDBR, PDIA, CHTW, DRHO(2)

COMMON /BARH3/ PRNO, VISG

COMMON /BARJ/ QORF(100), PRPRES

BIT=VISG\*CV\*GAM/PRNO\*\*0.600

DO 10 I=1,NDIM

QORF(I)=0.00

IF(T(I),LT,TWALO) GO TO 10

REY=RHO(I)\*U(I)\*DB/VISG

REY=DABS(REY)

QORF(I)=CHTW/DB/DB\*(T(I)-TWALO)\*REY\*\*0.800\*BIT

10 CONTINUE

RETURN

END

SUBROUTINE DUTFLD(KK,XBP,XBF,DT,SGN)

BOUNDARY VALUES AT GAS PERMEABLE BOUNDARY VENTING TO  
ATMOSPHERE.

ARGUMENT KK POINTS TO STORAGE LOCATION FOR BOUNDARY DATA.  
XBP IS THE LENGTH OF THE GAS COLUMN AT THE PRESENT UPDATE  
LEVEL AND XBF IS THE VALUE AT THE FUTURE UPDATE LEVEL. DT  
IS THE TIME STEP THROUGH WHICH THE SOLUTION IS BEING ADVANCED.  
SGN IS SET EQUAL TO 1 AT A LEFT HAND BOUNDARY AND -1 AT A RIGHT  
HAND BOUNDARY.

IMPLICIT REAL\*8(A-H,O-Z)  
REAL\*8 MOL

COMMON /BARA/ GS1(100,3), GS2(100,3), GS3(100,3)  
COMMON /BARB/ RHO(100), P(100), E(100), T(100), U(100), ETA(100)  
COMMON /BARC/ NDT, NI, NE, NP, INT, NDIM, MAXDIM  
COMMON /BARD/ DXMIN, DELTAX  
COMMON /BARE/ GAM, BV, MOL, ECHEM, RHOP, B1(20), B2(20), BN(20),  
1 CV, ZR(20)  
COMMON /BARF/ YPR, VPR, CM, XB, VE, AB, PRM, RDOT, SIG, SSTART  
COMMON /BARH/ AUP,ADWN,VISLYR,DELYR,AMUV(10),AMU(10),DB,  
\* BRX(10),BR(10),AIRGAM,AIRPO,AIRTO,AIRMW,TWALO,  
\* PRPF,CDMUZ,ASBR,COBR,PDIA,CHTW,DRHO(2)  
COMMON /BARJ/ QDRF(100),PRPRES  
DATA R,G /18550.00,386.1500/

UNF=U(KK)  
QDRFBT=QDRF(KK)\*(GAM-1.00)/(1.00-BV\*RHO(KK))\*DT  
CALL CARAC(KK,UNF,PNF,DPDU,XBP,1.00,DT,SGN,C,0.00)  
NWAY=0  
IF(DABS(UNF/C).LT.1.00) GO TO 50

SEARCH FOR SUPERSONIC EFFLUX

SGN2=-SGN  
CALL CARAC(KK,UNF,PNF2,DPDU2,XBP,1.00,DT,SGN2,C,SGN)  
SAVE=UNF  
UNF=UNF+(PNF2-PNF)/(DPDU-DPDU2)  
SAVEP=PNF  
PNF=PNF+DPDU\*(UNF-SAVE)  
NWAY=1

50 DIFF=-SGN\*UNF\*DT/XBP/DELTAX  
IF(KK.EQ.NDIM) GO TO 54  
DIFFA=1.00-DIFF  
IA=1  
GO TO 56  
54 DIFFA=DIFF  
DIFFB=1.00-DIFF

```

56 IA=NDIM-1
   IB=IA+1
   P2=P(IA)*DIFFA+P(IB)*DIFFB
   RHO2=RHO(IA)*DIFFA+RHO(IB)*DIFFB
   C=0.5D0*(C+DSQRT(G*GAM*P2/RHO2/(1.D0-BV*RHO2)))
   GC2=G/C/C
60 RHONF=RHO2+((PNF-P2)+QDRFBT)*GC2
   ENF=PNF*(1.D0-BV*RHONF)/(GAM-1.D0)/RHONF
   TNF=ENF/CV
   IF(NWAY.EQ.0) GO TO 100
   IF(NWAY.EQ.2) GO TO 110
   CBIT=DSQRT(G*GAM*PNF/RHONF/(1.D0-BV*RHONF))
   IF(DABS(UNF/CBIT).GE.1.D0) GO TO 104
90 NWAY=0
   UNF=SAVE
   PNF=SAVEP
   GO TO 50

```

C  
C  
C

SEARCH FOR SUBSONIC EFFLUX

```

100 ITER=0
   LSET=0
   LHSET=0
   NWAY=2
104 IF(KK.NE.1) GO TO 105
   CDB=CDBR
   AST=ASBR
   GO TO 110
105 CDB=CDMUZ
   AST=AB

```

C  
C  
C

QUASI-STEADY FLOW RATE

```

110 BIT=1.D0+UNF*JNF/2.D0/G/ENF/GAM
   NEXT=0
130 PS=PNF*BIT** (GAM/(GAM-1.D0))
   IF(NEXT.EQ.1) GO TO 140
   NEXT=1
   BIT=BIT-BV*(PS-PNF)/ENF/GAM
   GO TO 130
140 TS=TNF*BIT
   BITP=BV*PS/R/TS*MJL
   CRIT=CDB*AST*PS*DSQRT(GAM*G*MJL/R/TS*(2.D0/(GAM+1.D0)))**
   * ((GAM+1.D0)/(GAM-1.D0))
   * *(1.D0-0.224D0*BITP+0.104D0*BITP*BITP)
150 IF(NWAY.EQ.2) GO TO 155
   CRIT2=AB*RHONF*DABS(UNF)
   IF(CRIT2.LE.1.01D0*CRIT) GO TO 190
   GO TO 90
155 UNFA=UNF

```

```

UNFP=-SGN*CRIT/AB/RHONF
IF(DABS(UNFB-JNFA).LT.1.0-2*DABS(UNFA)) GO TO 190
UNF=UNFB
ITER=ITER+1
IF(ITER.GT.50) GO TO 200
IF(UNF.GT.UNFA) GO TO 160
UNFH=UNFA
LHSET=1
GO TO 170
160 UNFL=UNFA
LSET=1
170 IF(LSET*LHSET.EQ.0) GO TO 180
UNF=0.500*(UNFH+UNFL)
PNF=PNF+DPDU*(UNF-UNFA)
GO TO 60
180 DELP=DPDU*(UNF-UNFA)/2.00
PNF=PNF+DELP
UNF=UNFA+DELP/DPDU
GO TO 60

C
C
C
VALUES CONVERGED
190 U(KK)=UNF
P(KK)=PNF
T(KK)=TNF
E(KK)=ENF
BIT=XBF*RHONF
RHO(KK)=RHONF
GS1(KK,NF)=BIT
GS2(KK,NF)=BIT*UNF
GS3(KK,NF)=BIT*(ENF+UNF*UNF/2.00/G)
RETURN

C
C
C
ERROR MESSAGE
200 WRITE(6,210)
210 FORMAT(42H EXCESSIVE NUMBER OF ITERATIONS IN OUTFLO.)
CALL EXIT
END

```

SUBROUTINE REFIT (NWAY,N)

ROUTINE TO PERFORM ALLOCATION OF MESH. CALLED AFTER EACH UPDATE CYCLE BY BAR3 WITH NWAY = 1. ALSO CALLED INITIALLY BY BAR1 WITH NWAY = 0.

ARGUMENT N IS A POINTER TO THE LEVEL AT WHICH THE FLOW PARAMETERS ARE BEING INTERPOLATED.

REFIT ESTABLISHES MESH IN ACCORDANCE WITH VALUES OF INPUT QUANTITIES DXMIN AND MAXDIM WHERE:

DXMIN - MINIMUM VALUE OF MESH INTERVAL (IN PHYSICAL UNITS)  
MAXDIM - MAXIMUM NUMBER OF MESH POINTS DESIRED.

NDIM MESH POINTS ARE ESTABLISHED SUCH THAT  $3 \leq NDIM \leq MAXDIM$ . AS THE PROPELLANT MOVES, POINTS ARE ADDED FROM TIME TO TIME AND VALUES OF THE COMPUTATIONAL VARIABLES ARE DEDUCED BY A CUBIC SPLINE INTERPOLATION.

IF THE INITIAL VALUE OF XB IS LESS THAN DXMIN, TERMINATION OCCURS. IF XB IS GREATER THAN DXMIN BUT LESS THAN  $2 \times DXMIN$ , A WARNING IS PRINTED BUT EXECUTION CONTINUES.

IMPLICIT REAL\*8(A-H,O-Z)  
REAL\*8 MOL

COMMON /BARA/ GS1(100,3), GS2(100,3), GS3(100,3)  
COMMON /BARC/ NDT, NI, NF, NP, INT, NDIM, MAXDIM  
COMMON /BARD/ DXMIN, DELTAX  
COMMON /BARE/ GAM, BV, MOL, ECHEM, RHOP, B1(20), B2(20), BN(20),  
1 CV, ZR(20)  
COMMON /BARE/ XPR, VPR, CM, XB, VB, AB, PRM, RDOT, SIG, SSTART  
COMMON /BARG/ XBE, DELTBX, NPRC, NDIM1, NDIM2  
COMMON /BARJ/ QORF(100), PRPRES  
DIMENSION X(100,3,3), Y(100), SP(100), SPL(100)  
EQUIVALENCE (X(1,1,1), GS1(1,1))

NDIMA=NDIM  
NDIM1A=NDIM1  
NDIM2A=NDIM2  
K=XB/DXMIN+0.500  
K=K+1  
K1=0  
IF(NPRC.EQ.0) GO TO 5  
IF(CM.GT.1.D-10) GO TO 4  
NPRC=0  
GO TO 5  
4 K1=XBB/DXMIN+0.500  
K1=K1+1  
5 IF (NWAY.EQ.1) GO TO 30  
SP(1)=1.00

```

DO 10 I=2,MAXDIM
10 SP(I)=1.00-0.062500/SP(I-1)
   IF (K.GE.3) GO TO 30
   IF (K.EQ.2) GO TO 20
   WRITE (6,120)
   CALL EXIT
20 WRITE (6,130)
30 K=MAX0(K,3)
   IF(NPRC.EQ.0) GO TO 34
   IF(K1.GE.3) GO TO 35

```

C  
C  
C  
C

PROPELLING CHARGE TOO SHORT TO BE TREATED AS CONTINUUM.  
DEFAULT TO LUMPED PARAMETER.

```

NPRC=0
RHDP=CM/AB/XR3
PRPRES=QDRF(NDIM1)
34 NDIM=MNO(K,MAXDIM)
   GO TO 38
35 IF(K+K1.GT.MAXDIM) GO TO 37
36 NDIM=K
   NDIM1=K+1
   NDIM2=K+K1
   DELTBX=1.00/(DFLOAT(K1)-1.00)
   GO TO 38
37 BIT=DFLOAT(MAXDIM)/DFLOAT(K+K1)
   K=DFLOAT(K)*BIT
   K=MAX0(K,3)
   K1=MAXDIM-K
   IF(K1.GE.3) GO TO 36
   K1=3
   K=MAXDIM-3
   GO TO 36
38 DELTAX=1.00/(DFLOAT(NDIM)-1.00)
   IF (NWAY.EQ.0) RETURN
   IF (NDIM.EQ.NDIMA.AND.NPRC.EQ.0) RETURN
   IF(NDIM.EQ.NDIMA.AND.NDIM2.EQ.NDIM2A.AND.NPRC.EQ.1) RETURN
   DO 110 MM=1,3
     IL=2
     IR=NDIMA
     ILA=1
     IRA=NDIM
     MMM=NDIM
39 BIT=1.00/DFLOAT(IR-(IL-1))
     BITA=1.00/DFLOAT(IRA-ILA)
     BITD=1.500/3BIT/BIT
     IRM=IR-1
     IL1=IL
     ISHFT=IL-2
     IF (IL.GT.IRM) GO TO 60

```

```

SPL(1)=0.DO
DO 40 J=IL,IRM
SPLB=BITD*(X(J+1,N,MM)+X(J-1,N,MM)-2.DO*X(J,N,MM))
IF (J.GT.IL) SPLB=SPLB-0.25DO*SPL(J-1-ISHFT)/SP(J-2-ISHFT)
40 SPL(J-ISHFT)=SPLB
SPL(IR-ISHFT)=0.DO
KSHFT=IRM+IL-ISHFT
DO 50 J=IL,IRM
JSHFT=KSHFT-J
50 SPL(JSHFT)=(SPL(JSHFT)-0.25DO*SPL(JSHFT+1))/SP(JSHFT-1)
60 DO 90 I=ILA,IRA
ZA=BITA*DFLOAT(I-ILA)
DO 70 J=IL1,IR
Z=BIT*DFLOAT(J-(IL-1))
IF (Z.GE.ZA) GO TO 80
70 CONTINUE
J=IR
80 JJ=J-1
IL1=J
C1=(Z-ZA)/BIT
C2=(ZA+BIT-Z)/BIT
Y(I)=C1*X(JJ,N,MM)+C2*X(J,N,MM)
IF (IL.GT.IRM) GO TO 90
Y(I)=Y(I)-C1*C2/6.DO*BIT*BIT*((1.DO+C2)*SPL(JJ-ISHFT)+
*(1.DO+C1)*SPL(J-ISHFT))
90 CONTINUE
IF(NPRC.EQ.0) GO TO 95
IF(MMM.GT.NDIM) GO TO 95
IL=NDIM1A+1
IR=NDIM2A
ILA=NDIM1
IRA=NDIM2
MMM=NDIM2
GO TO 39
95 DO 100 M=1,MMM
100 X(M,N,MM)=Y(M)
110 CONTINUE
RETURN
C
120 FORMAT (44H ILLEGAL VALUES OF XB AND DXMIN. TERMINATING)
130 FORMAT (45H MARGINAL VALUES OF XB AND DXMIN. CONTINUING.)
END

```



FUNCTION RESP(X,V,A)

RESISTIVE PRESSURE ACTING ON PROJECTILE AS A FUNCTION OF  
TRAVEL (X), VELOCITY (V). ARGUMENT A IS RETURNED IN CASES  
WHEN RESISTANCE IS PROPORTIONAL TO PROJECTILE ACCELERATION.

IMPLICIT REAL\*8(A-H,O-Z)  
REAL\*8 MOL

COMMON /BARE/ GAM, BV, MOL, ECHEN, RHOP, B1(20), B2(20), BN(20),  
1 CV, ZR(20)  
COMMON /BARH/ AUP,ADWN,VISLYR,DELYR,AMUV(10),AMU(10),DB,  
\* BRX(10),BR(10),AIRGAM,AIRPO,AIRTO,AIRMW,TWALO,  
\* PPPF,COMUZ,ASBR,CDBR,PDIA,CHTW,DRHO(2)  
COMMON /BARH2/ PRMB,ELB,ANU,BMUV(10),BMU(10),NBRES3  
COMMON /BARH4/ RESAIR,RESOB  
COMMON /BARF/ XPR, VPR, CM, XB, VB, AB, PRM, RDOT, SIG, SSTART  
COMMON /BARI/ NWF2,NBRES1,NBRES2,NHTW,NMUZBL,NBRV  
DATA G/386.1500/,R/18550.00/

RESP=0.00  
A=0.00  
IF(NBRES1.EQ.0) GO TO 40

RESISTANCE DUE TO FRICTION ON OBTURATOR GIVEN IN TABULAR FORM

IF(X.GT.BPX(1)) GO TO 10  
RESP=BR(1)  
GO TO 40  
10 DO 20 I=2,NBRES1  
IF(BRX(I).GE.X) GO TO 30  
20 CONTINUE  
RESP=BR(NBRES1)  
GO TO 40  
30 BIT=(BRX(I)-X)/(BRX(I)-BRX(I-1))  
RESP=BR(I-1)\*3BIT+3R(I)\*(1.00-BIT)  
40 PESOB=RESP  
IF(NBRES2.EQ.0) GO TO 60

RESISTANCE DUE TO SHOCK AHEAD OF PROJECTILE

50 BIT=(AIRGAM-1.00)/(AIRGAM+1.00)  
BITC=DSQRT(G\*AIRGAM\*P\*AIRTO/AIRMW)  
BITL=1.00-BIT  
BITU=(V+DSQRT(V\*V+4.00\*BITL\*BITL\*BITC\*BITC))  
\* /(2.00\*BITL\*BITC)  
RESAIR=AIRPO\*((1.00+BIT)\*BITU\*BITU-BIT)  
RESP=RESP+RESAIR  
60 IF(NBRES3.EQ.0) RETURN

```

C      RESISTANCE DUE TO FRICTION ON OBTURATOR AS DETERMINED
C      BY SETBACK PRESSURE AND TABULAR COEFFICIENT OF FRICTION
      IF(V.GT.BMU(1)) GO TO 70
      BITMU=BMU(1)
      GO TO 100
70     DO 80 I=2,NBRES3
      IF(BMU(I).GE.V) GO TO 90
80     CONTINUE
      BITMU=BMU(NBRES3)
      GO TO 100
90     BIT=(BMU(I)-V)/(BMU(I)-BMU(I-1))
      BITMU=BMU(I-1)*BIT+BMU(I)*(1.00-BIT)
100    RESOB=BITMU/BMU(1)*SSTART
      RESP=RESP+RESOB
      DENOM=(1.00-ANU)/ANU*AB-BITMU*ELB*1.570796*DB
      IF(DENOM.LT.1.0-10) DENOM=1.0-10
      A=4.00*BITMU*ELB/DB*PRMB/G/DENOM
      RETURN
      END

```

FUNCTION RNOM(X)

NOMINAL DENSITY CURVE FOR PROPELLANT AS A FUNCTION OF  
PRESSURE (X).

IMPLICIT REAL\*8(A-H,O-Z)

REAL\*8 MOL

COMMON /BARE/ GAM, EV, MOL, ECHEM, RHOP, B1(20), B2(20), BN(20),  
1 CV, ZR(20)

COMMON /BARH/ AUP,ADWN,VISLYR,DELYR,AMUV(10),AMU(10),  
\* BRX(10),BR(10),AIRGAM,AIRPO,AIRTO,AIRMH,TWALO,  
\* PBRF,CDMUZ,ASBR,CDBR,PDIA,CHTW,DRHO(2)

DATA G/386.16D0/

RNOM=RHOP\*(3.D0\*G\*X/AUP/AUP/RHOP+1.D0)\*\*(1.D0/3.D0)

RETURN

END

SUBROUTINE SIGCHK

C  
C  
C  
CHECKS THAT PRESSURE IN SOLID PROPELLANT DOES NOT LIE  
ABOVE NOMINAL LOADING CURVE.

IMPLICIT REAL\*8(A-H,O-Z)  
COMMON /BARA/ GS1(100,3), GS2(100,3), GS3(100,3)  
COMMON /BARC/ NDT, NI, NF, NP, INT, NDIM, MAXDIM  
COMMON /BARS/ XBB,DELTEX,NPRC,NDIM1,NDIM2

C  
DO 10 I=NDIM1,NDIM2  
X=SNOM(GS1(I,NF))  
IF(GS3(I,NF).GT.X) GS3(I,NF)=X  
10 CONTINUE  
RETURN  
END

FUNCTION SNOM(X)

NOMINAL STRESS CURVE FOR PROPELLANT AS A FUNCTION OF DENSITY  
(X).

IMPLICIT REAL\*8(A-H,O-Z)

REAL\*8 MDL

COMMON /BARE/ GAM, BV, MDL, ECHM, RHOP, B1(20), B2(20), BN(20),

1 CV, ZR(20)

COMMON /BARH/ AUP,ADWN,VISLYR,DELYR,AMUV(10),AMU(10),

\* BRX(10),BR(10),AIRGAM,AIRPO,AIRTO,AIRMW,TWALO,  
\* PBRF,CDMUZ,ASBF,COBR,PDIA,CHTW,DRHD(2)

DATA G/386.16D0/

SNOM=AUP\*AUP\*RHOP/3.D0/G\*((X/RHOP)\*\*3-1.D0)

RETURN

END

SUBROUTINE VELCHK

C  
C  
C  
C  
CHECKS THAT VELOCITY HAS NOT BEEN REVERSED AS A  
CONSEQUENCE OF FRICTION

IMPLICIT REAL\*8(A-H,O-Z)

C  
COMMON /BARA/ GS1(100,3), GS2(100,3), GS3(100,3)  
COMMON /BARC/ NDT, NI, NF, NP, INT, NDIM, MAXDIM  
COMMON /BARG/ XEB, DELTAX, NPRC, NDIM1, NDIM2  
COMMON /BARJ/ QORF(100), PRPRES

C  
NB=NI  
IF(INT.EQ.0) NB=NP  
DO 10 I=NDIM1,NDIM2  
IF(DABS(GS2(I,NB)).LT.1.D-10) GO TO 10  
IF(GS2(I,NF)\*QORF(I).GT.0.D0) GS2(I,NF)=0.D0  
10 CONTINUE  
RETURN  
END

SUBROUTINE WFR

FRICITION BETWEEN SOLID PROPELLANT AND TUBE WALL

IMPLICIT REAL\*8(A-H,O-Z)

REAL\*8 MOL

COMMON /BAR3/ RHO(100), P(100), E(100), T(100), U(100), ETA(100)

COMMON /BARE/ GAM, RV, MOL, ECHEM, RHOP, B1(20), B2(20), BN(20),

1 CV, ZR(20)

COMMON /BARG/ XBP, DELTBX, NPROC, NDIM1, NDIM2

COMMON /BARH/ AUP, ADWV, VISLYR, DELYR, AMUV(10), AMU(10), DB,

\* BRX(10), BR(10), AIRGAM, AIRPO, AIRTO, AIRMW, TWALO,

\* PBPF, CDMUZ, ASBR, CDBR, PDIA, CHTW, DRHO(2)

COMMON /BARI/ NWFR, NRES1, NRES2, NHTW, NMUZBL, NBRV

COMMON /BARJ/ QORF(100), PRPRES

IF(NWFR.GT.0) GO TO 20

FRICITION DUE TO GAS FILM LAYER

DO 10 I=NDIM1,NDIM2

QORF(I)=-4.DO/DB\*VISLYR/DELYR\*U(I)

10 CONTINUE

RETURN

FRICITION DUE TO NORMAL STRESS

20 DO 70 I=NDIM1,NDIM2

QORF(I)=0.DO

IF(P(I).LE.0.DO) GO TO 70

IF(I.EQ.NDIM1) GO TO 22

IF(I.EQ.NDIM2) GO TO 24

PATI=0.2500\*(P(I-1)+P(I+1))+2.DO\*P(I))

GO TO 26

22 PATI=0.500\*(P(I)+P(I+1))

GO TO 26

24 PATI=0.500\*(P(I)+P(I-1))

26 BITU=U(I)

IF(BITU.GT.AMUV(1)) GO TO 30

BITMU=AMU(1)

GO TO 60

30 DO 40 J=2,NWFR

IF(AMUV(J).GE.BITU) GO TO 50

40 CONTINUE

BITMU=AMU(NWFR)

GO TO 60

50 BIT=(AMUV(J)-BITU)/(AMUV(J)-AMUV(J-1))

BITMU=AMU(J-1)\*BIT+AMU(J)\*(1.DO-BIT)

60 QORF(I)=-4.DO/DB\*BITMU\*PATI

```
IF(DABS(BITU).GT.1.D-10) QORF(I)=QORF(I)*BITU/DABS(BITU)  
70 CONTINUE  
RETURN  
END
```



# DISTRIBUTION LIST

<u>No. of Copies</u>	<u>Organization</u>	<u>No. of Copies</u>	<u>Organization</u>
2	Commander Defense Technical Info Center ATTN: DDC-DDA Cameron Station Alexandria, VA 22314	4	Commander US Army Armament Research & Development Command ATTN: DRDAR-LCE-MP, Dr.H. Fair DRDAR-LCE-D, Dr.J. Hershkowitz DRDAR-TSS (2 cys) Dover, NJ 07801
1	HQDA (SAUS-OR, D. Hardison) Washington, DC 20310		
1	HQDA (DAMA, LTC H. Glock) Washington, DC 20310	1	Commander US Army Armament Materiel Readiness Command ATTN: DRSAR-LEP-L, Tech Lib Rock Island, IL 61299
1	Commander US Army Materiel Development & Readiness Command ATTN: DRCDMD-ST 5001 Eisenhower Avenue Alexandria, VA 22333	1	Director US Army ARRADCOM Benet Weapons Laboratory ATTN: DRDAR-LCB-TL Watervliet, NY 12189
1	Commander US Army Materiel Development & Readiness Command ATTN: DRCDMD, MG R. Baer 5001 Eisenhower Avenue Alexandria, VA 22333	1	Commander US Army Aviation Research & Development Command ATTN: DRSAR-E P.O. Box 209 St. Louis, MO 63166
1	Commander US Army Materiel Development & Readiness Command ATTN: DRCPM-GCM-WF, LTC P. McVey 5001 Eisenhower Avenue Alexandria, VA 22333	1	Director US Army Air Mobility Research & Development Laboratory Ames Research Center Moffett Field, CA 94035
3	Commander US Army Armament Research & Development Command ATTN: DRDAR-TO, Dr.R. Weigle DRDAR-LC, Dr.J. Frasier DRDAR-SC, S. Jacobson Dover, NJ 07801	1	Commander US Army Communications Research & Development Command ATTN: DRDCO-PPA-SA Fort Monmouth, NJ 07703
		1	Commander US Army Electronics Research & Development Command Technical Support Activity ATTN: DELSD-L Fort Monmouth, NJ 07703

# DISTRIBUTION LIST

<u>No. of Copies</u>	<u>Organization</u>	<u>No. of Copies</u>	<u>Organization</u>
1	Commander US Army Missile Command ATTN: DRSMI-R Redstone Arsenal, AL 35809	1	Paul Gough Associates, Inc. ATTN: P. S. Gough Portsmouth, NH 03801
1	Commander US Army Missile Command ATTN: DRSMI-YDL Redstone Arsenal, AL 35809	1	Shock Hydordynamics, Inc. ATTN: Dr. H. Anderson 4710-16 Vineland Avenue N. Hollywood, CA 91602
3	Commander US Army Tank Automotive Research & Development Command ATTN: DRDTA-UL DRDTA-RKA, Mr. H. Spiro DRDTA-RE, Mr. C. Bradley Warren, MI 48090	1	Teledyne McCormick Selph ATTN: Mr. Charles S. Leveritt 3601 Union Road P.O. Box 6 Hollister, CA 95023
1	Director US Army TRADOC Systems Analysis Activity ATTN: ATAA-SL, Tech Lib White Sands Missile Range NM 88002	1	Princeton University Guggenheim Laboratories Dept. of Aerospace and Mechanical Science ATTN: Dr. L.H. Caveny Princeton, NJ 08540
1	Commander US Army Armor School ATTN: CPT E. Bryla Fort Knox, KY 40121	1	University of Illinois Dept. of Aeronautical Engineering ATTN: Prof. H. Krier Urbana, Illinois 61801
			<u>Aberdeen Proving Ground</u>
1	Commander Naval Weapons Center ATTN: Propulsion Systems Div Mr. R.M. Price China Lake, CA 93555		Dir, USAMSAA ATTN: DRXSY-D DRXSY-MP, H. Cohen
			Cdr, USATECOM ATTN: DRSTE-TO-F
1	AFATL (DLDG, Mr. O. Heiney) Eglin AFB, FL 32542		Dir, Wpns Systems Concepts Team Bldg E3516, EA ATTN: DRDAR-ACW
1	Battelle Columbus Laboratories ATTN: Dr. D. Trott 505 King Avenue Columbus, OH 43201		

## USER EVALUATION OF REPORT

Please take a few minutes to answer the questions below; tear out this sheet and return it to Director, US Army Ballistic Research Laboratory, ARRADCOM, ATTN: DRDAR-TSB, Aberdeen Proving Ground, Maryland 21005. Your comments will provide us with information for improving future reports.

1. BRL Report Number \_\_\_\_\_

2. Does this report satisfy a need? (Comment on purpose, related project, or other area of interest for which report will be used.)  
\_\_\_\_\_  
\_\_\_\_\_  
\_\_\_\_\_

3. How, specifically, is the report being used? (Information source, design data or procedure, management procedure, source of ideas, etc.) \_\_\_\_\_  
\_\_\_\_\_  
\_\_\_\_\_

4. Has the information in this report led to any quantitative savings as far as man-hours/contract dollars saved, operating costs avoided, efficiencies achieved, etc.? If so, please elaborate.  
\_\_\_\_\_  
\_\_\_\_\_  
\_\_\_\_\_

5. General Comments (Indicate what you think should be changed to make this report and future reports of this type more responsive to your needs, more usable, improve readability, etc.) \_\_\_\_\_  
\_\_\_\_\_  
\_\_\_\_\_  
\_\_\_\_\_

6. If you would like to be contacted by the personnel who prepared this report to raise specific questions or discuss the topic, please fill in the following information.

Name: \_\_\_\_\_

Telephone Number: \_\_\_\_\_

Organization Address: \_\_\_\_\_  
\_\_\_\_\_  
\_\_\_\_\_